

**Comparing the provision of ecosystem services of an anthropogenically modified salt
marsh to a natural salt marsh**

by

Makadunyiswe Doublejoy Ngulube

A Thesis Submitted to
Saint Mary's University, Halifax, Nova Scotia
in Partial Fulfillment of the Requirements for
the Degree of Master of Science in Applied Science.

August, 2024, Halifax, Nova Scotia

Copyright [Makadunyiswe Doublejoy Ngulube, 2024]

Approved: Dr. Danika van Proosdij
Supervisor
Department of Geography
and Environmental Studies

Approved: Dr. Jeremy Lundholm
Supervisory Committee
Member

Approved: Dr. Colleen Barber
Supervisory Committee
Member

Approved: Kirsten Ellis, MSc.
Supervisory Committee

Approved: Joanna Eyquem, PGeo.,
ENV SP., CWEM. CEnv.
External Examiner

Date: August 30th, 2024

Comparing the provision of ecosystem services of an anthropogenically modified salt marsh to a natural salt marsh.

by

Makadunywiswe Doublejoy Ngulube

Abstract:

Natural marshes are valued for their biodiversity and ecosystem services. This research quantified the functions of ecosystem services (wave energy dissipation, habitat, primary productivity, blue carbon) of a natural salt marsh in the Acadian Peninsula, New Brunswick, and compared them to those of an anthropogenically modified salt marsh pre-restoration on the Chiasson Office Spit, adjacent to the Shippagan Gully. This is a habitat offsetting project to mitigate unavoidable alterations to Piping Plover (*Charadrius melodus*) Critical Habitat. Maximum wave heights were measured from August – November 2022, vertical biomass distribution was analyzed using binarized images. Vegetation surveys were carried out and sediment cores were collected for carbon content and soil nutrient analysis. Key findings indicate that seasonal vegetation variability impacts wave energy dissipation, with the natural marsh exhibiting higher annual net primary productivity and greater carbon content than the modified salt marsh. This research provides essential data for coastal restoration and protection strategies.

August 30th, 2024

Acknowledgements

Thank you to my dear supervisor, Dr. Danika van Proosdij, who has always been supportive in many ways. I consider it an honour to have been under her mentorship and tutelage. Thank you for believing in me, and always seeing the bigger picture. To my supervisory committee, Dr. Jeremy Lundholm, Dr. Colleen Barber, and Kirsten Ellis, MSc., thank you for your unwavering support. To my External Examiner, Joanna Eyquem, PGeo. ENV SP. CWEM. CEnv., thank you for availing yourself to read, review and provide guidance on my thesis – I appreciate your perspective and feedback!

This thesis taught me many lessons, but the most important one I'll share is “to ask for help”. This was the true test of vulnerability on my part, overthrowing the lie of self-sufficiency and individualism, as I found myself constantly seeking counsel from various experts in the field. It was also a true test of humility. As King Solomon once said, “...lean not on your own understanding...”

Having learned that, I truly understand the meaning of “it takes a village”, as it applies to me both figuratively and literally. So, to my village in Zimbabwe, *abakoNgulube, labakoNdlovu*, and the Sindah Clan – *enkosi* (thank you). To my parents, Bishops Sindah and Suzen, thank you for laying down your lives for mine, so that I may pursue tertiary education. I will forever be grateful for it and bring honor to you and the family name. To my sister Makabongwe, and her lovely husband, Vincent, thank you for your support - look how far we've come!

To my village in Canada, thank you CBWES (Tony Bowron, Jennie Graham, Samantha Lewis, Kailey Nichols, Kayla Williams, Katie Sonier, Jocelyn Kickbush, Samantha Battaglia, and Tom Johnson), SMU and TransCoastal Adaptations for being supportive throughout this journey. A special thanks to Brittney Roughan, Chelsea Fourgère, Christian Hart, Christopher Ross, Emma Poirier, Emily Baker, Emily Hodgson, Jane Heeney, Jubin Thomas, Jordan Dunham,

and Leah Rudderham. Thanks to Greg Baker for listening to my never-ending rants and for sharing your knowledge on all things GIS and beyond. I would also like to thank the Dalhousie University CERC lab, specifically Claire Normandeau for providing training and lab space for my work, and the Nova Scotia Agriculture Lab in Truro. A special thank you to MITACS, and the Department of Fisheries and Oceans Canada - Small Craft Harbours program for providing funding for this work.

To my mentoring pod, through the Coastal and Estuarine Research Federation Rising TIDES Program (Dr. Johnny Quispe, Gabriela Jamir Reyes, Alexandra Cormack, Christian Pryor and Zlatka Rebolledo Sanchez) – thank you for your support and for creating a space for me share my research, to grow, and to be challenged by other early career professionals and academics.

To my dear friend, Arthur Munyaradzi Mataure, CPA, who lost the battle to cancer during my Masters, I'll forever be grateful for his words of encouragement and motivation. Up until his passing, he encouraged me to keep going. To all my friends, especially Han, Tanaka, Sophia, Sara, Neema, Nickel, Karen, Nonie and Sam – thank you for putting up with my love-hate relationship with grad school – we did it!

Now, to my younger self, the little black girl that grew up playing in the streets of Glen Norah B, thank you for always dreaming, for always seeking a way out, for always believing that you are capable and for holding on to the fact you will do great things. Thank you for not giving up, even when the odds were up against you. Thank you for your resilience - your tenacity is highly admirable!

To every black girl that has a dream, remember you are the epitome of brilliance. Be creative. Be diligent. Be authentic. This is my promise to you; I will create space for you in

whatever capacity I can because I know there is room for all of us to shine. Simply put your best foot forward and keep going. Here's to brilliant minds!

- *From a Brilliant one!*

Table of Contents

Abstract:	ii
Acknowledgements	iii
Table of Contents	vi
List of Figures	viii
List of Tables	xiii
Chapter 1 - Literature Review.....	1
1.1. Introduction.....	1
1.2. Salt Marshes and their importance for coastal protection.....	1
1.3. Nature-based solutions.....	4
1.3.1. Sand nourishment.....	8
1.3.2. Living shorelines.....	9
1.4. Ecosystem services	12
1.4.1. Regulating and maintenance	13
1.4.1.1. Coastal flooding/erosion protection: Wave energy dissipation	13
1.4.1.2. Habitat provision: Vegetation cover, species diversity and abundance.....	14
1.4.1.3. Climate regulation: Blue carbon (carbon storage)	15
1.4.2. Provisioning	16
1.4.3. Habitat provision: Primary productivity	16
1.5. Rationale and Research Questions.....	17
Chapter 2: Study Area.....	20
2.1. Chiasson Office Spit and Shippagan Gully	20
2.2. History of the Shippagan Gully	23
2.3. Restoration work at the Shippagan Gully	27
2.3.1. Chiasson Office Spit Study Site (SHP).....	27
2.4. Reference Site – Baie de Pokemouche	30
2.5. Climate at the Chiasson Office Spit and at the Baie de Pokemouche	31
2.6. Hydrodynamic processes	33
Chapter 3: Methodology	35
3.1. Wave energy dissipation	35
3.1.1. Vegetation surveys.....	39

3.2. Habitat.....	41
3.2.1. Vegetation Surveys	41
3.2.1.1 Statistical Methods.....	42
3.2.2. Soil Nutrient Analysis.....	42
3.3. Primary Productivity	43
3.3.1. Aboveground Biomass Sampling	43
3.4. Blue carbon	45
3.4.1. Field sampling procedure.....	45
3.4.2. Sediment Core Analysis - Laboratory Analysis.....	48
3.4.3. Carbon Stocks	53
3.4.3.1. Statistical Analysis.....	53
3.5. Grain Size Analysis.....	54
3.5.1. Statistical Analysis.....	54
Chapter 4: Results	55
4.1. Wave energy dissipation	55
4.1.1. Vegetation height and stem density using image obscuration ratio.....	60
4.2. Habitat.....	62
4.2.1. Soil Nutrients	66
4.3. Primary Productivity	68
4.4. Organic, Inorganic and Total Carbon	69
4.5. Bulk Density, Organic, and Total Carbon changes with core depth.....	74
Chapter 5: Discussion	77
5.1. Research objectives and interpretation	77
5.2. Hydrology as a driver for salt marsh processes	77
Chapter 6: Conclusion and Future Recommendations.....	90
References:.....	93
Appendix.....	101
List of Tables:	101

List of Figures

Figure 1. Salt marsh processes that enable adaptation and mitigation despite climate change impacts. (Modified from Duarte et al., 2013).	3
Figure 2. With rising sea level, foreshore marshes can adapt due to the dynamic processes.....	4
Figure 3. Range of potential for building with nature along main axes of given bed slope and hydrodynamic energy. (Modified from Figure 1. de Vriend et al., 2015).	5
Figure 4. Types of sand nourishment, with the MKL zone (Momentane KustLijn i.e., current coastline) shown in each scenario (modified from Brand et al., 2022).	9
Figure 5. Types of Shorelines: A) Bulkhead, B) Riprap revetment, C) Sill (Modified from Figure 1. Gittman et al., 2014).	12
Figure 6. Three different categories of ecosystem services.	13
Figure 7. Location of the Shippagan Gully inlet and the Acadian Peninsula near Le Goulet, New Brunswick. A – Eastern Canada; B – Acadian Peninsula, North-eastern New Brunswick; C – Chiasson Office Spit, Shippagan Gully inlet. Site location is shown by white outline.....	21
Figure 8. Study area map, CBWES 2021 Report Baseline interim monitoring report (reprinted with permission from CBWES Inc.).	22
Figure 9. Images of Study Site (Shippagan), photos taken in August 2022.	22
Figure 10. Historical engineering works at Shippagan Gully from the late nineteenth century to the mid-twentieth century (photo taken in 1980) (Provan et al., 2018).....	24
Figure 11. Google Earth Imagery of Shippagan (Google Earth, 2024).	24
Figure 12. Original Big Shippagan Lighthouse and its replacement (image from Library and Archives Canada).	27

Figure 13. Map of Chiasson Office Spit showing locations of proposed offsets (reprinted with permission from CBWES Inc). 29

Figure 14. Images of Reference Site (SHP_R), photos taken in August 2022. 31

Figure 15. Temperature and Precipitation Graph for 1981 to 2010 Canadian Climate Normals, Shippagan, New Brunswick..... 32

Figure 16. Wind Rose diagram represents the wind speed and direction in the Shippagan region. (May 2022 to January 2023), based on the meteorological data collected on site at the Chiasson Office Spit, via the TransCoastal Adaptations weather station. 33

Figure 17. 4 RBRduet³ T.D|wave16 — temperature and pressure sensors deployed along a 30 m transect at the study site (SHP); (HHWLT - The average of the highest high waters, 1 from each of 19 years of predictions, from Shippagan Gully CHS station). 38

Figure 18. 4 RBRduet³ T.D|wave16 — temperature and pressure sensors deployed along a 10 m transect at the reference site (SHP_R); (HHWLT - The average of the highest high waters, 1 from each of 19 years of predictions, from Shippagan CHS station). 39

Figure 19. Portable digital photograph frame used to capture side-on photographs of marsh vegetation. Left: (From Figure 2. Möller et al., 2006), Right: (Re-designed by Ngulube, 2022). 40

Figure 20. Schematic diagram illustrating how to derive obscuration ratio (black pixel coverage (%) of image) and canopy height from field image, to classified image and classified binary black and white image. 41

Figure 21. Vegetation plot layout and 30 m wave logger transect at the Study Site, Chiasson Office Spit, New Brunswick (MS = Marsh Sill, SW = Sea Wall, W = Wetland). 44

Figure 22. Vegetation plot layout and 10 m wave logger transect at the Reference site, Boudreau Channel, New Brunswick. 45

Figure 23. Layout map showing where sediment cores were collected at the study site, Chiasson Office. 47

Figure 24. Layout map showing where sediment cores were collected at the reference site, Boudreau Channel, New Brunswick..... 48

Figure 25. Bulk density disc cut out of sediment core sample 50

Figure 26. Grinding and homogenization of soil sample with mortar and pestle..... 51

Figure 27. A. Scale used to measure sample weights, B. Capsule holder and forceps for compressing capsule, C. Compressed capsules containing sample for EA. 52

Figure 28. Maximum wave height recorded at RBR 1, RBR 2, RBR 3 and RBR 4 at Shippagan (Study Site) throughout the duration of the study from August to November 2022. 49

Figure 29. Event 1 - Maximum wave height recorded at RBR 1, RBR 2, RBR 3 and RBR 4 at Shippagan (Study Site) from September 15th to September 19th, 2022. 50

Figure 30. Event 2 - Maximum wave height recorded at RBR 1, RBR 2, RBR 3 and RBR 4 at Shippagan (Study Site) from September 22nd to October 5th, 2022. 51

Figure 31. Event 3 - Maximum wave height recorded at RBR 1, RBR 2, RBR 3 and RBR 4 at Shippagan (Study Site) from October 25th to November 5th, 2022..... 51

Figure 32. Maximum wave height recorded at RBR 1, RBR 2, RBR 3 and RBR 4 at Shippagan (Reference Site) throughout the duration of the study from August to November 2022. 53

Figure 33. Event 1 - Maximum wave height recorded at RBR 1, RBR 2, RBR 3 and RBR 4 at Shippagan (Reference Site) from September 15th to September 19th, 2022. 54

Figure 34. Event 2 - Maximum wave height recorded at RBR 1, RBR 2, RBR 3 and RBR 4 at Shippagan (Reference Site) from September 22nd to October 5th, 2022..... 55

Figure 35. Event 3 - Maximum wave height recorded at RBR 1, RBR 2, RBR 3 and RBR 4 at Shippagan (Reference Site) from October 25th to November 5th, 2022..... 55

Figure 36. Percentage of attenuation, water depth and significant wave height at the study site (SHP), for entire deployment..... 57

Figure 37. Percentage of attenuation, water depth and significant wave height at the reference site (SHP_R), for entire deployment. 58

Figure 38. Relationship between aboveground biomass (dry weight) of photographed vegetation and image obscuration ratio for SHP and SHP_R at RBR 3 and RBR 4..... 61

Figure 39. Percent cover for top 5 dominant species at Shippagan study site (SHP) (arranged in order of top 2 dominant species, with standard deviation bars.) 64

Figure 40. Percent cover for top 5 dominant species at Shippagan reference site (SHP_R) (arranged in order of top 2 dominant species, with standard deviation bars). 64

Figure 41. Frequency at Shippagan study site (SHP), which is the % of all plots at the site where the species occurs..... 65

Figure 42. Frequency at Shippagan reference site (SHP_R), which is the % of all plots at the site where the species occurs. 65

Figure 43. Plot average coverage at Shippagan Study Site (SHP) with standard deviation bars.. 66

Figure 44. Plot average coverage at Shippagan Reference Site (SHP_R), with standard deviation bars..... 66

Figure 45. Average aboveground biomass at Shippagan Study Site (SHP)and Shippagan Reference Site (SHP_R)..... 69

Figure 46. Total carbon at the Study and Reference Sites, within the shoreline, low marsh and mid to high marsh zones (x represents the mean within the data range (no statistically significant differences)). 70

Figure 47. Organic carbon at the Study and Reference Sites, within the shoreline, low marsh and mid to high marsh zones (x represents the mean within the data range (statistically significant interaction)). 71

Figure 48. Inorganic carbon at the Study and Reference Sites, within the shoreline, low marsh and mid to high marsh zones (x represents the mean within the data range). 72

Figure 49. Percentage of Organic Carbon and Organic Matter from LOI at both the Reference and Study Sites. 73

Figure 50. Percentage of Total Carbon and Organic Matter at both the Reference and Study Sites. 73

Figure 51. Changes with depth in bulk density, organic carbon, and total carbon for each marsh zone at the study site (SHP). 75

Figure 52. Changes with depth in bulk density, organic carbon, and total carbon for each marsh zone at the study site (SHP_R). 76

List of Tables

Table 1. Ecosystem services and corresponding functions.....	13
Table 2. Historical works at Shippagan Gully (Table 1, modified from Provan et al., 2018).....	25
Table 3. Sample statistics used for grain size analysis (modified from Blott & Pye, 2001)	54
Table 4. Measured parameters for each ecosystem service variable.	55
Table 5. Summary of Events 1 -3, at SHP and SHP_R (Event 1 – Sept 15 – 19; Event 2 – Sept 22 – Oct 5; Event 3 – Oct 25 – Nov 5).	56
Table 6. Wave heights and water depths for SHP and SHP_R, showing similar vegetation species found at each site, that quantify wave energy dissipation at initial instrument * (at the transect section considered) (RBR 1 and RBR 3 were used for calculation).....	59
Table 7. Image obscuration for August and September 2022 at SHP and SHP_R.....	62
Table 8. Wave heights and water depths for field studies with similar vegetation species to those found in salt marshes in Canada, that quantify wave energy dissipation (modified from Table 1 in Tempest et al., 2015, and Table 1 in Vuik et al., 2016).....	81

Chapter 1 - Literature Review

1.1. Introduction

Coastal communities and low-lying areas face threatening impacts of climate change and sea level rise (IPCC, 2022). Storms and hurricanes have an impact on the coastal zone, and there has been an increase in the cost of impacts associated with these hazards (Shepard et al., 2011). Intensified storms have led to an increased risk of flooding in coastal communities and as a result, urgent implementation of sustainable measures is needed to cope with the problem (Duarte et al., 2013; Foster-Martinez et al., 2018; Greenan et al., 2019; Michener et al., 1997). In Canada, according to Reed et al. (2024), these changes are particularly concerning, impacting infrastructure and various ecosystems. Natural ecosystems such as salt marshes, which are crucial for coastal protection are being impacted (Bridges et al., 2021; Eyquem, 2021; Greenan et al., 2019). The development of adaptation strategies as a means for coastal protection is therefore essential to address the hazards posed by climate change (Duarte et al., 2013; Nicholls et al., 2008). As a response to these intensified storms, nature-based solutions are being implemented in different coastal regions globally (Bridges et al., 2015; Duarte et al., 2013, Eyquem, 2021).

1.2. Salt Marshes and their importance for coastal protection

Salt marshes are natural ecosystems that occur in temperate and high latitudes (Allen & Pye, 1992; Davidson-Arnott et al., 2019). They occur along coastal areas where physical energy is low enough to allow salt tolerant grasses to establish in the intertidal zone (Friedrichs et al., 2001; Allen and Pye, 1992). These areas are regularly inundated by tidal waters and this hydrology is a major driver of salt marsh functions and its ecological services (Allen, 2000; Byers & Chmura, 2014). Rates of subsidence, concentration of nutrients, organic matter, and oxygen are also influenced by subsurface hydrology (Byers & Chmura, 2014).

The vital benefits provided by salt marshes are known as protective and ecosystem services. These services are often a result of components of the ecosystem or underlying processes (Duarte et al., 2013) (*Figure 1*).

Salt marshes play an important role as buffers in protecting coastlines. They absorb wind and wave energy before it reaches inland (Allen, 2000; Foster-Martinez et al, 2018; Möller et al., 2014). Additional benefits of salt marshes include their ability to sequester carbon, keep pace with sea level rise, provide rich wild-life habitat, and improve water quality (Allen, 2000). Salt marshes also export and store nutrients and have the ability to trap particles suspended in tidal waters, storing them in the soil (Duarte et al., 2013). Salt marshes are an important ecosystem which should be prioritized in coastal protection studies.

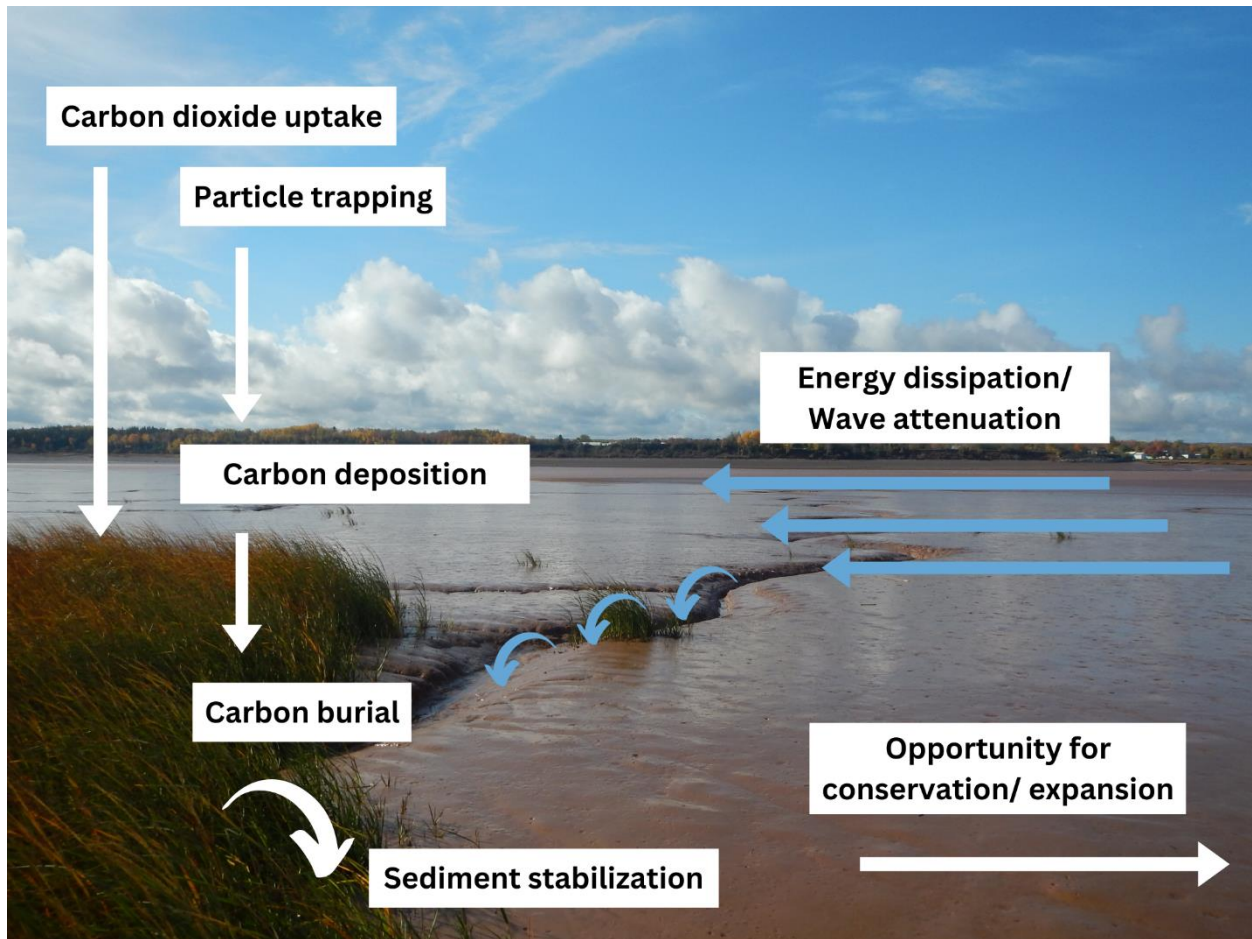


Figure 1. Salt marsh processes that enable adaptation and mitigation despite climate change impacts. (Modified from Duarte et al., 2013).

Incorporating salt marshes in coastal hazard mitigation and climate change adaptation strategies is essential (Shepard et al., 2011). Salt marshes occupy the same low-lying coastal areas that are especially vulnerable to sea level rise (Mitchell & Bilkovic, 2019; Shepard et al., 2011). As a result, they are a practical choice for inclusion in mitigation and adaptation approaches as they can maintain the coastline, by means of accreting sediment at a level that is comparable or even higher than sea level rise (Figure 2). This provides a further reduction in vulnerability to hazards and climate change (Shepard et al., 2011). It is therefore vital to implement policies that propose restoration or construction of natural systems that will maximize the benefits and ecosystem services of salt marshes (Shepard et al., 2011, Rahman et al., 2019, Vouk & Eyquem, 2024).

To keep pace with sea level: a) Marshes migrate b) Marshes accrete

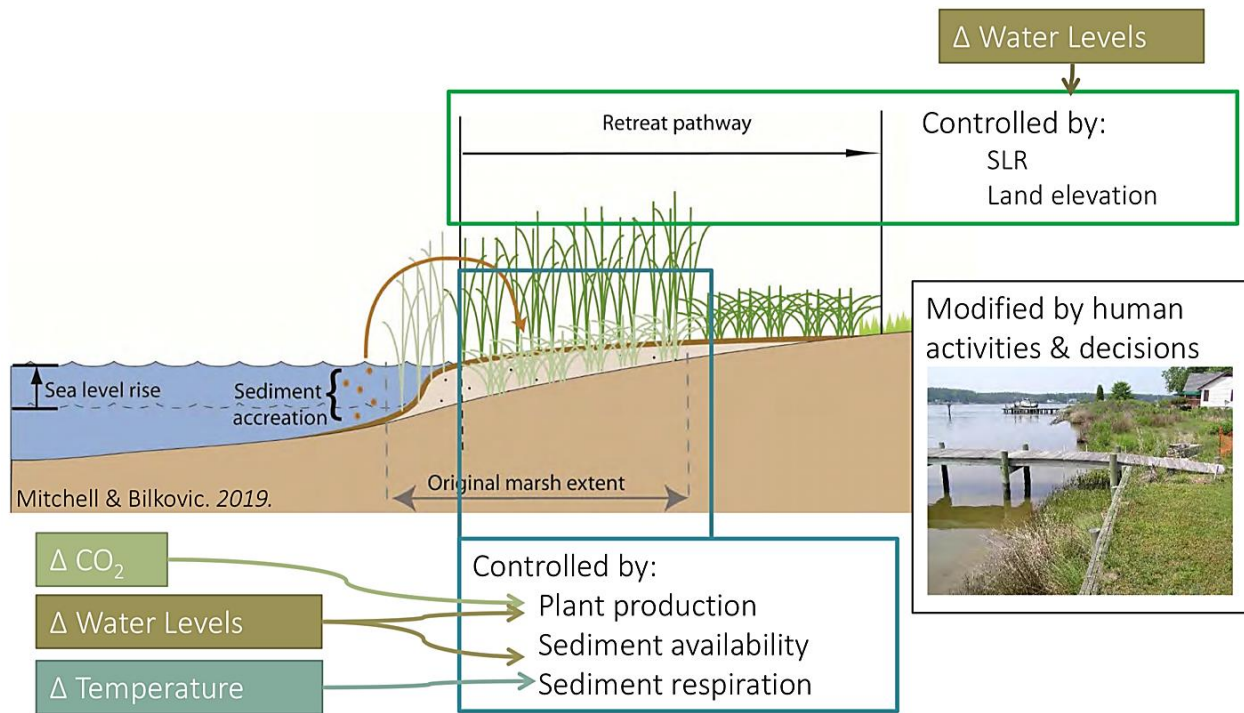


Figure 2. With rising sea level, foreshore marshes can adapt due to the dynamic processes. The presence of tall dense marsh vegetation allows for wave energy dissipation and the collection of sediment which leads to an increase in marsh elevation; the roots of marsh vegetation also contribute to sediment accretion. Low elevation lands allow for the retreat of marshes into upland areas as sea level rises, maintaining marsh extent under changing conditions (Figure 1., modified from Mitchell & Bilkovic, 2019).

1.3. Nature-based solutions

The International Union for Conservation of Nature (IUCN) defines Nature-based Solutions (NbS) as "actions to protect, sustainably manage, and restore natural or modified ecosystems, which address societal challenges effectively and adaptively, simultaneously providing human well-being and biodiversity benefits" (IUCN, 2020). Natural features are defined as features that are created and evolve over time through the actions of physical, biological, geologic, and chemical processes operating in nature (Bridges et al., 2015). Nature-based features are those that mimic the characteristics of natural features but are created by human design, engineering, and construction to provide specific services such as coastal risk reduction (Bridges et al., 2015) (Figure 3). With

increasing global sea-level rise, many low-lying developed shoreline areas are already experiencing flooding at extreme high tides (Griggs & Patsch, 2019). The use of natural and nature-based features for coastal resilience and climate change adaptation has increased as research has progressed (Bilkovic et al., 2016; Bridges et al., 2015; Murphy et al., 2024). There has been a rise in the implementation of ecosystem-based approaches to reduce the risks of coastal storms (Bouma et al., 2005; Bridges et al., 2015; Duarte et al., 2013; Murphy et al., 2024).

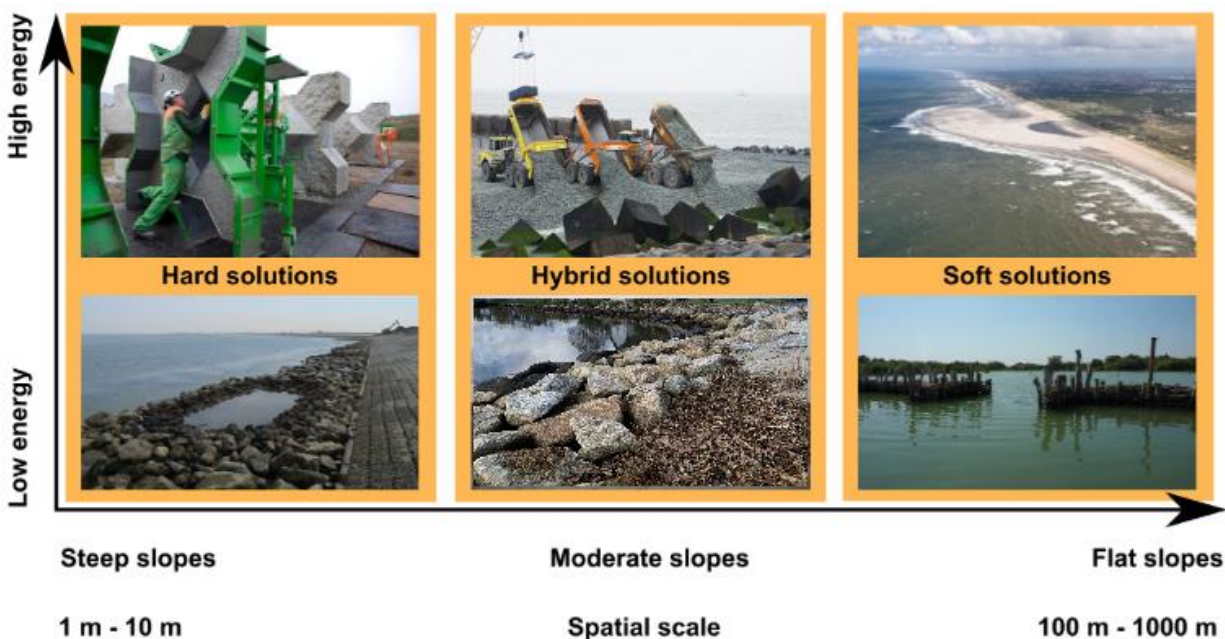


Figure 3. Range of potential for building with nature along main axes of given bed slope and hydrodynamic energy. (Modified from Figure 1. de Vriend et al., 2015).

In the past, civil engineering solutions have been implemented as a means of coastal protection. These solutions involve hard structures such as groynes, seawalls, breakwaters, and surge barriers (van der Meulen et al., 2023). These hard structures have often led to the narrowing of coastal zones, a term referred to as “coastal squeeze”, and a decrease in species biodiversity (Gittman et al. 2016). It is also known that coastal squeeze causes depreciation of coastal habitat (Gittman et al. 2016, Dethier et al., 2017, Powell et al., 2019, van der Meulen et al., 2023). Other

negative effects of hard solutions include a reduction in sediment supply in downdrift sites, which in turn accelerates erosion on the inshore of the barriers. Hard structures that are parallel to the shore reflect wave energy, which leads to deepening of the foreshore and narrowing of the beach to open water (van der Meulen et al., 2023).

In contrast, soft structures are those that incorporate the use of nature, specifically in low energy environments. These soft solutions utilize local materials for coastal adaptation. Solutions which have both hard and soft components are known as hybrid solutions and are often applied in moderate environments (Murphy et al., 2024; Vouk et al., 2021). The inclusion of natural components in infrastructure designs allows for adaptability to changing environments and optimization of ecosystem services (de Vriend et al., 2015). The different types of nature-based solutions (NbS) relevant to coastal systems, that will be addressed in the following sections include but are not limited to sand nourishment and living shorelines, specifically marsh creation.

Different types of Nature-based Infrastructure (NBI) are often preferred in different types of coastal settings.

Sediment-based solutions

Sediment-based solutions are crucial for coastal infrastructure across diverse environments such as estuarine, deltaic, wetland, and open coast areas (Murphy et al., 2024). They harness sediment's resilience against floods and erosion by leveraging natural coastal processes to support plant and biota habitats (Murphy et al., 2024). Sediment-based solutions integrate natural sediment dynamics, engineered structures, and vegetation to improve coastal resilience through dynamic formations like beaches, dunes, berms, and shoals (Davidson-Arnott et al., 2019; Osborne et al., 2024). Unlike static grey infrastructure, sediment-based solutions necessitate larger accommodation spaces and continuous monitoring due to their dynamic nature and reliance on

natural processes (Eyquem et al., 2021, Murphy et al., 2024). They are particularly suitable for sediment-rich coasts and vary in suitability based on sediment type and wave exposure, with coarser sediments fitting best in high-exposure or limited-cross-shore-width areas, and finer sediments in wider cross-shore settings or fine-sediment-dominated coasts (Murphy et al., 2024, Osborne et al., 2024).

Vegetation-based solutions

Vegetation-based solutions are an integral component for coastal flood and erosion risk management (FERM), particularly on coasts with moderate wave exposure or as part of a multi-layered defense strategy, where climate, hydrodynamic, and soil conditions support vegetation growth (van Proosdij et al., 2024, Vouk et al., 2021). These solutions maximize the natural plant's capacities for soil stabilization, wave attenuation, and water quality improvement. They encompass a diverse array of plants—from submerged aquatic vegetation and kelp to tidal wetland species and riparian vegetation—which provide additional benefits like carbon sequestration and habitat creation (van Proosdij et al., 2024).

To implement vegetation-based solutions more effectively, it is essential to match species to specific environmental conditions, including salinity, light availability, sediment composition, and exposure to waves and ice (van Proosdij et al., 2024). Design considerations must account for seasonal variability in plant form and lifecycle, as well as future sea level rise impacts. Vegetation-based solutions can be resilient and adaptive; however, they do require robust monitoring and adaptive management strategies to be implemented throughout their lifecycle to optimize their protective and ecological functions.

1.3.1. Sand nourishment

Nourishment involves the increase in the volume of a beach or nearshore by adding sediment that is similar in size or slightly coarser, from an offsite source, such as a gravel and sand pit or dredge material. Sand nourishments are a common engineering solution that is implemented globally to mitigate coastal erosion. They are a soft solution for coastal protection, as they are considered to be more environmentally friendly and less disruptive compared to traditional hard solutions such as groynes, dykes and seawalls (Brand et al., 2022). Sandy shores are valuable areas of flood safety, tourism, and ecology; however, they are susceptible to erosion evermore so due to sea level rise (Brand et al., 2022, Stronkhorst et al., 2018). Sand nourishments lead to a more resilient coast as they can provide a sufficiently substantial beach to accommodate natural dynamics as well as sea level rise and future climate change (Brand et al., 2022). Nourishment via dredging and placement of sand resources directly on the beach or in the nearshore and shoreface is a method often used to counteract degradation of beaches (Bridges et al., 2015). The goal of nourishments is to slow landward migration of the beach or dune system (Bridges et al., 2015, de Schipper et al., 2021). A vital factor of nourishment is to place the material where the system can naturally redistribute it appropriately. Nourishment design is dependent on many factors such as the local morphology, the regional setting (e.g., proximity of a harbour), rate of erosion, ecological considerations, and stakeholder requests (Brand et al., 2022).

There are four main types of nourishment which are dune nourishment, beach nourishment, shoreface nourishment and channel wall nourishment. Dune nourishments are carried out above the dune foot, while beach nourishments are placed directly in the MKL-zone (MKL-position (Momentane KustLijn, i.e., current coastline) which is used as a proxy to determine the current position of the coastline) (Brand et al., 2022) (*Figure 4*). Shoreface nourishments are carried out

in the lower part of the MLK-zone or below, and channel wall nourishments are placed on the landward side of the channel.

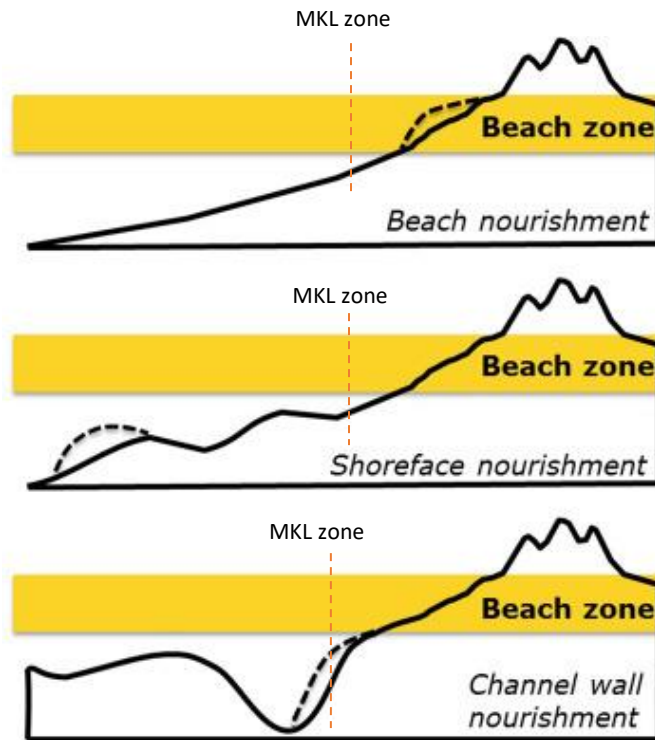


Figure 4. Types of sand nourishment, with the MKL zone (Momentane KustLijn i.e., current coastline) shown in each scenario (modified from Brand et al., 2022).

Sand for projects comes from two sources: offshore and terrestrial quarries such as canals, ports, and borrow pits. Hydraulic pumping or truck haul is used to deposit sand on the beach, then the material is spread over the beach with various types of heavy equipment such as backhoes, graders, and dozers (Fletemeyer et al., 2018). In some cases, the material is allowed to redistribute naturally through longshore sediment transport (Brand et al., 2022).

1.3.2. Living shorelines

Created marshes with ancillary stabilization structures are a type of living shoreline and are valued for their ability to enhance ecological function and promote shoreline stabilization (Mitchell et al., 2019) (Figure 2). While living shorelines are considered as a method to increase community resilience to sea level rise, their resilience under changing climate should also be considered. The

responses to coastal retreat and the implemented methods depend on the site and cost of implementation (Griggs & Patsch, 2019). While coastal armouring such as concrete sea walls or rock revetment, provides some form of shoreline protection, Griggs & Patsch (2019) state that many of the protective structures eventually fail by scour, outflanking or overtopping. When looking at nature-based forms of coastal protection, it is vital to note that not all coastlines are and can be vegetated (Chamber et al., 2021; Currin et al., 2010). For example, the 1760 km exposed outer coast of California, characterised by high energy, has no living green or organic approaches that are capable of significantly reducing the effects of storm waves and high tides (Griggs & Patsch, 2019).

Factors that affect the viability of living shorelines include the design, their setting, and the maintenance provided by humans (Mitchell et al., 2019). The longevity of living shorelines can be attributed to siting. The three main siting factors that influence the persistence of the living shorelines are the wave energy at the site, the potential for upland marsh retreat and the sediment supply. Living shorelines should be designed to minimize wave energy and have the potential for upland marsh retreat (*Figure 5*). Living shorelines will naturally be able to migrate landward if they are built in low elevation areas with no topographic or anthropogenic barrier behind them. It is important to ensure that designs for living shorelines are dynamic. An ideal living shoreline design takes advantage of natural processes that enhance sediment accretion, marsh surface elevation, marsh stability and adaptability (Mitchell et al., 2019; Sutton-Grier et al., 2015).

An integral component of living shoreline sustainability is marsh plantings; the growth of plants is vital for the enhancement of natural marsh processes. Alternative techniques for stabilizing shorelines such as replanting saltmarsh or restoring oyster reefs have been developed by practitioners, researchers, and private sector (Berman et al., 2005; Currin et al., 2010; Gittman

et al., 2016). The plant height and root growth can be maximized by addition of fertilizer to the initial plantings, while plant density can be maximized through denser initial planting or encouraging plant spread. Rock or oyster sill structures can help to achieve edge stabilization. Marsh sills are shore-parallel structures that consist of an offshore low relief mound made of rock or oyster shell called a sill, and an intertidal area between the offshore sill and the upland which contains emergent marsh vegetation. Given sufficient sediment supply and wave reduction capacity, both sediment deposition and accretion can be enhanced by including sills in living shorelines. This can lead to an increase in resilience of living shorelines. The resilience of living shorelines can also be affected by its slope and the way water enters and leaves the marsh. In living shorelines, water access may be through more constricted channels than in natural marshes, leading to changes in inundation periods, sedimentation patterns and plant species distributions. The plants used to vegetate living shorelines are tidal wetland species or other coastal plants such as dune species, as they are adapted to saltwater environments, and other biotic and abiotic conditions of the site (Isdell et al., 2021; Michener et al., 1997).

Ecological services provided by living shorelines include nursery, nesting, feeding habitat, filtering sediments and nutrients from water ways, wave energy reduction, and carbon storage. Recent research has found that various outcomes including the abundance of ecologically and economically important fish and invertebrates, water quality, and erosion control are influenced by the design of living shorelines (e.g., width of marsh and presence of sill) (Bilkovic and Mitchell 2013; La Peyre et al., 2013; Scyphers et al., 2011; Toft et al., 2013).



Figure 5. Types of Shorelines: A) Bulkhead, B) Riprap revetment, C) Sill (Modified from Figure 1. Gittman et al., 2014).

1.4. Ecosystem services

Ecosystems provide a range of services that are of vital importance to human well-being, for health, livelihoods, and survival (deGroot et al., 2012). Ecosystem services are “*the benefits people obtain from ecosystems*” that are complex in structure and function, various in size, and dynamic in time (MEA, 2005; Dasgupta, 2021). Ecosystem services are grouped into three different categories (Figure 6): 1. Provisioning services supply materials and energy, including food, fresh water, fuel, fiber, biochemicals, genetic resources, and ornamental resources. 2. Regulating and maintenance services encompass the regulation and maintenance of ecosystem processes, such as climate regulation, water purification, erosion control, disease regulation, pollination, and protection against natural hazards. 3. Cultural services provide non-material benefits that enhance human well-being through spiritual enrichment, education, recreation, and aesthetic enjoyment. These services are essential for maintaining ecological balance and human health, and their disruption can significantly impact human societies (Dasgupta, 2021).

Ecosystem services depend on ecosystem structures and functions, specifically roles of ecosystem processes that are influenced by biodiversity (Dasgupta, 2021). Ecosystem functions such as primary productivity, soil nutrient retention and resilience against disturbances and invasions, are increased by biodiversity (Constanza et al., 1997, Dasgupta, 2021).

The ability of ecosystems to continuously supply the flow of ecosystem services for present and future generations is threatened by ecosystem degradation and the loss of biodiversity (Brondízio et al, 2019; deGroot et al., 2012; Norström et al., 2022). A changing climate has also led to an alteration on ecosystem services that are critical to coastal communities and livelihoods, creating an urgent need for adaptation and mitigation strategies (Berman et al., 2018; Brondízio). This thesis seeks to quantify following functions of ecosystem services of a salt marsh: (*Table 1*).

Table 1. Ecosystem services and corresponding functions

Category of Ecosystem Services	Ecosystem service	Function
Regulating and Maintenance	Coastal flooding/erosion protection	Wave energy dissipation
	Habitat provision	Vegetation cover Species diversity and abundance Soil nutrient regulation
	Climate regulation	Blue carbon (carbon storage)
	Provisioning	Habitat provision

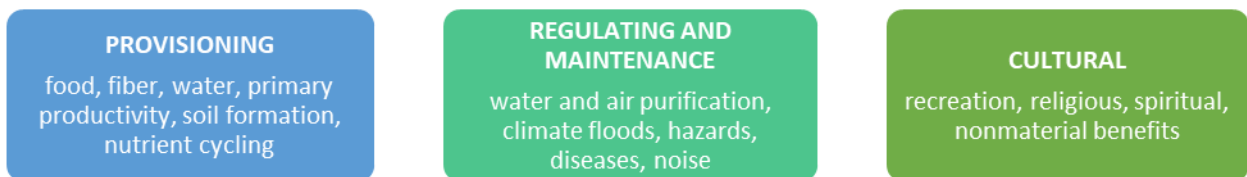


Figure 6. Three different categories of ecosystem services.

1.4.1. Regulating and maintenance

1.4.1.1. Coastal flooding/erosion protection: Wave energy dissipation

Vegetated coastal habitats provide coastal protection, which is a regulating service, involving wave attenuation (decrease in wave height) of wave transmission onshore (Duarte et al., 2013, Neumeier, 2005).). This can be achieved by inducing wave breaking as the main damping mechanism, energy

dissipation through flow separation, porous friction, friction on rough surfaces and producing a barrier effect which reflects energy in the offshore direction (Duarte et al., 2013). Wave energy dissipation is the decrease in wave energy as the wave propagates towards the shore. This can be achieved by wave shoaling/breaking, and by drag from the plant canopy (Möller et al., 2014). Vegetation dissipates waves better with decreasing submergence ratio (Rupprecht, 2017), which is the ratio of water depth to canopy height. Wave energy dissipation also depends on the wave height to water depth ratio (Foster-Martinez et al., 2018; Möller, 2006).

A combination of these mechanisms is also an effective way to attenuate waves. Wave heights can be reduced by seasonal variations in aboveground biomass. A combination of low water depth and high biomass results in wave dissipation (Vuik et al., 2016). This is reflected in the summer, where salt marshes are more effective at decreasing wave heights, in contrast with winter where there is minimal or no vegetation coverage.

Mechanical fragility of vegetation also impacts wave heights (Vuik et al., 2016). Stems often sway or bend at the impact of oncoming waves, and if the waves overpower the stems, breakage can occur. However, studies have shown that even broken stems potentially dissipate wave energy, as they provide a friction surface for the oncoming waves (Leonardi et al., 2019; Möller et al., 2014; Rupprecht et al., 2015; Vuik et al., 2016).

1.4.1.2. Habitat provision: Vegetation cover, species diversity and abundance

Occurring in mid- and high latitudes, and in some tropical areas, salt marshes contain salt-tolerant vegetation which includes grasses, herbs, and small shrubs (Allen & Pye, 1992; Davidson-Arnott et al., 2019). Salt marshes consist of three marsh zones – the low marsh, mid marsh, and high marsh zone, with hydrology having a significant influence on each zone (Davidson-Arnott et al., 2019). The low and mid marsh zones are largely dominated by one or two species, due to the

high stresses in this zone. It is characterized by vegetation which can be submerged on almost every tide, for more than six hours (Allen, 2000; Davidson-Arnott et al., 2019). A decrease in frequency of submersion and depth occurs within the high marsh zone; the vegetation may be submerged briefly during high tides (Davidson-Arnott et al., 2019, Hutchinson, 1982) The high marsh zone has more favorable conditions that allow for a wider range of plants, hence there is a greater species diversity in this zone (Broome et al., 2019; Davidson-Arnott et al., 2019; Dawe et al., 1982; Raposa, 2008).

Salt marshes provide high quality habitat to various species such as invertebrates, fish, birds, and mammals (Broome et al., 2019). Salt marshes also serve as nurseries for fish and crustaceans due to the high production of vascular plant detritus (Broome et al., 2019). The shallow, spatially complex habitats offer protection from predation (Boesch & Turner, 1984).

1.4.1.3. Climate regulation: Blue carbon (carbon storage)

Vegetated coastal ecosystems, particularly tidal marshes, seagrass meadows and mangroves, have exceptional capacities to sequester carbon dioxide (CO₂). They are the most productive habitats on earth, and through photosynthesis fix CO₂ as organic matter, hence removing CO₂ from the atmosphere (Duarte et al., 2005). The term blue carbon refers to the capacity of vegetated coastal ecosystems to store organic carbon (C) in their canopies and soils over centennial to millennial time scales (Nellemann & Corcoran, 2009; Duarte et al., 2013). The capacity of a marsh to sequester carbon is influenced by patterns of belowground production. When the production of belowground root and rhizome material outpaces remineralization, carbon sequestration occurs (Davis et al., 2015, Vaughn et al., 2020).

The high primary productivity of vegetated coastal ecosystems and their ability to efficiently trap sediments and associated carbon from outside their ecosystem boundaries, allow

them to act as natural sinks (blue carbon sinks). These vegetated coastal habitats are efficient at trapping suspended matter and associated organic carbon during tidal inundation. The carbon sequestration rate can increase over time through increased primary productivity or an increase in areal extent. Tidal marshes are highly efficient carbon sinks (Mcleod et al., 2011), as they sequester carbon within underlying sediments, within living biomass aboveground (leaves, stems, branches) and belowground (roots), and within non-living biomass (e.g., litter and dead wood). Blue carbon sequestration that occurs over the short term (decennial) centers on biomass, whereas the long-term sequestration (millennial) centers on time scales in sediments (Mcleod et al., 2011).

Salt marshes account for 46.9 % of the total carbon burial in marine sediments (Duarte et al., 2013). Salt marshes can store carbon for millennia, however if there is a disturbance, the salt marsh sink capacity can be affected (Macreadie et al., 2013). Loss of salt marsh plant material following a disturbance can reduce the particulate carbon trapping capacity which leads to a reduction in carbon stock accumulation (Macreadie et al., 2013). Salt marsh disturbance can also result in a reduction in the overall plant biomass which contributes to carbon capture via photosynthesis. This can reduce the total amount of carbon captured by salt marshes due to the loss of photosynthesis capacity (Macreadie et al., 2013). Plant die-off can be another cause of carbon loss. Erosion, leaching and microbial mineralization could also result in the release of buried ancient sedimentary carbon (Macreadie et al., 2013).

1.4.2. Provisioning

1.4.3. Habitat provision: Primary productivity

The fixation of sunlight by plants and other autotrophic organisms leads to the flow of energy through any ecosystem (Mitsch & Gosselink, 1993). The energy accumulated is known as primary production, and the rate at which this accumulation occurs is known as primary

productivity. Globally, salt marshes have the highest primary productivity. Physical conditions of soil and nutrient availability control the primary productivity of salt marshes (Bertness et al., 2008). Brackish intertidal marshes are productive due to the increased exposure to tidal flow (Mitsch & Gosselink, 1993). Competition, salinity, and degree of waterlogging also play vital roles in regulating primary productivity (Neves et al., 2007). Primary productivity regulates the quality and quantity of most of the ecological services provided by salt marshes (Bertness et al., 2008).

Salt marshes also play a role in the cycling of nutrients in estuaries (Palomo & Niell, 2009). Upon being transported to marshes, inorganic nutrients are transformed to organic compounds through plant uptake and then released as organic and inorganic forms through plant decay and detritus mineralization (Palomo & Niell, 2009). As a result, salt marshes act as sources and sinks of organic matter and nutrients (Palomo & Niell, 2009).

1.5. Rationale and Research Questions

Limited research has been conducted on the sandy coastal ecosystem response to nature-based adaptation methods in a cold climate. While numerous studies have identified living shorelines as protective features that have the capacity to reduce storm surge, wave, and wind impacts to coastal communities (Bridges et al., 2015; Denny et al., 2021; John et al., 2015), there is still a need to further quantify the co-benefits of these nature-based features to improve coastal resilience. Numerous studies have identified ecosystem services provided by natural marshes, but the quantification of these services has been limited. My work focuses on quantifying these ecosystem services to provide quantitative data on both a natural marsh and an anthropogenically modified marsh. Knowledge gap exists on natural marshes which have been anthropogenically altered or modified and whether they have any ecosystem services value, particularly for those that exist in cold regions.

In Canada, the Federal government is undertaking the Census of the Environment, a crucial component that will contribute to a better understanding of the value of salt marsh ecosystem services. The Census of Environment (CoE) aims to establish a comprehensive national register of Canada's ecosystems, including wetlands, coastal areas, and urban forests (CoE, 2024). It seeks to quantify their size, condition, and the ecosystem services they provide. By cataloguing and monitoring these ecosystems over time, the CoE aims to support evidence-based policymaking at all levels of government, inform urban planning, and aid decision-making in various sectors such as industry and agriculture (CoE, 2024). It also intends to help Canadians understand the benefits of ecosystems and their role in achieving sustainability goals, particularly in the context of climate change impacts (CoE, 2024). The CoE will utilize data from various sources, including earth observation and environmental monitoring datasets, and will adhere to international standards to ensure data quality and accessibility. This effort is vital for understanding and preserving the ecosystem services provided by salt marshes (Rabinowitz, 2022). Quantifying these services will help improve the design and implementation of nature-based solutions for coastal resilience.

The Shippagan Gully, located in northeastern New Brunswick's Acadian Peninsula (47.7238749° N, -64.6601559° W), serves as a vital navigation channel between communities in the area and Baie de Chaleurs to the Gulf of Saint Lawrence. Between 1983 and 2017, dredging was periodically conducted, including emergency dredging that inadvertently affected piping plover (*Charadrius melodus*) habitat, leading to the broader Shippagan Gully Dredging and Breakwater project. Over recent decades, sediment accumulation at the inlet mouth has posed hazards for vessel passage (Ellis, 2021). The main objective of the Shippagan Gully Dredging and Breakwater Construction Project was to ensure safe passage for fishing vessels under the mandate of DFO-SCH. While the project did not obtain approval for sea disposal of dredged material, some

of this material was re-purposed to nourish the shoreline and expand tidal wetland habitat, including the construction of a marsh sill. This measure aimed to compensate for habitat loss caused by the project, particularly affecting piping plovers (*Charadrius melodus*) and mitigating impacts on fish and fish habitat (Ellis, 2021).

My work provides preliminary data to establish a baseline, through the quantification of functions of ecosystem services of the anthropogenically modified marsh on the Chiasson Office Spit, pre-restoration. My research will quantify and compare the following functions of ecosystem services: wave energy dissipation, habitat, primary productivity, and blue carbon. Results obtained from the anthropogenically modified marsh will be compared to those of the natural marsh (47.6417910° N, 67.7952839° W), which is located southwest of the Baie de Pokemouche and Pokemouche Gully. (For the purposes of this study, *anthropogenically modified marsh* refers to an existing tidal wetland habitat which has been modified by anthropogenic/human activity including the addition of rip rap sill, and a partially failing wooden seawall) and uncontrolled ATV traffic.

This work will provide empirical data for climate change adaptation and mitigation studies to inform policy making and decisions on coastal protection. A key pathway to adaptation is understanding how these coastal systems function. Providing site-specific data will allow for site-specific adaptation strategies to be put in place.

The research will address the following key questions:

1. Do anthropogenically modified marshes perform functions that support the delivery of ecosystem services (wave energy dissipation, habitat, primary productivity, blue carbon)?
2. How do the functions of ecosystem services of an anthropogenically modified marsh compare to those of a natural marsh?

Chapter 2: Study Area

2.1. Chiasson Office Spit and Shippagan Gully

The Chiasson Spit is a sand spit peninsula located adjacent to the Shippagan Gully and consists of low sand dunes and intertidal saltwater marshes (Figure 7) (CEAA, 2012). The Shippagan Gully is a narrow channel at the mouth of a highly dynamic tidal inlet situated on the Gulf of Saint Lawrence, in Northeast New Brunswick, Canada (Provan et al., 2014). This area has been assessed as having high vulnerability to climate change impacts including storm surge and sea level rise (Cornett et al., 2013; Provan et al., 2013).

The Chiasson barrier spit is 2 km long, and located in a wave-dominated environment, where the process of longshore drift moves sandy sediments in a net southward direction past the Shippagan Gully to the beach in Le Goulet, New Brunswick, Canada. The spit is at risk of erosion partially associated with rising sea levels and increasing storm intensity (CEAA, 2012). The interior is a flat, low intertidal zone with interconnected marshes while the seaward side consists of a low, gently sloping sand beach. The spit is backed by a low foredune ridge and dominated by beachgrasses, while the present wetlands are dominated by *S. alterniflorus* and *S. pumilus* (CEAA, 2012). The drainage along the spit follows the topography and flow to the north towards Shippagan Bay or south towards the Gulf of St. Lawrence (CEAA, 2012).

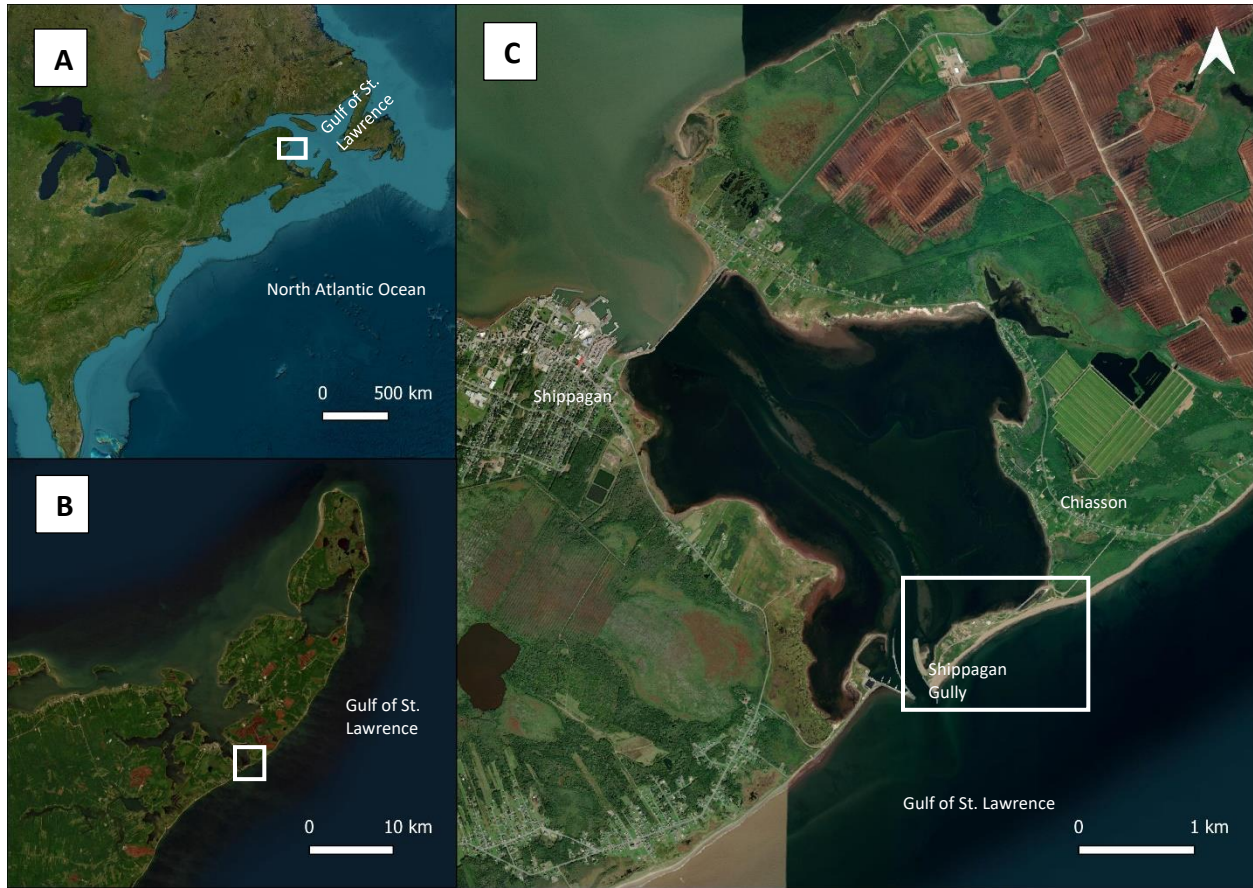


Figure 7. Location of the Shippagan Gully inlet and the Acadian Peninsula near Le Goulet, New Brunswick. A – Eastern Canada; B – Acadian Peninsula, North-eastern New Brunswick; C – Chiasson Office Spit, Shippagan Gully inlet. Site location is shown by white outline.



Figure 8. Study area map, CBWES 2021 Report Baseline interim monitoring report (reprinted with permission from CBWES Inc.).



Figure 9. Images of Study Site (Shippagan), photos taken in August 2022.

2.2. History of the Shippagan Gully

The Shippagan Gully holds a long history of its importance as a navigation channel between communities in the Acadian Peninsula and the Baie des Chaleurs, to the open waters of the Gulf of St Lawrence (Ellis et al., 2021; Provan et al., 2014). It is in understanding the history of the Shippagan gully that one can gain in-depth knowledge on the anthropogenic changes at the Chiasson office site, and how they influence remnant structures – this includes, sediment core profile and the existing vegetation.

The gully is used extensively by the fishing industry and relies on safe navigation through the inlet. The fishing industry supports the local economy servicing both the commercial fishery and recreational users (Ellis et al., 2021; Provan et al., 2014; Provan et al., 2018). Since the 1800s, there have been attempts to control and stabilize the inlet with coastal structures, such as the construction of numerous breakwaters, training walls and sea walls. These man-made coastal structures were also constructed to promote its use as a shipping channel (Provan et al., 2018).

Additionally, pre-construction, the original coastal structures were severely degraded. Between 1998 and 2004, the outer 40 m of the newer east jetty collapsed (Provan et al., 2018). Before 2004, the configuration of structures included a short 25-m-long damaged jetty on the east side of the inlet mouth, a 325-m-long jetty on the west side, and a 600-m-long curved vertical training wall extending northward along the west side of the inlet from the tip of the west jetty (Provan et al., 2018). These modifications impact or disrupt natural coastal processes of sediment transport.



Figure 10. Historical engineering works at Shippagan Gully from the late nineteenth century to the mid-twentieth century (photo taken in 1980) (Provan et al., 2018).



Figure 11. Google Earth Imagery of Shippagan (Google Earth, 2024).

Table 2. Historical works at Shippagan Gully (Table 1, modified from Provan et al., 2018).

Year of project	Scope of work	Reason for construction
1882	Two 300-m-long jetties constructed on either side of the inlet mouth	Attempt to control and stabilize the inlet
Late nineteenth century	Periodic extensions of the east jetty	Jetty extension required as sediment was accumulating on the east (updrift) face and passing into the inlet
1960–1970	New 90 m jetty constructed on the east side of the inlet, parallel to the shoreline that also reduced the inlet width	Try to trap longshore sediment from entering the inlet
1960–1970	Two phase construction of a 600-m-long curved, vertical sheet pile training wall on the west side of the inlet	Attempt to establish a stable, self-scouring navigation channel; a sheltered small craft harbor was also formed between the west jetty and curved training wall
2021	Construction of breakwater at the seaward end of the gully (as shown in <i>Figure 11</i>)	To minimize future maintenance dredging requirements in the channel and a nearby ebb delta
	Shoreline protection/reconfiguration on the eastern side of the channel	To minimize erosion along shoreline
	Dredging of main channel	To increase cross-sectional area of the channel, thus reducing water flow and increasing marine safety.

One of the last major construction installations was a vertical sheet pile breakwater installed in the 1960s and 70s which resulted in the tidal lagoon. Between 1983 and 2017, dredging was frequently undertaken (Ellis et al., 2021; Provan et al., 2018). Natural processes had led to an accumulation of significant volumes of sediment within the inlet mouth which led to an increase in hazards for vessel passage due to the accumulation of significant volumes of sediment within the inlet mouth. Larger vessels were no longer able to safely navigate through the channel and had to

circumnavigate Lamèque and Miscou Islands (CEAA, 2012; Ellis et al., 2021; Provan et al., 2018). The site had complex hydrodynamics due to the effects of coastal structures that were constructed in the past; the high energy environment of the gully and the age of the structure impacted its deterioration (CEAA, 2012). The extensive history of engineering activities at Shippagan Gully led to a complicated morphological structure of the spit (Provan et al., 2018).

The Shippagan lighthouse (Big Shippagan Lighthouse) is located at the end of Domitien Lane on Chiasson Office Spit. The lighthouse commenced operation at the opening of the navigation channel in 1906 and is one of the nine octagonal wooden towers remaining in New Brunswick. In 1924, the lighthouse was remodelled to feature a keeper's dwelling. It still supports a beautiful Barbier, Bernard et Turenne lantern, which is the only one of its kind remaining in the province (Provan et al., 2018). As a result, the Big Shippagan Lighthouse holds sentimental and touristic value, and its removal remains a controversial feature for many locals.



Figure 12. Original Big Shippagan Lighthouse and its replacement (image from Library and Archives Canada).

2.3. Restoration work at the Shippagan Gully

The Shippagan Gully Dredging and Breakwater Construction Project was undertaken to address these navigation issues in 2020. The implemented project addressed the problem by improving and realigning the access road to the Shippagan Gully, land-based dredging, construction of a breakwater and channel realignment. Dredged material that was not used for construction was disposed at two shoreline sites. However, the implementation of the project would result in the destruction of 48,000 m² of Piping Plover (*Charadrius melodus*) critical habitat. To mitigate these adverse impacts, conservation allowances (conservation offsets) were undertaken to compensate for the impact.

2.3.1. Chiasson Office Spit Study Site (SHP)

My research will be focused on Conservation Offset C3 (*Figure 8*), which entails of the extension of Wetland 1 to the Lower Low Water Mean Tide (LLWMT) and the stabilization of marsh toe

using living shoreline techniques (Marsh with sill) and material generated from partial removal of historic dredge spoil as part of Offset I (*Figure 13*). All my research and data were obtained before any interventions or changes were made at Offset C3. Offset C3 is right behind the sea wall and is a disturbed wetland with uneven vegetation cover, and a limited number of species. Offset C3 lies right behind the wooden sea wall or the sea wall footprint; marsh sill and salt marsh plantings will take place as a part of the salt marsh sill creation, as a means of coastal protection and restoration. Restoring the wetland by planting a variety of vegetation species will restore the species biodiversity and the overall primary production, and reduce the impact of oncoming waves, as the presence of vegetation will provide a friction surface. This will improve the overall state of the wetland, with hydrology being restored, an improvement in ecosystem services offered should be notable. Evidently, the hydrology at the study site is impaired. The movement of water at the site is through already existing channels that have developed over time. The presence of the broken-down wooden wall serves as a barrier for a short time before the water can flow through the cracks and openings, and therefore delays the flood tide into the site (*Figure 9*). Under normal conditions, the 1 to 2 m tides enter and exit the site through existing tidal channels. Under severe storm conditions, there are often differences in the flooding patterns at the site.

The anthropogenically modified marsh has a unique species distribution throughout the entire marsh. *S. alterniflorus* and *Sporobolus pumulis* (*S. pumulis*) species were found in the lower and high marsh area, respectively, at the site (SHP). However, due to disturbance, there is a clear uneven distribution of vegetation species at the site.

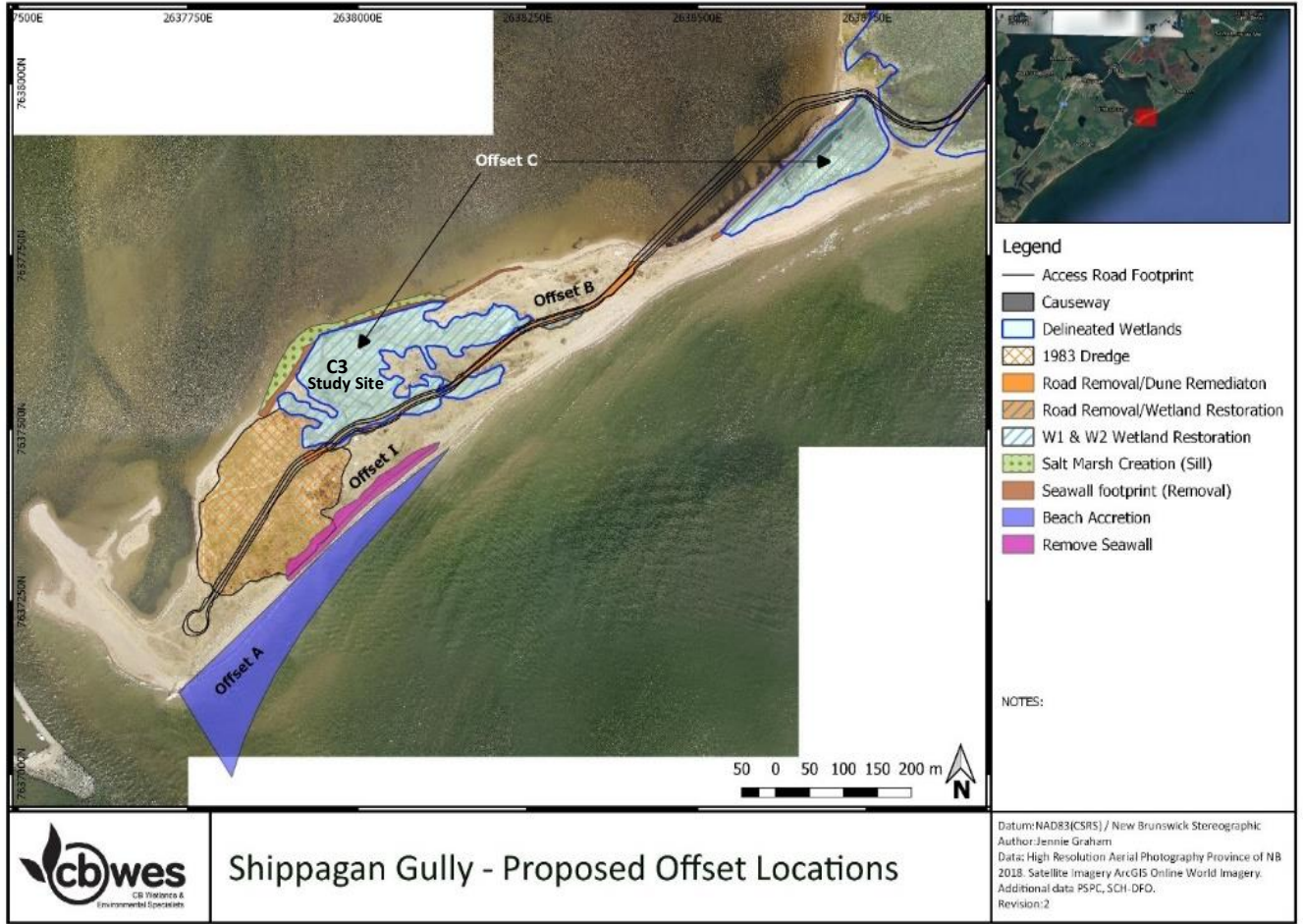


Figure 13. Map of Chiasson Office Spit showing locations of proposed offsets (reprinted with permission from CBWES Inc).

2.4. Reference Site – Baie de Pokemouche

Southwest of the Pokemouche Gully lies the Baie de Pokemouche which is the reference site for my research and for the broader offsetting and monitoring plan. This site was identified based on its proximity to the study site, similar habitat type representation (beach, dune, backshore, wetland), similar geomorphology (barrier spit), limited human impacts, and likelihood that plovers have used the beach in the recent past based on signage and symbolic fencing (string with flagging tape stretched between poles) present during site visit (pers. obs., July 2020).

The natural salt marsh (SHP_R) has a variety of plant species. Similar to the study site, SHP, the reference site (SHP_R) has *S. alterniflorus* and *S. pumilus* as the dominant species in the low and high marsh areas, respectively. Contrary to the Study Site, the Reference Site, is a fully vegetated salt marsh with functional hydrology which is a key driver for salt marsh processes. Other dominant species which can be found at the Reference Site are *Juncus gerardii*, *Lysimachia maritima* and *Hordeum jubatum*, which are species that are found in a healthy salt marsh environment.

The tidal range at the SHP_R is between 1 and 2 m, with the low marsh areas being inundated all year round, as they are lower in elevation. The high marsh areas are often inundated when there is a storm surge and high tide.

A single reference site was selected based on regional restoration monitoring standards (e.g., GPAC protocol; Neckles and Dionne, 2000). There are other similar sites in the region, however due to the increased distance from the study site, a greater difference is expected, which decreases representativeness.



Figure 14. Images of Reference Site (SHP_R), photos taken in August 2022.

2.5. Climate at the Chiasson Office Spit and at the Baie de Pokemouche

Canadian Climate Normals (1981-2010) for the Bathurst climate station (47°37'45.050''N and -65°44'54.020''W), the station located closest to the study and reference sites, indicate a mean annual temperature of 4.8°C with extremes ranging from -35.6°C to 37.4°C. Measurable precipitation per year is approximately 1110.1 mm. Extreme daily precipitation of up to 96.3 mm has been recorded (Environment Canada, 2015a) (*Figure 15*). The wind is generally from the south

or west based on wind-rose diagrams generated from the weather station located on the Chiasson Office Spit and those generated for the Lamèque area, (météoblue.com, nd). (Figure 15).

On dry, windy days, fine particulate matter can be created due to the surrounding industrial peat bog harvesting operations proximal to the study and reference sites.

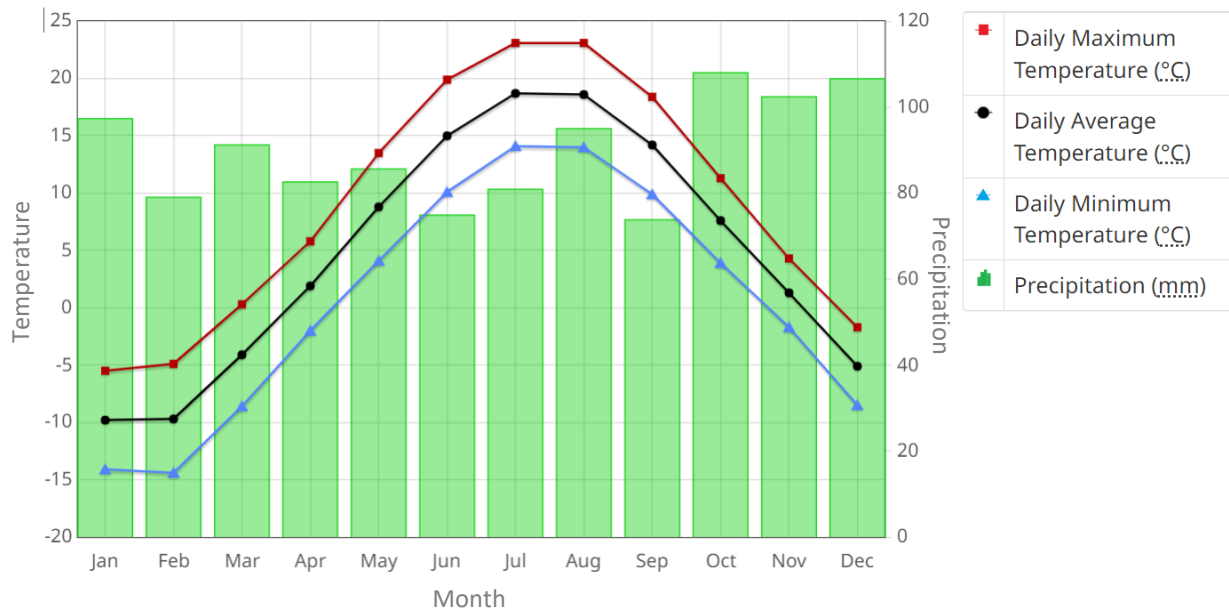


Figure 15. Temperature and Precipitation Graph for 1981 to 2010 Canadian Climate Normals, Shippagan, New Brunswick.

An Automatic Weather Station (AWS) was installed near the Shippagan Lighthouse (AWS geographical coordinates: 47.720402 N and -64.662873 W). The Ultrasonic Wind Speed and Direction Smart Sensor record wind direction and speed at the Shippagan site. The wind direction accuracy is ± 4 degrees of 0.2 to $3 \text{ m}\cdot\text{s}^{-1}$ and ± 2 degrees of $>3 \text{ m}\cdot\text{s}^{-1}$, whilst the wind speeds that can be measured are as low as $0.4 \text{ m}\cdot\text{s}^{-1}$. Data recorded between May 2022 and January 2023, were plotted using a rose diagram (Figure 16). These data were stored at an interval of 5 minutes. Based on the figure, the dominant wind direction is NW and SW, with maximum speed winds from NW greater than $16 \text{ m}\cdot\text{s}^{-1}$. However, in the winter, the prevailing wind direction shifted to NE.

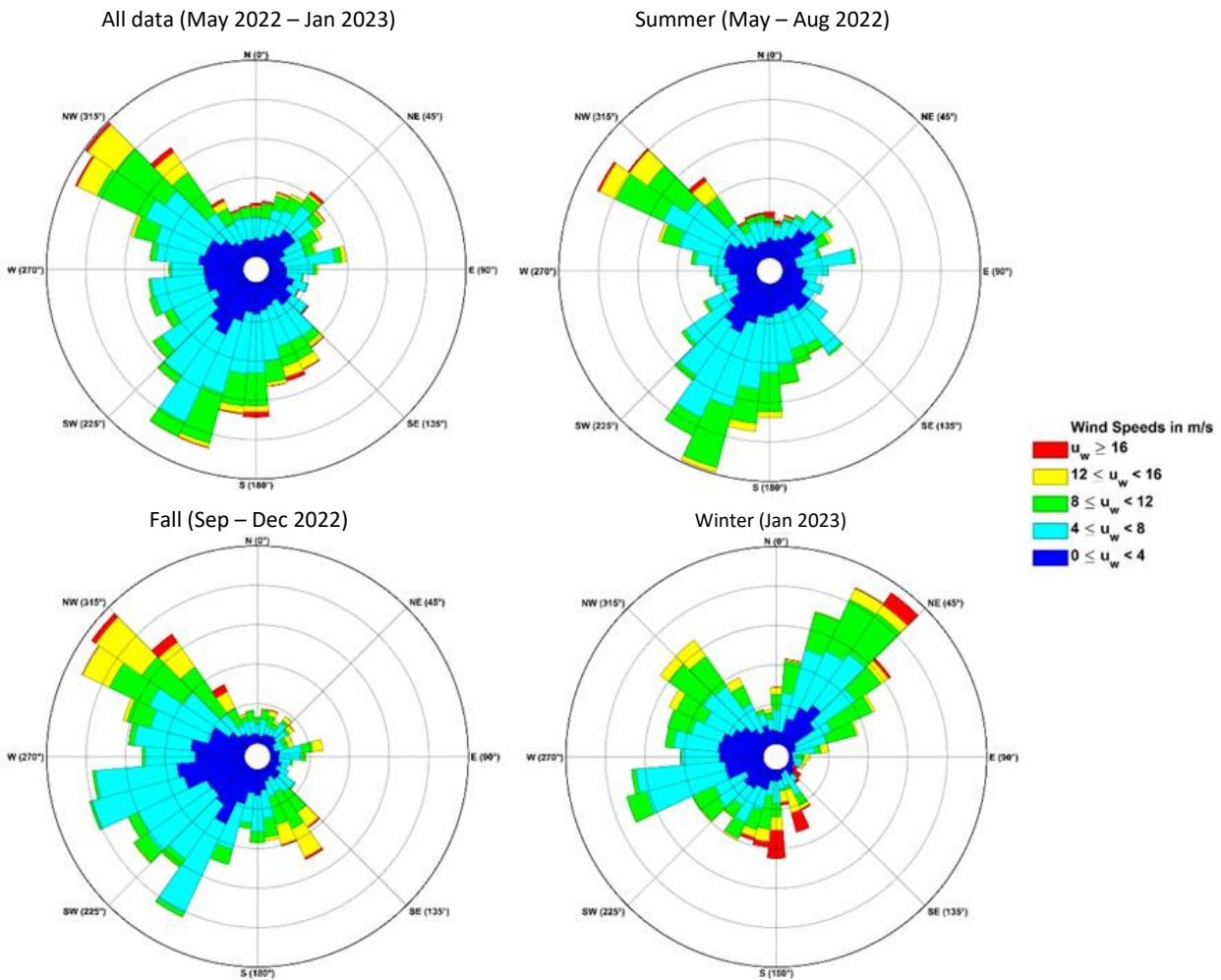


Figure 16. Wind Rose diagram represents the wind speed and direction in the Shippagan region. (May 2022 to January 2023), based on the meteorological data collected on site at the Chiasson Office Spit, via the TransCoastal Adaptations weather station.

2.6. Hydrodynamic processes

The Shippagan Gully transects the Acadian Peninsula and is influenced by tidal forcing from the Gulf of Saint Lawrence and the Bay de Chaleurs. As a result, the tidal flows through the inlet were driven by the phase lag between tides of the Gulf of St. Lawrence and the Baie de Chaleurs. The hydrodynamic and sedimentary processes that occur in the Shippagan Gully are affected by its unique phase-lag in the tidal cycle. The tidal range at the site is between 1 and 2 m. The phase-lag generated is due to the Gully's tidal lagoon which bisects the Acadian Peninsula and is open to the sea at two locations (*Figure 7*). Ebb flows through the Shippagan Gully are known to exceed 2

$\text{m}\cdot\text{s}^{-1}$, which is approximately twice as strong as the velocities of the flood stage (Provan et al., 2014). The Shippagan Gully is a micro-tidal system, with a tidal range of 2 m or less; its tides are mixed semi-diurnal (Provan et al., 2014).

Chapter 3: Methodology

In this research, two of the three categories of ecosystem services were assessed: 1. Regulating and maintenance and 2. Provisioning. In the following sections, we will look at the methods used to quantify each of the corresponding variables which are: wave energy dissipation, habitat, primary productivity, and blue carbon.

3.1. Wave energy dissipation

Following the method outlined in Vuik et al., 2016, modified by Ngulube, 2021 – RBRduet³ T.D|wave16 — temperature and pressure sensors (wave loggers) were deployed at each site in a transect. A 30 m – long transect was set up at the Shippagan Study site (SHP). Instruments were spaced out at 15, 22 and 30 m from the open water, respectively as shown in the figure below. A shorter transect of 10 m was set up at the reference site (SHP_R). Instruments were spaced out at 3, 5, and 10 m from the open water, respectively. The difference in spacing at both sites was due to the impact of relict structures at the study site (SHP). The first instrument (RBR 1) is important as it serves as a reference point for wave energy dissipation calculations throughout the duration of the deployment. Past studies also provided further guidance on how to set up the transect, and how waves are dissipated over shorter distances or within a small area (Ngulube, 2021). The instruments were deployed over a duration of four months from August 14 to November 9, 2022. This deployment was carried out over a range of 2 Spring and Neap tides, hence focusing on these 2 cycles.

At both sites, the wave loggers were deployed in the same configuration, and the elevation heights were determined using a Leica GS14 Antenna RTK (Horizontal datum: NAD83 (CSRS) UTM Zone 20N, mean measurement accuracy = 7 mm; vertical datum: CGVD2013, mean measurement accuracy = 11 mm) (instrument coordinates are provided in the Appendix). The wave loggers were

programmed to record the pressure with a frequency of 4 Hz over a period of 8.5 minutes, every 10 minutes. This means that every burst contains 2048 samples. The measured pressure is the result of atmospheric pressure, the hydrostatic pressure, and the dynamic wave pressure (Vuik et al., 2016) (The Ruskin software allows for input for compensation of atmospheric concentration). The pressure sensors were mounted 0.05 m above the sediment surface. Below are some of the wave equations that the software used to generate existing parameters:

Equation 1

$$f = 1/T$$

Where f is the frequency, and T is the period.

Equation 2

$$\frac{H}{H_0} = \frac{1}{1 + \beta x}$$

Where H is the wave height recorded at the end of the transect, while H_0 is the wave height recorded at the beginning of the transect by the logger in the open water, and x is the distance between the two measurements.

To calculate the attenuation percentage, the following formula was used:

Equation 3

$$\% \text{ attenuation} = 1 - \frac{H}{H_0}$$

Vegetation attenuates wave energy via plants on the water column. Where vegetation is submerged entirely throughout the water column, and water depths are shallow, a higher attenuation percentage is expected (Garzon et al., 2019, Möller, 2006). The work done by plants on the water column is proportional to the drag force that acts on the vegetation, which is roughly proportional to the orbital velocity squared (neglecting the plant motion). As a result, energy dissipation is roughly proportional to the wave height cubed. To estimate the spatial dissipation of waves across a flat, rigid vegetation field, the following formula is used:

Equation 2

$$\frac{H}{H_0} = \frac{1}{1 + \beta x}$$

Equation 4

$$\beta = \frac{4}{9\pi} C_D b_V N H_0 k \frac{\sin h^3(k\alpha h) + 3 \sin h(k\alpha h)}{(\sin h(2kh) + 2kh) \sin h(kh)}$$

where H is the wave height [m], H_0 is the incident wave height [m], x is the horizontal coordinate [m], β is the energy dissipation coefficient, C_D is the drag coefficient [-], b_V is the plant area per unit height [m²], N is the number of plants per unit area [-], α is the submergence ratio ($\alpha = hv/h$) [-], h is the water depth [m], hv is the plant height [m], k is the wave number ($k = 2\pi/L$) [m⁻¹], and L is the wavelength [m]. These equations show how important plants are in dictating dissipation.

To understand the changes in maximum wave heights along each transect and over time, figures were created to illustrate the maximum wave heights of all four instruments at the study and reference sites (SHP and SHP_R) throughout the duration of the experiment (August 16 –

November 9, 2022). The maximum wave height recorded by each instrument at each location was recorded. The Ruskin software accounted for removal of the tidal signal and atmospheric pressure. The results obtained from the wave logger deployments were analysed to assess the wave energy dissipation throughout the duration of the research for three events that were selected. These events were chosen based on peaks that were higher than the average calculated maximum wave height. A script was created to calculate the maximum water depth over the marsh platform, the average wave height reduction, and the exponential wave decay constant.



Figure 17. 4 RBRduet³ T.D/wave16 — temperature and pressure sensors deployed along a 30 m transect at the study site (SHP); (HHWLT - The average of the highest high waters, 1 from each of 19 years of predictions, from Shippagan Gully CHS station).

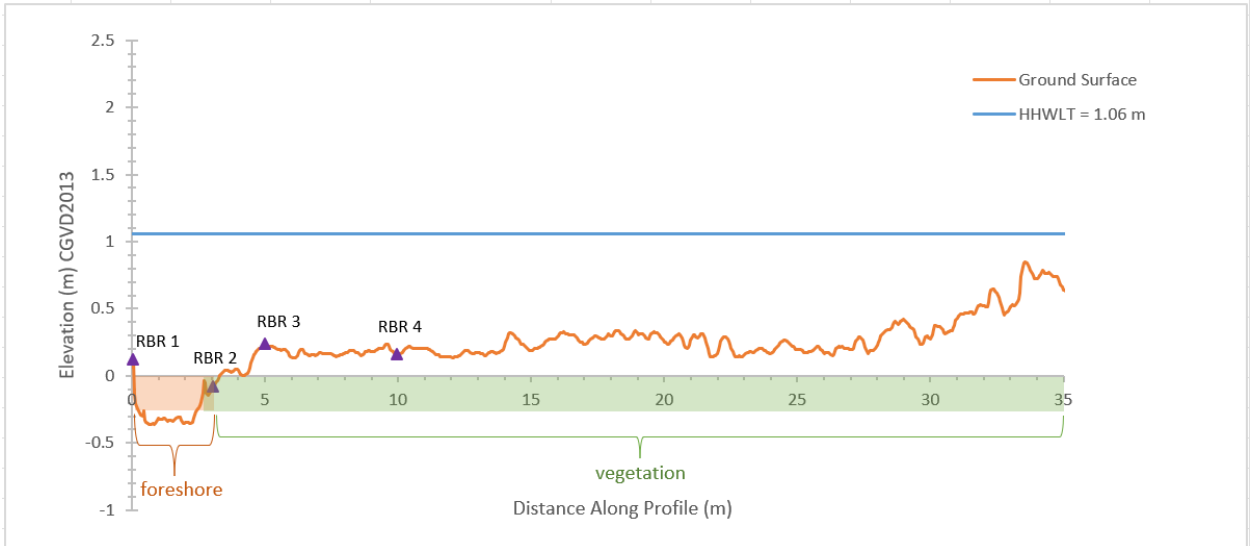


Figure 18. 4 RBRduet³ T.D/wave16 — temperature and pressure sensors deployed along a 10 m transect at the reference site (SHP_R); (HHWLT - The average of the highest high waters, 1 from each of 19 years of predictions, from Shippagan CHS station).

3.1.1. Vegetation surveys for wave analysis

Vegetation data for wave analysis were obtained by counting the number of stems and measuring the stem height at all RBR wave logger stations. Each RBR wave logger station consisted of a 0.6 m x 0.2 m plot - the stem heights were measured using a 1 m rule, while the stems were physically counted by hand to determine the total number of stems within each plot. The stem density was derived by calculating the number of stems per square metre within each plot.

Additionally, vegetation data were obtained using digital side-on photographs as shown in Figure 19. Digital side-on photographs of a 0.6 m wide and 0.2 m deep strip of vegetation were taken against a red background plate (this provided maximum colour contrast against the brown to green tones of the vegetation) (Möller et al., 2006). The portable digital frame design was modified to suit the conditions of the study and reference sites. A light wood frame was used to flatten the vegetation rather than a steel frame to avoid stem breakage along the transect. The hard plastic board was replaced with a plaskolite (general-purpose acrylic sheet) to avoid excessive bending and folding of stems.

The digital images captured were classified into binary black (vegetation) and white (background) images using the ArcGIS software and output as binary matrix files for further quantitative analysis. A supervised classification was performed on each of the images obtained per station per site, throughout the duration of the study. Images were obtained only during the August and September surveys because both sites were too windy during the November survey.

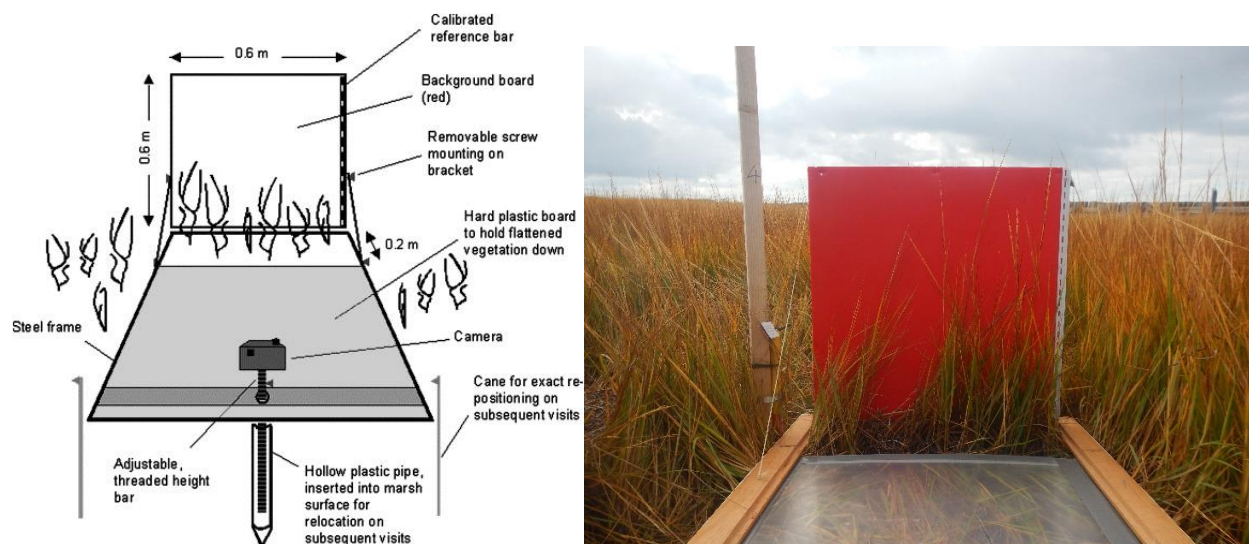


Figure 19. Portable digital photograph frame used to capture side-on photographs of marsh vegetation. Left: (From Figure 2. Möller et al., 2006), Right: (Re-designed by Ngulube, 2022).

Upon performing the supervised classification, the area of vegetation versus the background was calculated in the ArcGIS software (*Table 7*). The area of vegetation was compared to the dry biomass at each station.



Figure 20. Schematic diagram illustrating how to derive obscuration ratio (black pixel coverage (%) of image) and canopy height from field image, to classified image and classified binary black and white image.

Vegetation species in salt marshes exist due to a wide range of abiotic factors such as hydrology, salinity, wrack deposition, edaphic factors, topography and the presence or lack of ice thereof (Broome et al., 1988; Chang et al., 2016; Desplanque and Mossman, 2004; Lyon and Lyon, 2011). Physical stresses and the tolerance and competitive ability of vegetation species lead to the formation of zones within a salt marsh (Anastasiou and Brooks, 2003; Batzer and Baldwin, 2012; Pennings et al., 2005; Porter et al., 2015).

3.2.1. Vegetation Surveys

Vegetation surveys were carried out at each site. A species list was created and used for reference during vegetation surveys. Using the stratified random sampling approach, 25 vegetation plots were surveyed at each site within monitoring quadrats (1 m²). Quadrats were spaced randomly using the visual method and based on the marsh zone. Marsh zones were established based on the vegetation species and the elevation difference as one advances from the shoreline to the high

marsh (the shoreline zone had seven plots, the low marsh zone had eight plots and the mid to high marsh zone had ten plots). The percent cover by species was measured using the point intercept method (Peet et al., 1988). The stem height of the observed species was recorded.

3.2.1.1 Statistical Methods

Plot percent cover and species richness were compared graphically across the study site and the reference site. Abundance data were point count frequencies taken within each plot (out of 25 possible points, multiplied by 4 to generate a % cover index); frequency data were the number of plots a species was encountered at within a site (Ellenberg and Mueller-Dombois, D, 1974). The Welch Two Sample t-test was applied to species grouped by site in R 4.1.2 (R core team 2021). The species that were compared were the top two dominant species: *Sporobolus alterniflous* and *Sporobolus pumilus*. A 2-way ANOVA test was conducted on the 25 vegetation plots at each site, per marsh zone (shoreline, low marsh and mid to high-marsh).

3.2.2. Soil Nutrient Analysis

Sediment cores were collected corresponding to each vegetation plot and subsampled at two different intervals, 0 – 15, and 15 – 50 cm. The samples were sent for processing at the PEI Analytical Laboratory. Mineral and nutrients in the soil were determined for each sub-sample. The nutrients in the soil were determined by ICP-OES using Mehlich 3 Extraction (Modified Laboratory Manual of Methods, Standards and Equipment, Section 5.0, 1996, Nutrients in Soil by Inductively Coupled Argon Plasma). The Carbon and Nitrogen in the soil was determined by combustion analysis using Leco CN828, Leco Form No. 203-821-627, 3/21-REV0. The salt content was determined by using a conductivity meter and measuring the electrical conductivity. The protocols and procedures for soil nutrient analysis were carried out at the PEI Analytical Laboratory.

3.2.2.1 Statistical Methods

A two-way ANOVA with crossed zone*site factors test was performed to analyze the changes in soil nutrients as we advance along the marsh from the shoreline to low marsh, to mid to high marsh areas.

3.3. Primary Productivity

3.3.1. Aboveground Biomass Sampling

The primary productivity by vegetation consisted of aboveground biomass sampling. Aboveground biomass was harvested at selected plots, by clipping vegetation at the sediment surface (Darby & Turner, 2008). Aboveground biomass was sampled, rather than belowground biomass because belowground biomass is a more destructive method to the marsh area. The biomass was harvested within a 0.2 m x 1m area of the quadrat. All standing live and dead culms and litter were removed and placed into pre-labeled plastic bags. The biomass bags were transported to the laboratory at Saint Mary's University, Halifax, NS for processing. The biomass was dried in a Fischerbrand Isotemp oven at 60°C for approximately 72 hours, then weighed to the nearest 0.01 g to determine the annual net primary production (Darby & Turner, 2008).



Figure 21. Vegetation plot layout and 30 m wave logger transect at the Study Site, Chiasson Office Spit, New Brunswick (MS = Marsh Sill, SW = Sea Wall, W = Wetland).

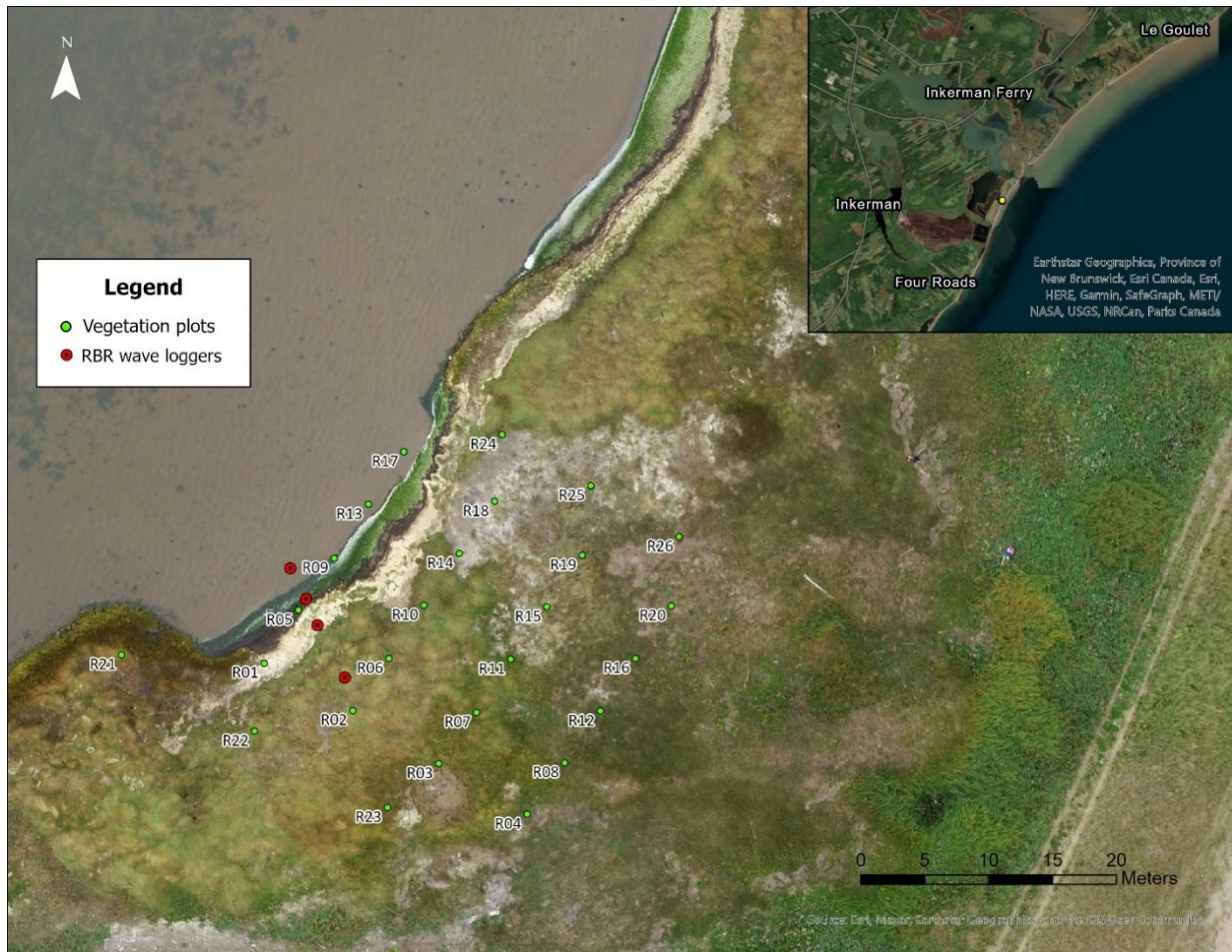


Figure 22. Vegetation plot layout and 10 m wave logger transect at the Reference site, Boudreau Channel, New Brunswick.

3.4. Blue carbon

3.4.1. Field sampling procedure

Sediment cores were collected corresponding to the vegetation plots, 1 m away from each vegetation plot in a linear direction. Sediment cores were collected from shoreline, low marsh, to mid to high marsh plots, to characterize variability across the transition of marsh zones along each transect. The shoreline, low marsh and, mid- to high marsh zones were differentiated through vegetation surveys at each coring plot. The shoreline zone had five plots, the low marsh zone had eight plots and the mid to high marsh zone had eight plots.

Prior to coring, any vegetation and litter found on the soil surface was removed from the soil surface before collecting the core. A 75-cm long PVC pipe was slowly inserted into the ground at a 50 cm depth, ensuring that the core remained vertical. Before retrieving the core, the distance between the top of the core (inside the PVC pipe) and the soil surface (outside the PVC) was measured using a ruler to determine compaction of the core (Howard et al., 2014). Using a rubber stopper to create suction, the PVC pipe was sealed and carefully pulled out of the ground. The top and bottom of the pipe were labeled, and the core identity were recorded. A total 21 cores were collected at each site and transported to the lab for storage. The cores were refrigerated at 4°C to minimize microbial activity. The cores were subsampled in the lab at 0 – 5, 5 – 15, 15 – 30 and 30 – 50 cm. Another set of increments were 0 – 5, 5 – 10, 10 – 15, 15 – 20, 20 – 25, 25 – 30, 30 – 35, 35 – 40, 40 – 45, 45 – 50 cm, in preparation for Bulk density, Loss on Ignition and Elemental Analysis procedures. These increments were chosen to assess the variation with depth.

Key	
shore	shoreline
low	low marsh
mid to high	high marsh

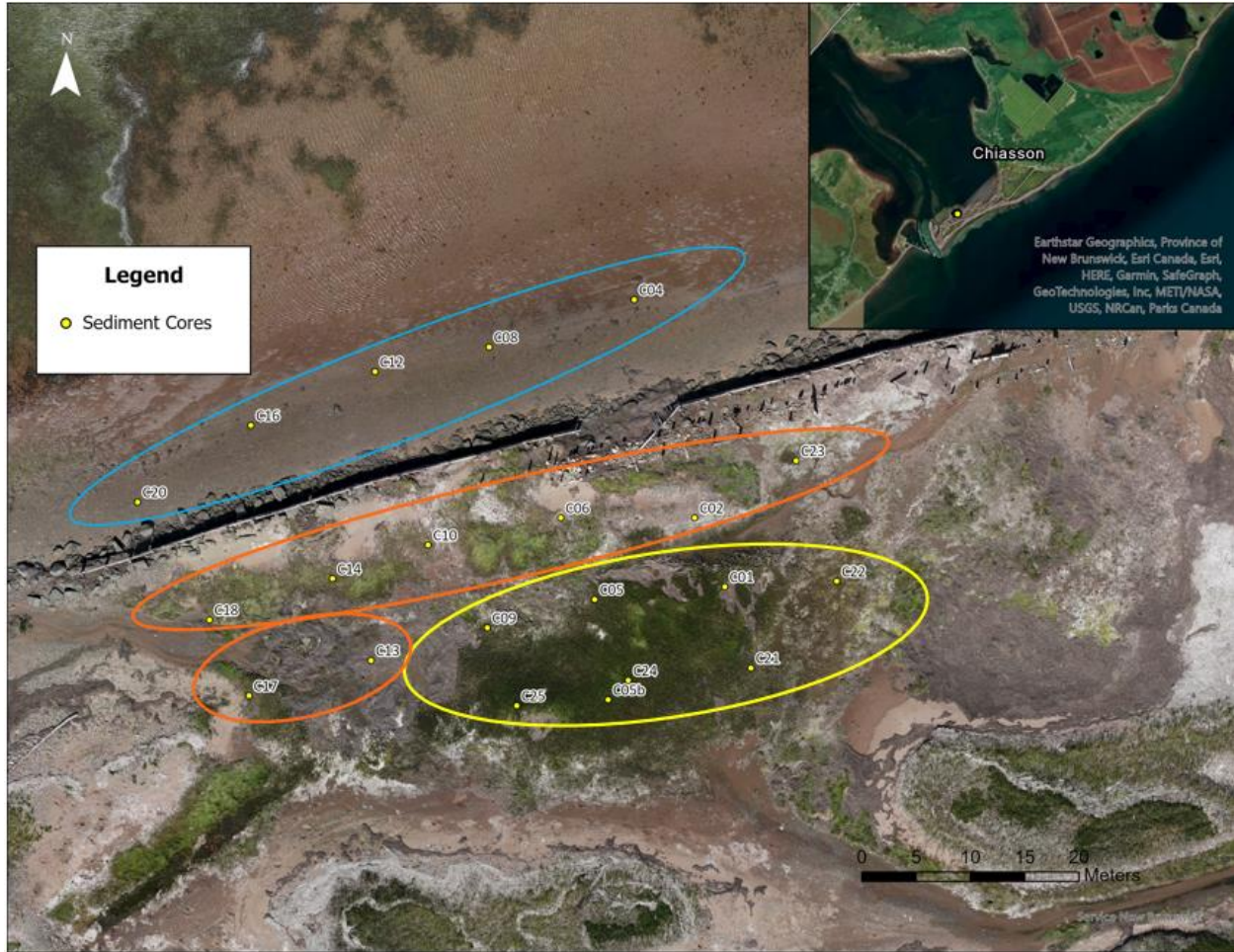


Figure 23. Layout map showing where sediment cores were collected at the study site, Chiasson Office.



Figure 24. Layout map showing where sediment cores were collected at the reference site, Boudreau Channel, New Brunswick.

3.4.2. Sediment Core Analysis - Laboratory Analysis

The Soil Organic Carbon (SOC) was determined using the three variables: bulk density, organic matter (OM) content, and % OC via elemental analysis (EA). The Bulk density is obtained from a known volume of dry soil, which is the dry weight of soil per unit volume (Mitsch & Gosselink, 2015). The Loss on ignition is a measurement of % OM in a soil sample, which is obtained by

heating a sample in a muffle furnace and weighing the before and after to determine the amount of material combusted (Howard et al., 2014). Elemental analysis is a direct measure of C in a soil sample and LOI (% OM) can be converted to % OC using a conversion equation developed by comparing estimates of OC via LOI to OC measured using an elemental analyzer (Craft et al., 1991; Howard et al., 2014).

Bulk density samples for each core were extracted from the centre of each increment, by cutting a circular disc from the mid-point of each sample. The volume of each extracted piece was calculated:

Equation 5

$$(V = \pi r^2 h)$$

where π is 3.14, r is 2.5 cm and h is 2 cm.

The samples were oven-dried in metal tins at $\sim 60^\circ\text{C}$ for 48 to 72 hours until a consistent weight was reached (Howard et al., 2014). To prevent any loss of soil organic matter (oxidation), that may occur at higher temperatures, samples were dried at 60°C (Howard et al., 2014). When the samples reached a stable weight, the mass of the sample, and volume were used to determine Dry Bulk Density (DBD).

Using the following equation, bulk density was calculated, where $1\text{ mL} = 1\text{ cm}^3$:

Equation 6

$$\text{Dry Bulk Density (g/ml)} = \text{net dry weight at } 60^\circ\text{C} / \text{volume (ml)}$$



Figure 25. Bulk density disc cut out of sediment core sample

When correcting for inorganic C content in samples, it is important to consider that higher temperatures (>500 °C) will result in the loss of water and CO₂ derived from inorganic C (e.g. calcium carbonate, CaCO₃, from shells) (Howard et al. 2014). If the samples have inorganic C, then the loss in weight is the total loss in both organic and inorganic carbon (total carbon – TC) (Howard et al., 2014).

For both LOI and elemental analysis (EA), the dried bulk density samples were used, as enough sample was obtained. These samples were dried and ground with a mortar and pestle prior to the LOI and EA procedures. Any large items such as stones and twigs were removed, and large clumps were broken up using a spatula. The mortar and pestle were cleaned with ethanol between each soil sample to reduce chances of cross-contamination (Howard et al., 2014).



Figure 26. Grinding and homogenization of soil sample with mortar and pestle.

When the samples had been ground, they were combusted in a muffle furnace for 4 hours at a temperature of 550 °C, and weighed to calculate LOI, to quantify the fraction of organic carbon lost (Howard et al., 2014):

Equation 7

$$\%LOI = (D_{wi} - D_{wf} / D_{wi}) * 100$$

Where D_{wi} is the initial dry weight and D_{wf} is the dry weight after combustion.

LOI represents the loss of organic matter, which is comprised of carbon, hydrogen, nitrogen, oxygen, sulfur etc., and not solely the loss of organic carbon. Therefore, elemental analysis was completed at the Dalhousie University Steele Oceans Building. Analysis for Carbon and Nitrogen content was determined by an Elementar MicroCube. The procedures and protocols for processing were carried out by the Canada Excellence Research Chairs (CERC) Ocean Lab, located at the Dalhousie University Steele Oceans Building. The samples were packed in tin capsules. The Vario

MicroCube is configured to run in CN mode and calibrated to obtain %C and %N. The technique consists of flash combusting samples at 1000 °C, reducing nitrogen and carbon compounds to N₂ and CO₂ products and separating the different elements with a temperature programmed desorption trap. The Elementar MicroCube determines the total carbon content of a sample, including organic and inorganic carbon, therefore, the inorganic carbon must be determined separately.

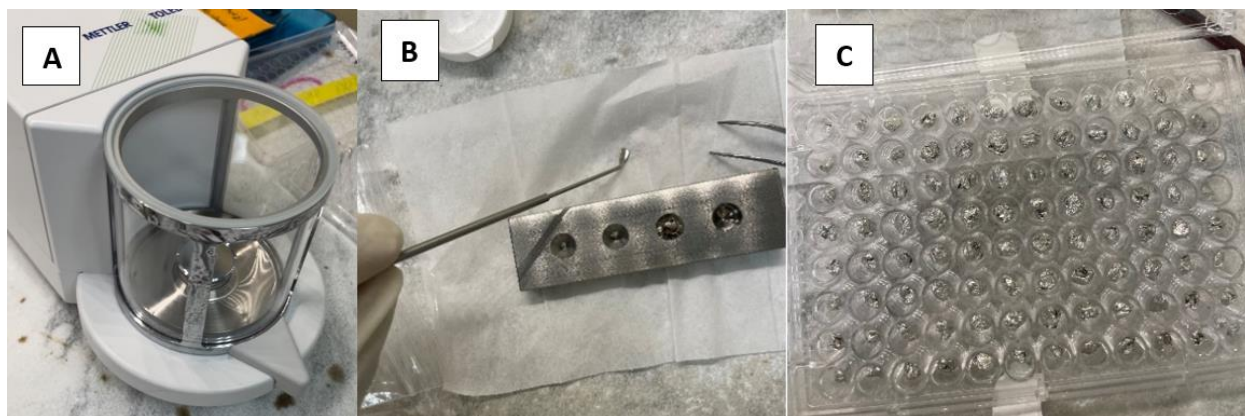


Figure 27. A. Scale used to measure sample weights, B. Capsule holder and forceps for compressing capsule, C. Compressed capsules containing sample for EA.

Coastal soils containing shells and pieces of coral are known to contain inorganic carbon in the form of carbonates such as calcium carbonate. Some mineral-rich soils found beneath layers of peat can also contain calcium carbonate (Howard et al., 2014).

A subset of the samples was acid-washed to remove inorganic C, which was essential in determining an inorganic C correction factor (TC/TOC) (Mossman et al., 2022). The process of acidification involved volatilizing inorganic carbon to CO₂. The soil subsample was treated with 10% Hydrochloric acid, rinsed twice with MilliQ water (centrifuged, decanted). The sediment samples were frozen before freeze-drying. The sediment samples were packed in tin capsules. Similar to the total carbon samples processing, the Vario Micro Cube was configured to run in CN mode and calibrated to obtain %C and %N. This technique consists of flash combusting samples at 1000 °C, reducing nitrogen and carbon compounds to N₂ and CO₂ products and separating the

different elements with a temperature programmed desorption trap. These different gaseous compounds are then carried by ultrapure helium to the thermos conductivity detector (TCD) to determine %C and %N.

Inorganic carbon content was estimated from the difference in weight of the subsample before and after treatment. Reactions with more dilute acids over a longer time frame minimize the loss of organic carbon due to composition, as there is often a risk that some organic carbon will also be removed during acidification (Howard et al., 2014, Pilskaln and Paduan, 1992, Weliky et al., 1983). To determine the organic carbon content, the inorganic carbon content is subtracted from the total carbon content. Once corrected for inorganic C, values of % C obtained via EA were considered %OC for the purposes of this study.

3.4.3. Carbon Stocks

To estimate the carbon, I initially measured carbon stocks in all cores at each site (n = 21 at the study site – SHP, n = 20 at the reference site – SHP_R). These measurements were scaled up to estimate the amount of carbon per hectare (Mg C/ha) in the low, mid, and high marsh zones at each site.

3.4.3.1. Statistical Analysis

Statistics were carried out where a 2-way ANOVA with crossed zone*site factors test was used. (A two-way ANOVA is used to determine whether there is a statistically significant difference between means of three or more independent groups that have been split on two variables). A two-way ANOVA test was performed to analyze the changes in carbon as we advance along the marsh from the shoreline to low marsh, to mid to high marsh areas. Another two-way ANOVA test was also performed to analyze the organic carbon changes along the marsh.

3.5. Grain Size Analysis

Sediment samples were dried at 105 °C in a Fischerbrand Isotemp oven for 24 hours and later placed in a desiccant cabinet for an hour to ensure that there was no moisture present. The dry sieving method was used, as samples were coarse (Blott and Pye, 2001). Dry sieves were prepared in order, with the largest sieve size at the top of the stack and the stack was placed into the shaker table. Each 100g subsample was placed into the stack at the top and spread evenly, and each sample was run for 10 minutes. Afterwards, each sieve was emptied completely into the container for weighing and record the weights of contents from each sieve.

3.5.1. Statistical Analysis

The statistical analysis was carried out in Microsoft Excel spreadsheet, which allows both tabular and graphical output (Blott and Pye, 2001). The values were input as a percentage of sediment present in several size fractions - this was the weight retained on a series of sieves. The sample statistics that were calculated are: mean, mode(s), sorting (standard deviation), skewness, and kurtosis.

Table 3. Sample statistics used for grain size analysis (modified from Blott & Pye, 2001)

Sorting (σ_1)		Skewness (Sk_1)		Kurtosis (K_G)	
Very well sorted	<0.35	Very fine skewed	+0.3 to +1.0	Very platykurtic	<0.67
Well sorted	0.35–0.50	Fine skewed	+0.1 to +0.3	Platykurtic	0.67–0.90
Moderately well sorted	0.50–0.70	Symmetrical	+0.1 to -0.1	Mesokurtic	0.90–1.11
Moderately sorted	0.70–1.00	Coarse skewed	-0.1 to -0.3	Leptokurtic	1.11–1.50
Poorly sorted	1.00–2.00	Very coarse skewed	-0.3 to -1.0	Very leptokurtic	1.50–3.00
Very poorly sorted	2.00–4.00			Extremely leptokurtic	>3.00
Extremely poorly sorted	>4.00				

Mean	Standard deviation	Skewness	Kurtosis
$M_z = \frac{\phi_{16} + \phi_{50} + \phi_{84}}{3}$	$\sigma_1 = \frac{\phi_{84} - \phi_{16}}{4} + \frac{\phi_{95} - \phi_5}{6.6}$	$Sk_1 = \frac{\phi_{16} + \phi_{84} - 2\phi_{50}}{2(\phi_{84} - \phi_{16})} + \frac{\phi_5 + \phi_{95} - 2\phi_{50}}{2(\phi_{95} - \phi_5)}$	$K_G = \frac{\phi_{95} - \phi_5}{2.44(\phi_{75} - \phi_{25})}$

Chapter 4: Results

This research quantified variables associated with four ecosystem services: wave energy dissipation, habitat, primary productivity, and blue carbon. The results from the study were consolidated and statistically analyzed to assess for trends or patterns at both the reference site and the study site.

Table 4. Measured parameters for each ecosystem service variable.

Variable	Parameter
Wave energy dissipation	<ul style="list-style-type: none">▪ Maximum wave height
Habitat	<ul style="list-style-type: none">▪ Vegetation species▪ Soil nutrients
Primary productivity	<ul style="list-style-type: none">▪ Aboveground biomass
Blue carbon	<ul style="list-style-type: none">▪ Total carbon▪ Organic carbon▪ Bulk density

4.1. Wave energy dissipation

The maximum wave height recorded throughout the duration of the experiment from August to November 2022 was analyzed. At each site, three events were selected by visual observation. The average calculated maximum wave height for the duration of the experiment was 0.03 m and 0.02 m, at SHP and SHP_R, respectively. Overall, the trend is clear in depicting wave energy dissipation along the transect (*Table 6*). As we advance from the open water to the marsh area, wave energy dissipation occurs. This is reflected by the reduction of the maximum wave height values recorded from RBR 1 to RBR 4.

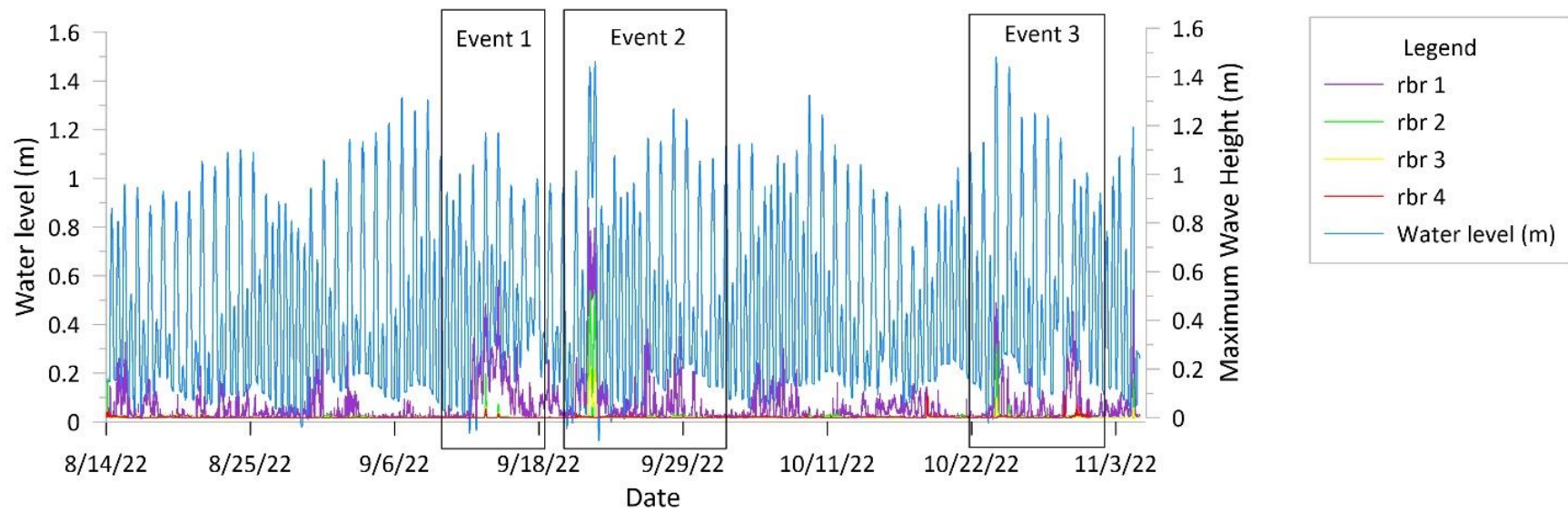


Figure 28. Maximum wave height recorded at RBR 1, RBR 2, RBR 3 and RBR 4 at Shippagan (Study Site) throughout the duration of the study from August to November 2022.

In Event 1, the average wave reduction between RBR 1 and RBR 3 is 15% and complete dissipation occurs by the time the waves reach RBR 4 (*Table 6*). The maximum wave height peak starts off at 0.6 m, where the peak water level is at 1.1 m, we see a steady rise and fall that corresponds to the water depths (*Figure 29*). The peaks in this Event are a result of the increase in wind speeds at the study site which are highly likely to have led to the surge and increase in water levels (See *Figure 16* on wind speeds throughout the duration of the experiment). The first instrument, RBR 1 which was deployed in the open water, recorded the maximum wave height values which ranging from 0 to 0.6 m. Complete dissipation occurs within this event, as the instruments RBR 2, 3, and 4 record a maximum wave height of 0, and the calculated exponential wave decay constant (β) is 0.02 m^{-1} (*Table 6*).

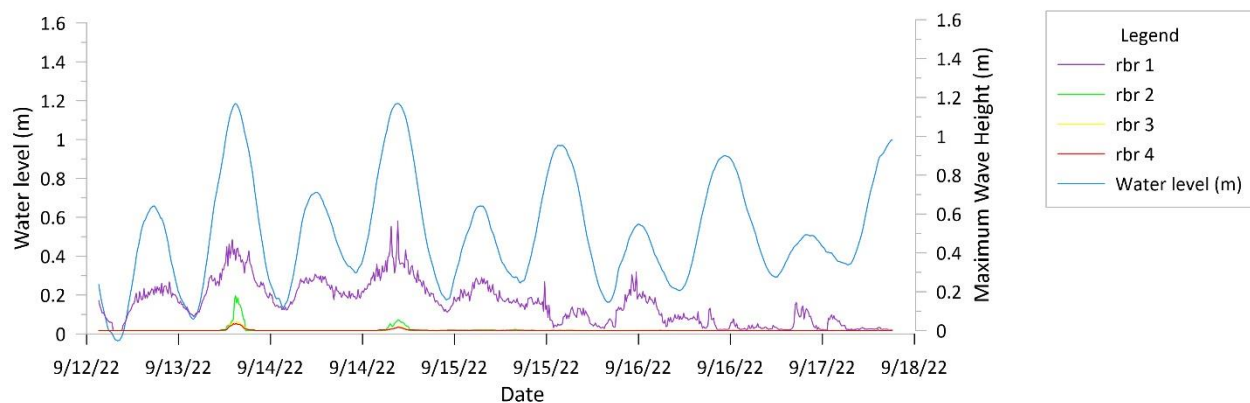


Figure 29. Event 1 - Maximum wave height recorded at RBR 1, RBR 2, RBR 3 and RBR 4 at Shippagan (Study Site) from September 15th to September 19th, 2022.

Event 2 shows a steady rise and fall in the water levels which corresponds to the maximum wave height recorded for RBR 1. The maximum wave height recorded was 0.8m during Hurricane Fiona which occurred between September 22 – 24, 2022 (*Figure 30*), and the water level during that time was 1.5 m. The increase in water levels corresponds to the increase in wind speeds ranging from 4 to $7 \text{ m}\cdot\text{s}^{-1}$ along the coast which caused a storm surge. The rest of the event is characterised by

much smaller maximum wave height values which range from 0.1 to 0.2 m. The average wave height reduction between RBR 1 and RBR 3 is 32%, with a calculated exponential wave decay constant (β) is 0.02 m^{-1} , as shown in Table 6.

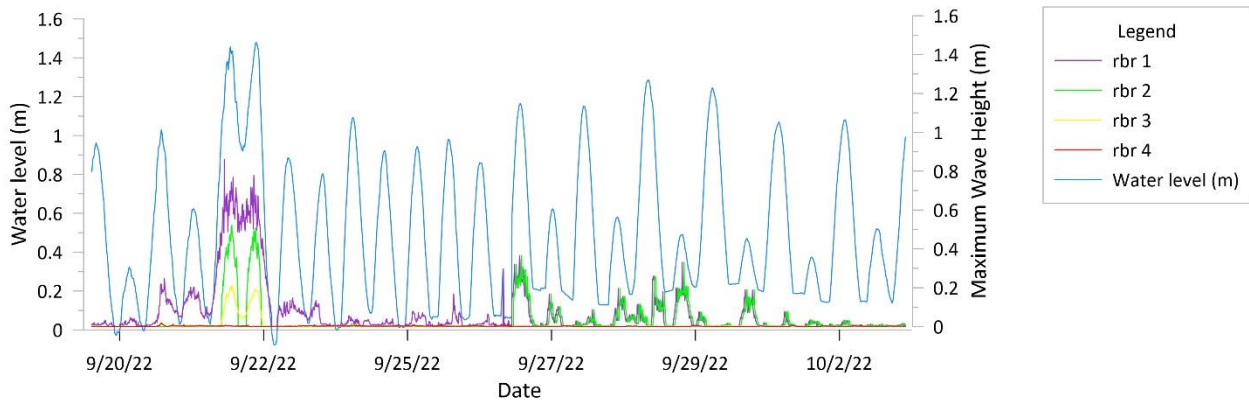


Figure 30. Event 2 - Maximum wave height recorded at RBR 1, RBR 2, RBR 3 and RBR 4 at Shippagan (Study Site) from September 22nd to October 5th, 2022.

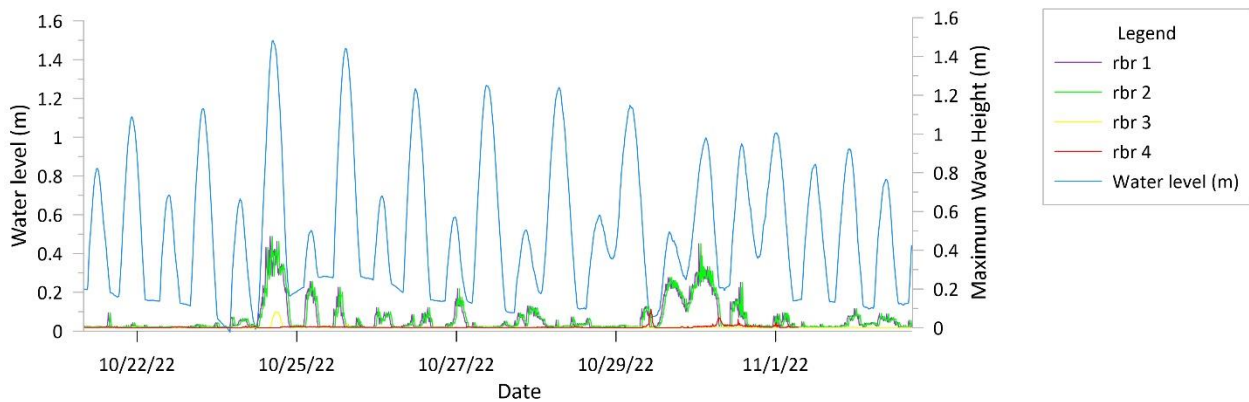


Figure 31. Event 3 - Maximum wave height recorded at RBR 1, RBR 2, RBR 3 and RBR 4 at Shippagan (Study Site) from October 25th to November 5th, 2022.

Event 3 shows a steady rise and fall in the water levels corresponding to the maximum wave height. The peak in maximum wave height between October 24 and October 25 was 0.5 m recorded at RBR 1. With complete dissipation having occurred along the transect, the maximum wave height

RBR 2, 3, and 4 was 0. The average wave height reduction between RBR 1 and RBR 3 is 27%, with a calculated exponential wave decay constant (β) is 0.04 m^{-1} , (Table 6).

The exact time frame of events was analyzed at the reference site (SHP_R) and were characterized and chosen according to the peaks and the average maximum wave height which was calculated for the duration of the experiment. Overall, the general trend is a decrease in the maximum wave height values as the waves advance along the transect towards the instrument at the end of the transect (RBR 1 to RBR 4). However, in this deployment, the maximum wave heights for RBR 1 and RBR 3 appear to be close, as the instruments are 5 m apart. In comparison to the transect setting at SHP, where the distance between RBR 1 and RBR 3 is 22 m, the distance is much shorter at SHP_R. RBR 2 was located right at the marsh edge. The relationship between RBR 1 and RBR 3 at SHP_R is closely monitored within the events and explored further in the following sections. In this research, we use both RBR 1 to determine the decrease in the maximum wave heights along the transect up until RBR 3, as complete dissipation eventually occurs when the waves reach RBR 4 in both cases.

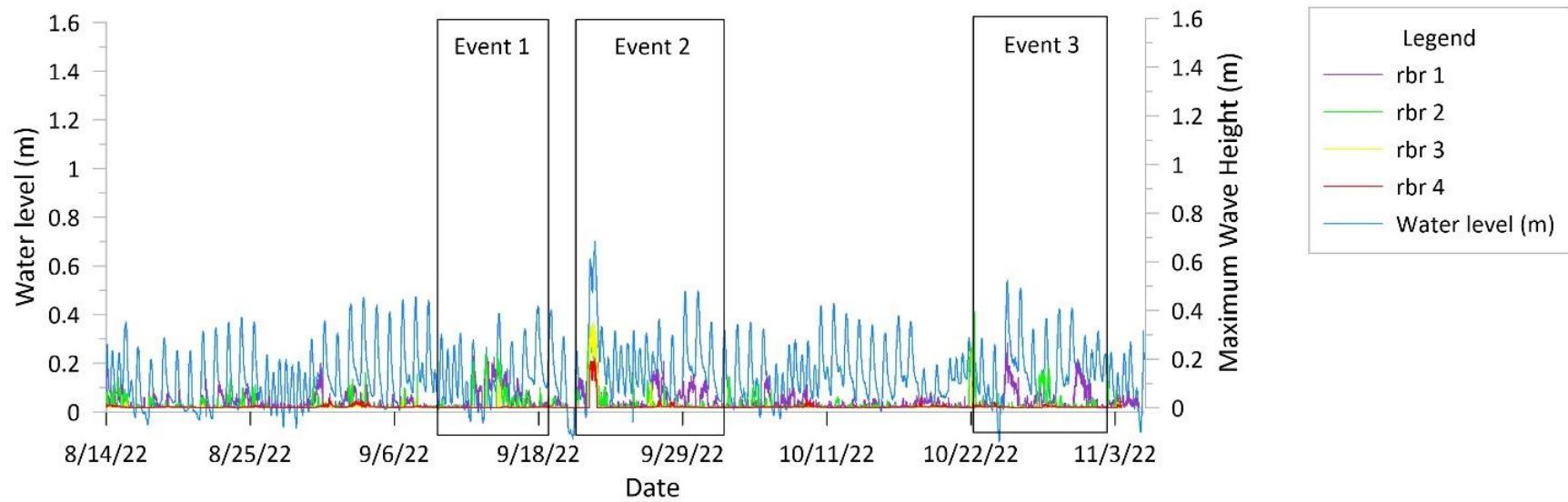


Figure 32. Maximum wave height recorded at RBR 1, RBR 2, RBR 3 and RBR 4 at Shippagan (Reference Site) throughout the duration of the study from August to November 2022.

Event 1 shows the maximum wave height recorded at each RBR (RBR 1 – RBR 4), from September 15th to September 19th, 2022. From this event, we can see a complete decrease in the maximum wave height from an average of 0.2 m at RBR 1 to 0 m by the time the waves reach RBR 4. It is important to note that this is a fully vegetated transect, where RBR 2, RBR 3 and RBR 4 were placed in the fully vegetated transect, whilst RBR 1 was placed in the open water.

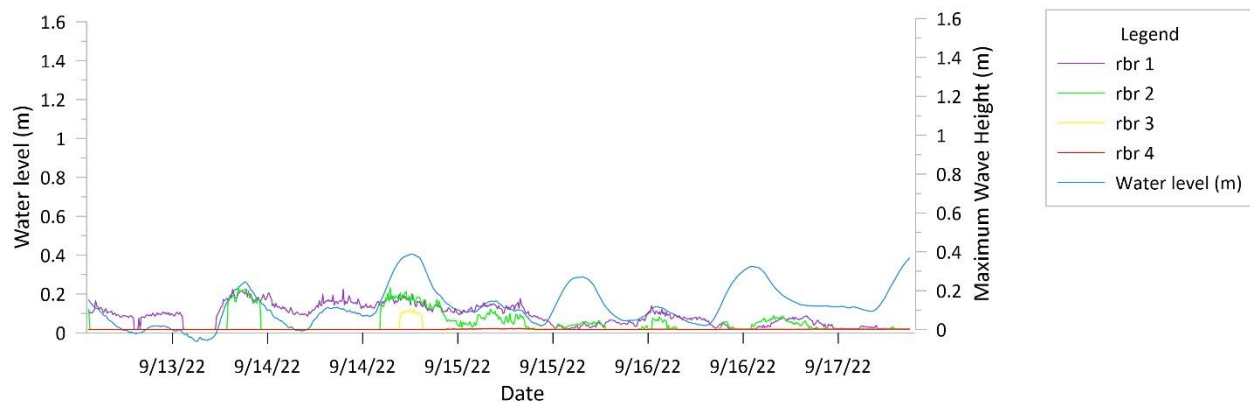


Figure 33. Event 1 - Maximum wave height recorded at RBR 1, RBR 2, RBR 3 and RBR 4 at Shippagan (Reference Site) from September 15th to September 19th, 2022.

Event 2 shows the maximum wave height recorded at each RBR (RBR 1 – RBR 4), from September 22nd to October 5th, 2022. Similar to Event 2 at the study site, Hurricane Fiona (September 22 – 24, 2022) was recorded and an increase in water levels is observed from 0.3 m to 0.7 m, which is twice as much as the values recorded under normal site conditions.

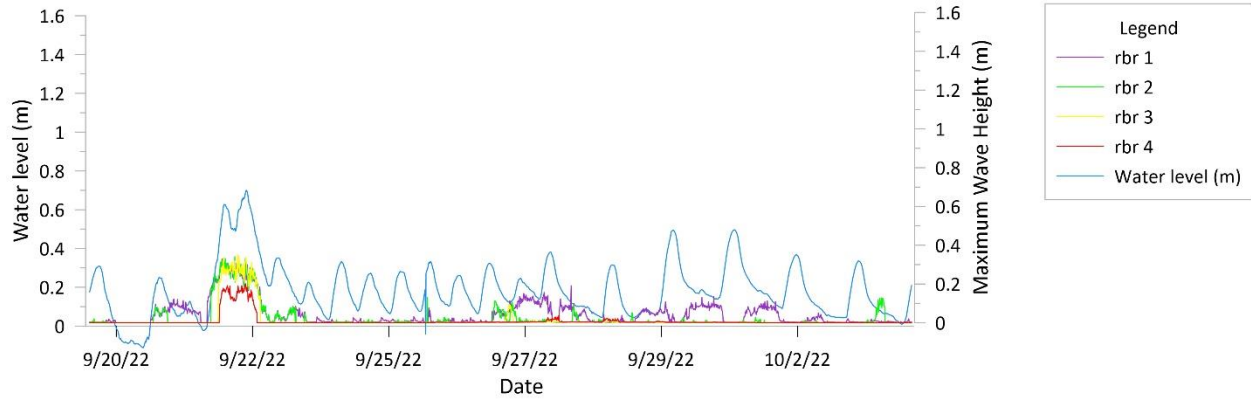


Figure 34. Event 2 - Maximum wave height recorded at RBR 1, RBR 2, RBR 3 and RBR 4 at Shippagan (Reference Site) from September 22nd to October 5th, 2022.

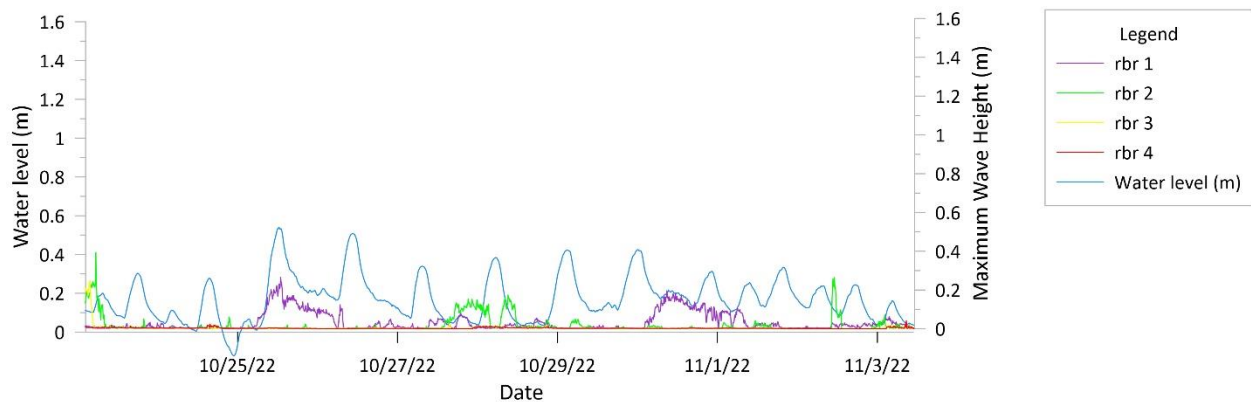
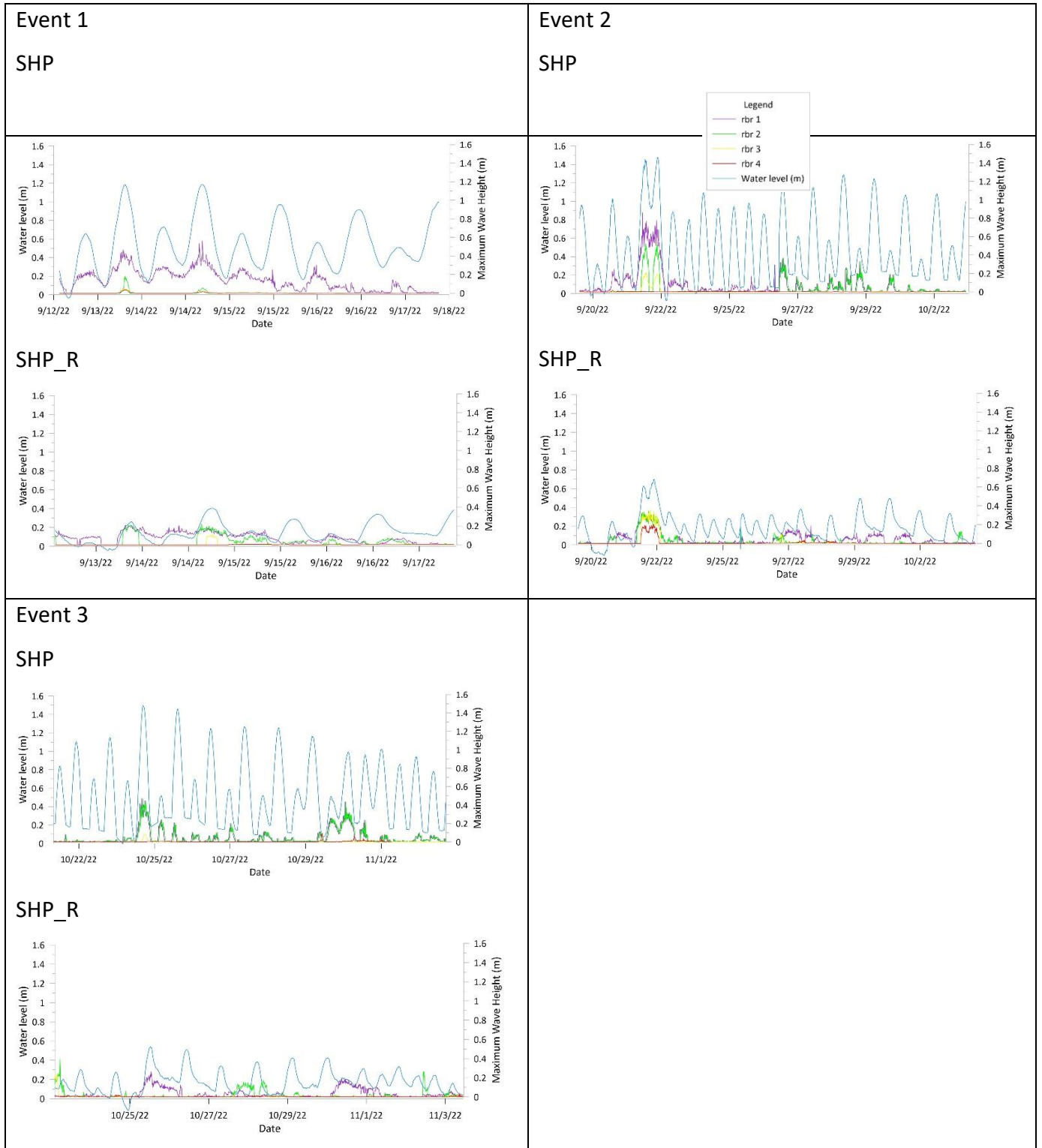


Figure 35. Event 3 - Maximum wave height recorded at RBR 1, RBR 2, RBR 3 and RBR 4 at Shippagan (Reference Site) from October 25th to November 5th, 2022.

Event 3 has a unique pattern in that the maximum wave heights are close in value to the water level values. The range for the water level and maximum wave heights in Event 3 is 0.1 to 0.5 m. The exponential wave decay constant (β) for event 3 at the reference site (SHP_R), is 0.12 m^{-1} , as shown in Table 6, and the average wave height reduction is 70%, between RBR 1 and RBR 3.

Table 5. Summary of Events 1 -3, at SHP and SHP_R (Event 1 – Sept 15 – 19; Event 2 – Sept 22 – Oct 5; Event 3 – Oct 25 – Nov 5).



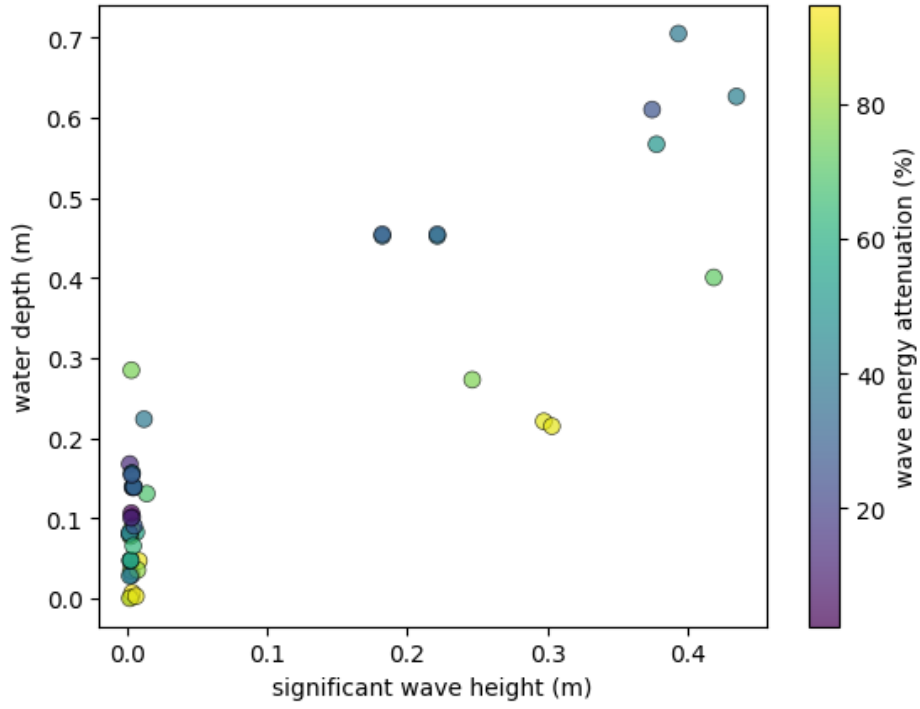


Figure 36. Percentage of attenuation, water depth and significant wave height at the study site (SHP), for entire deployment.

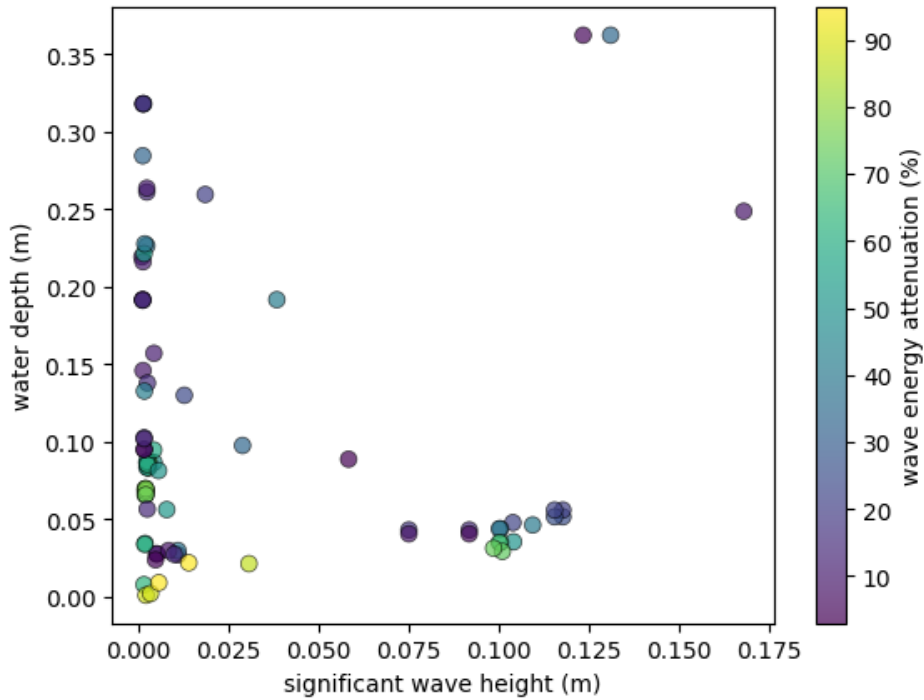


Figure 37. Percentage of attenuation, water depth and significant wave height at the reference site (SHP_R), for entire deployment.

The relationship between significant wave height (m) and water depth (m), with wave energy attenuation (%) is depicted through the color gradient of the data points (Figure 36 and Figure 37). Both figures show a cluster of data points at lower wave heights (0 to 0.1 meters) across varying water depths, indicating diverse attenuation levels. Figure 35 suggests a wider range of water depths (up to 0.7 meters) compared to Figure 36 (up to 0.35 meters), showing that the study site has deeper waters, and a wider range of wave conditions compared to the reference site. Both figures indicate that small waves are easily attenuated in shallow water. In some instances, as the wave height increases, the water depth also increases. Additionally, larger wave heights in slightly deeper waters show more consistent attenuation percentages.

4.1.1. Wave energy dissipation

The table below (Table 6) shows the maximum water depth over each marsh platform, at the Study (SHP) and Reference Site (SHP_R) for all three events, as well as the exponential wave decay constant obtained from the calculations. The maximum significant wave height the Study Site is 0.24 m, 0.43 m, and 0.27 m at the Study for events 1, 2, and 3, respectively. The average wave height reduction is 15%, 32% and 27%, with the corresponding exponential wave decay constants being 0.02 m^{-1} , 0.02 m^{-1} , and 0.04 m^{-1} .

*Table 6. Wave heights and water depths for SHP and SHP_R, showing similar vegetation species found at each site, that quantify wave energy dissipation at initial instrument * (at the transect section considered) (RBR 1 and RBR 3 were used for calculation).*

Research Site	Event	Vegetation Characteristics	Average stem height (m)	Maximum water depth over marsh platform, h (m)	Relative roughness (max water depth/stem height)	Maximum significant wave height, H_s (m) (at initial instrument RBR 1)	Transect Length (m)	Average wave height reduction (%)	Exponential wave decay constant, β (m^{-1})
SHP (study site)	1	<i>Sporobolus alterniflorus</i>	0.49	1.32	2.69	0.24	22	15	0.02
	2	<i>Sporobolus alterniflorus</i>	0.38	1.76	4.63	0.43	22	32	0.02
	3	<i>Sporobolus alterniflorus</i>	0.22	0.27	1.23	0.27	22	27	0.04
SHP_R (reference site)	1	<i>Sporobolus alterniflorus</i> , <i>Sporobolus pumilus</i>	0.65	x	x	x	5	x	x
	2	<i>Sporobolus alterniflorus</i> , <i>Sporobolus pumilus</i>	0.49	x	x	0.03	5	5	x
	3	<i>Sporobolus alterniflorus</i> , <i>Sporobolus pumilus</i>	0.36	0.37	1.02	0.15	5	70	0.12

The maximum significant wave height at the Reference Site is much less than the maximum significant wave height at the Study Site. Table 6 shows the maximum significant wave height for events 2 and 3 as 0.03 m and 0.15 m, respectively. The average wave height reduction were events 2 and 3 were 5% and 70%, this is much less than half the study site height. Values for the maximum significant wave height and average wave height reduction for event 1 could not be calculated in the script used to obtain results due to no values recorded or an extreme minimum reported in that dataset (Table 6).

4.1.1. Vegetation height and stem density using image obscuration ratio

The image obscuration and dry biomass were compared for each site. *Figure 19* shows that the black pixel density in the classified binary images and the dry biomass varied at each RBR station. The different canopy heights and stem density are shown in *Figure A2*. According to what we know from the literature (Möller, 2006, Neumeier, 2005), when the image obscuration ratios are compared to the dry biomass and the wave dissipation data, the wave energy dissipation occurs where there are larger amounts of dry biomass, and emergent vegetation as seen in the stem height values (*Figure A2*), and water level values (*Figures 27 and 31*). Overall, there is a higher increase in the image obscuration and the dry biomass at the reference site compared to the study site (*Figure 38*).

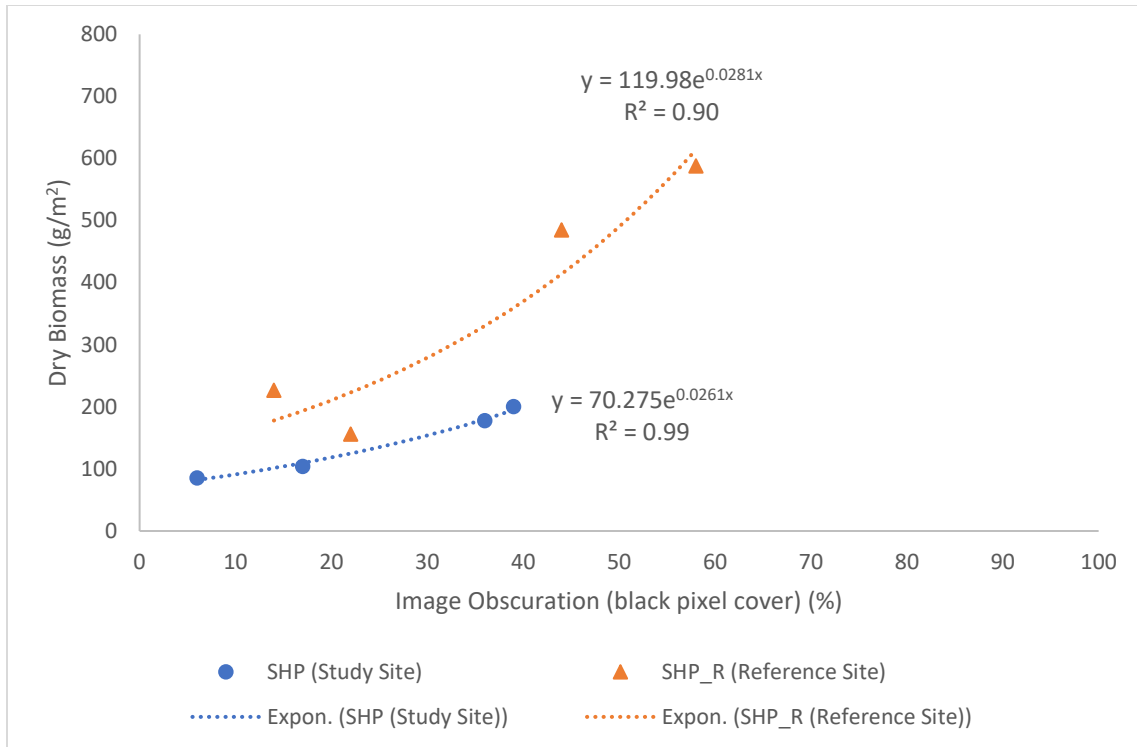


Figure 38. Relationship between aboveground biomass (dry weight) of photographed vegetation and image obscuration ratio for SHP and SHP_R at RBR 3 and RBR 4.

Table 7. Image obscuration for August and September 2022 at SHP and SHP_R.

Month	Site	Station	Dry biomass g/m ²	Image Obscuration (black pixel cover) (%)	Background (%)
Aug	SHP	RBR 3	103.92	17	83
		RBR 4	177.83	36	64
Sept	SHP	RBR 3	85.25	6	94
		RBR 4	200.33	39	61
Nov	SHP	RBR 3	57.17	n/a (windy site conditions)	
		RBR 4	165.75		
Aug	SHP_R	RBR 3	156.08	22	78
		RBR 4	587.92	58	42
Sept	SHP_R	RBR 3	226.42	14	86
		RBR 4	484.83	44	56
Nov	SHP_R	RBR 3	33.75	n/a (windy site conditions)	
		RBR 4	664.83		

The overall trend in Table 7, is that there is an increase in vegetation growth (denoted by the image obscuration percentage), over the growing season between August and November. The largest obscuration percentage was calculated at RBR 4, SHP_R (reference site) as 58% in August, while the lowest obscuration percentage was calculated at RBR 3, SHP (study site) as 17% (Table 7).

4.2. Habitat

A total of 9 species were detected at the anthropogenically modified salt marsh (SHP) plots, while 20 species were detected in the salt marsh area at the Shippagan reference site (SHP_R). The average plot coverage was slightly higher at the reference site, this is due to greater representation of mature communities and the high marsh species such as *Juncus gerardii*, *Sporobolus pumilis* and *Hordeum jubatum* (Figure 39, Figure 40). SHP has more bare ground represented in plots for many reasons. Bare ground caused by human disturbance such as ATV tracks and the existing road, were captured in the vegetation plots. The vegetation patterns found at SHP were sparser than those observed at SHP_R; this was also due to the natural disturbances such as overwash fans. *Sporobolus alterniflorus* (a low marsh species) was found present and dominant in 9 of the 16

vegetation plots at SHP. The average cover of vegetation in plots did not differ significantly between SHP and SHP_R (P value = 0.6523).

While some plots at SHP_R were also found to have *Sporobolus alterniflorus*, 14 out of 22 plots are dominated by *Sporobolus pumilus*, which is a high marsh species that develops where there is favorable tidal hydrology, allowing for these vegetation species to be saturated for a significant number of hours (Figure 39; Figure 40). *Sporobolus alterniflorus* and *Sporobolus pumilus* were the two dominant species at both sites. Statistical analysis using the Welch Two Sample t-test, which accounts for unequal sample sizes, showed that the p-value for *Sporobolus alterniflorus* was 0.3667, indicating no significant difference in its presence between the two sites. In contrast, the p-value for *Sporobolus pumilus* was 0.0423, suggesting a significant difference, with SHP_R having more *Sporobolus pumilus* compared to SHP. These results support that the reference site (SHP_R) has more favorable conditions for the growth of *Sporobolus pumilus*, likely due to optimal tidal hydrology, while *Sporobolus alterniflorus* shows no significant variation between the sites.

The top five dominant species found in the plots at each site were selected and the species abundance values were analysed. The results show that there is a clear variation in the dominant species at SHP compared to those found at SHP_R. *Sporobolus alterniflorus*, *Sporobolus pumilus*, *Puccinella maritima*, *Salicornia maritima* and *Suaeda maritima*, were the top five dominant species at SHP. *Sporobolus alterniflorus*, *Sporobolus pumilus*, *Juncus gerardii*, *Lysimachia maritima*, and *Hordeum jubatum* were the top five dominant species at SHP_R. Both *Sporobolus alterniflorus* and *Sporobolus pumilus* were found to be dominant at both sites, with a percent cover of 24 % and 20 % at SHP, respectively and 48 % and 56 %, at SHP_R respectively (Figure 39, Figure 40).

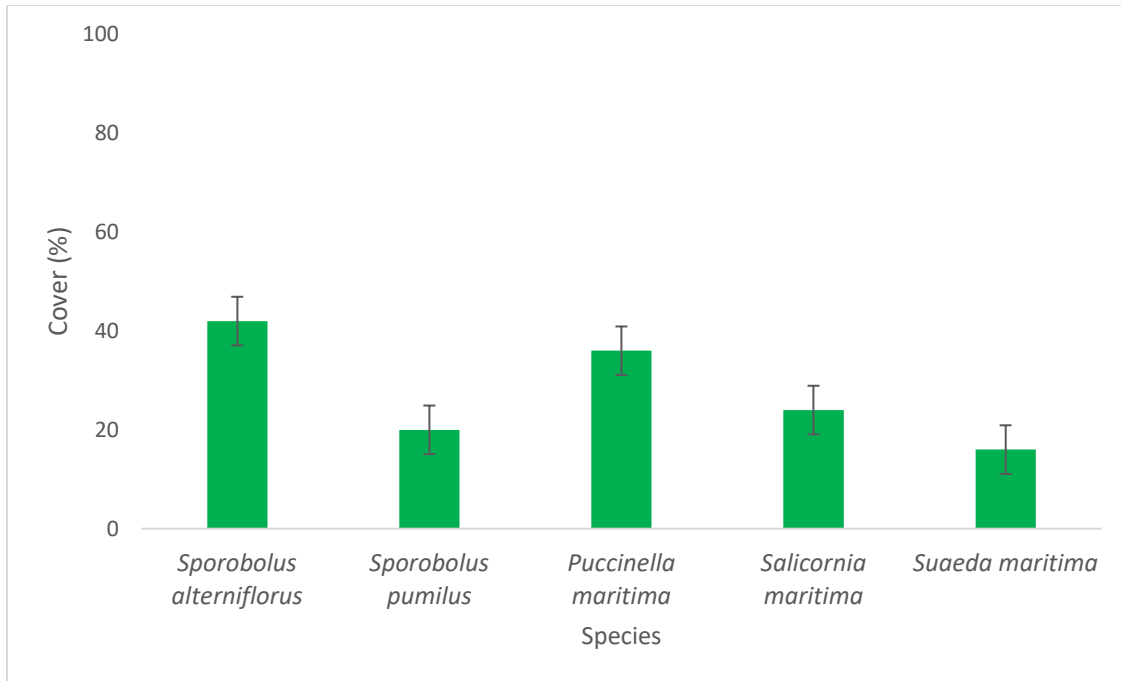


Figure 39. Percent cover for top 5 dominant species at Shippagan study site (SHP) (arranged in order of top 2 dominant species, with standard deviation bars.)

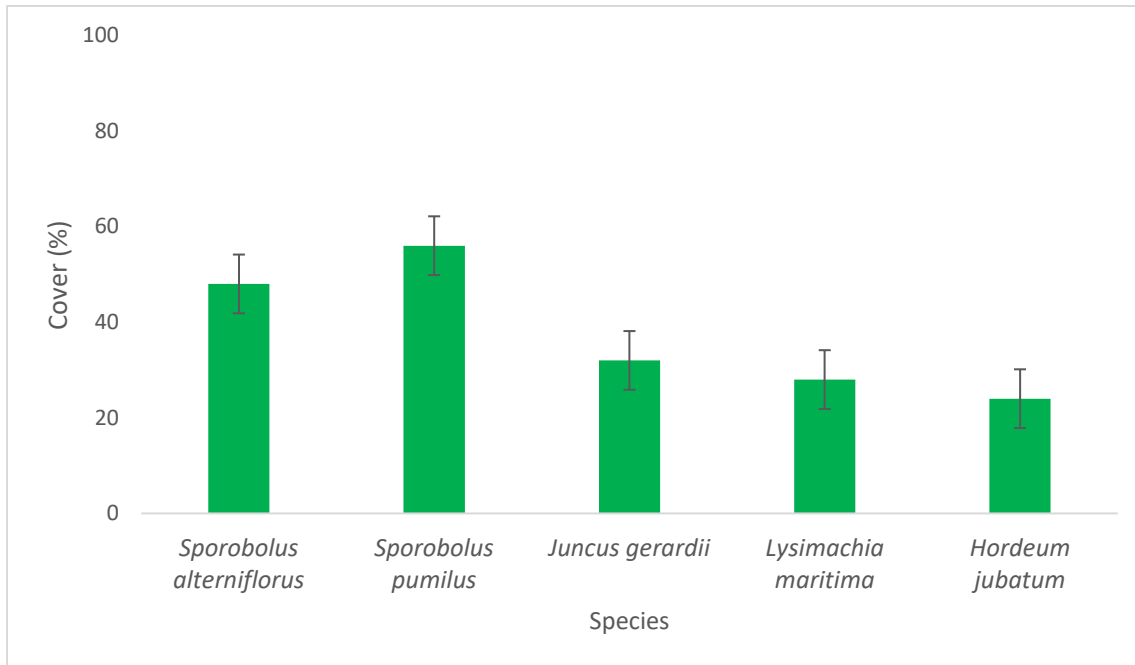


Figure 40. Percent cover for top 5 dominant species at Shippagan reference site (SHP_R) (arranged in order of top 2 dominant species, with standard deviation bars).

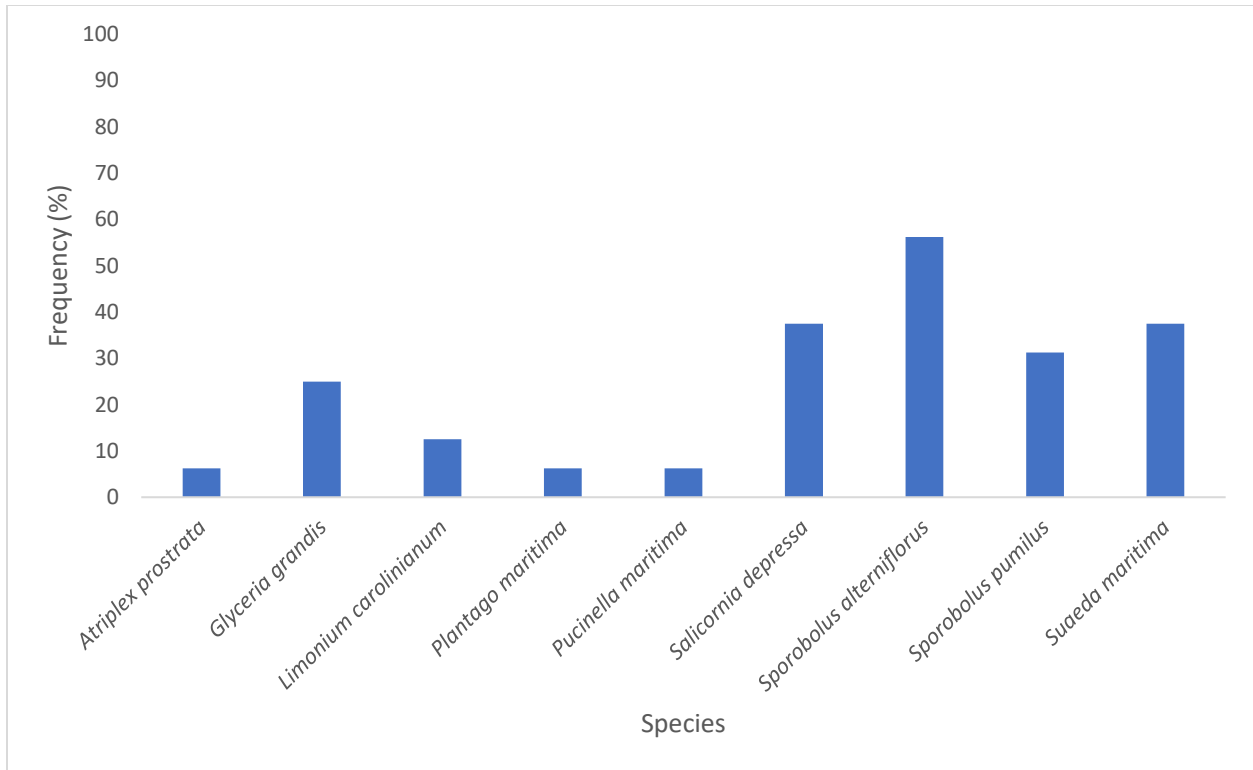


Figure 41. Frequency at Shippagan study site (SHP), which is the % of all plots at the site where the species occurs.

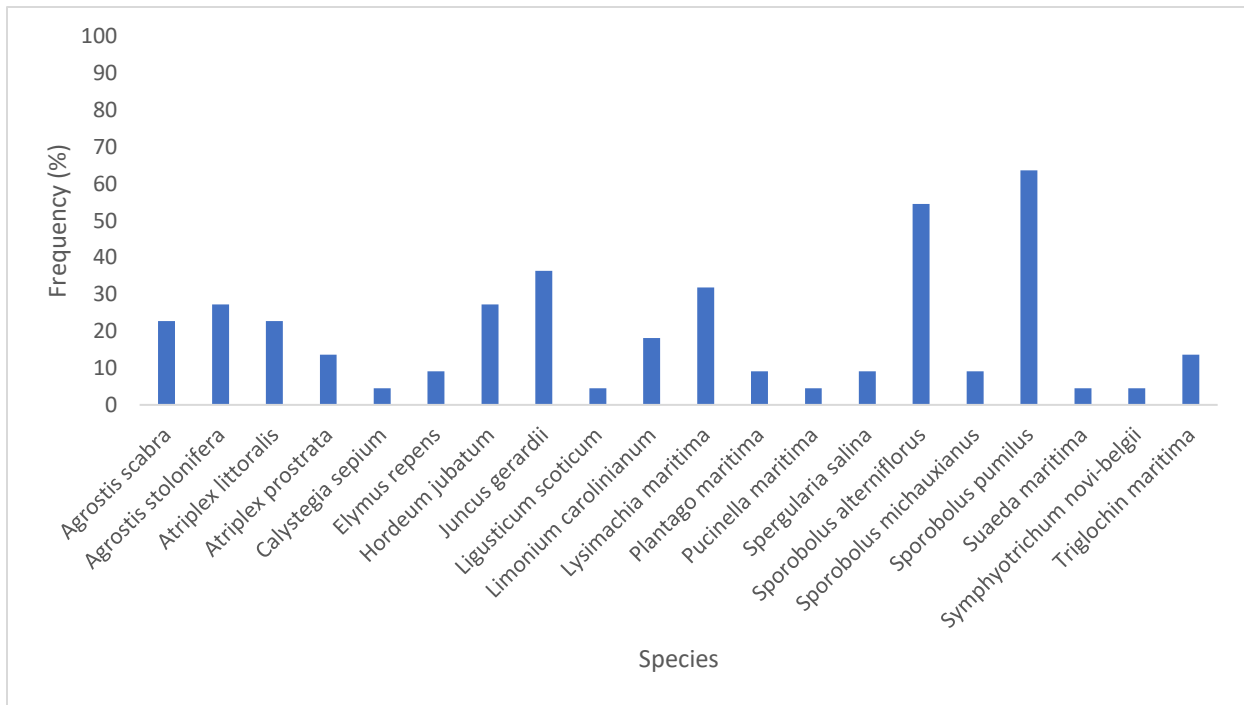


Figure 42. Frequency at Shippagan reference site (SHP_R), which is the % of all plots at the site where the species occurs.

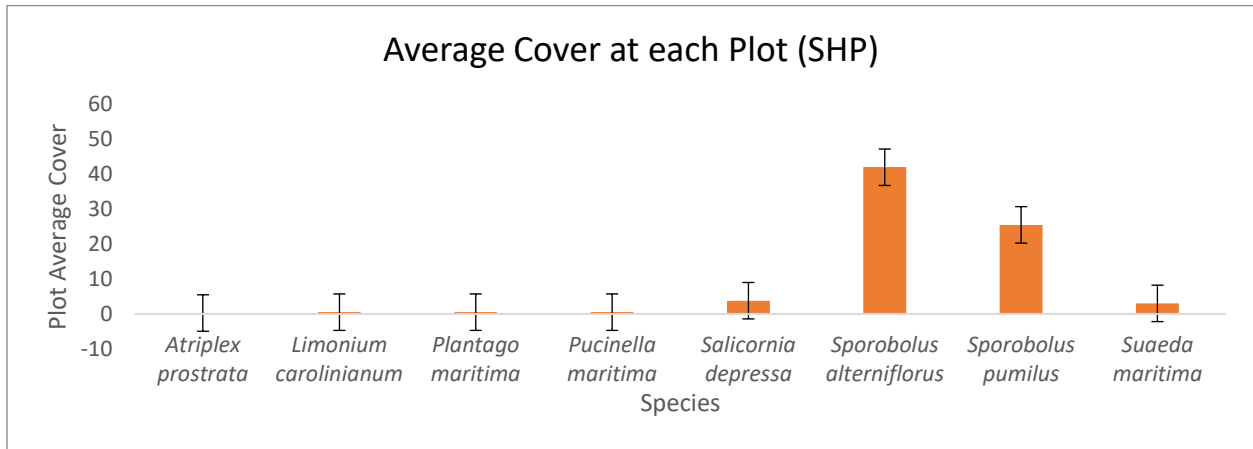


Figure 43. Plot average coverage at Shippagan Study Site (SHP) with standard deviation bars..

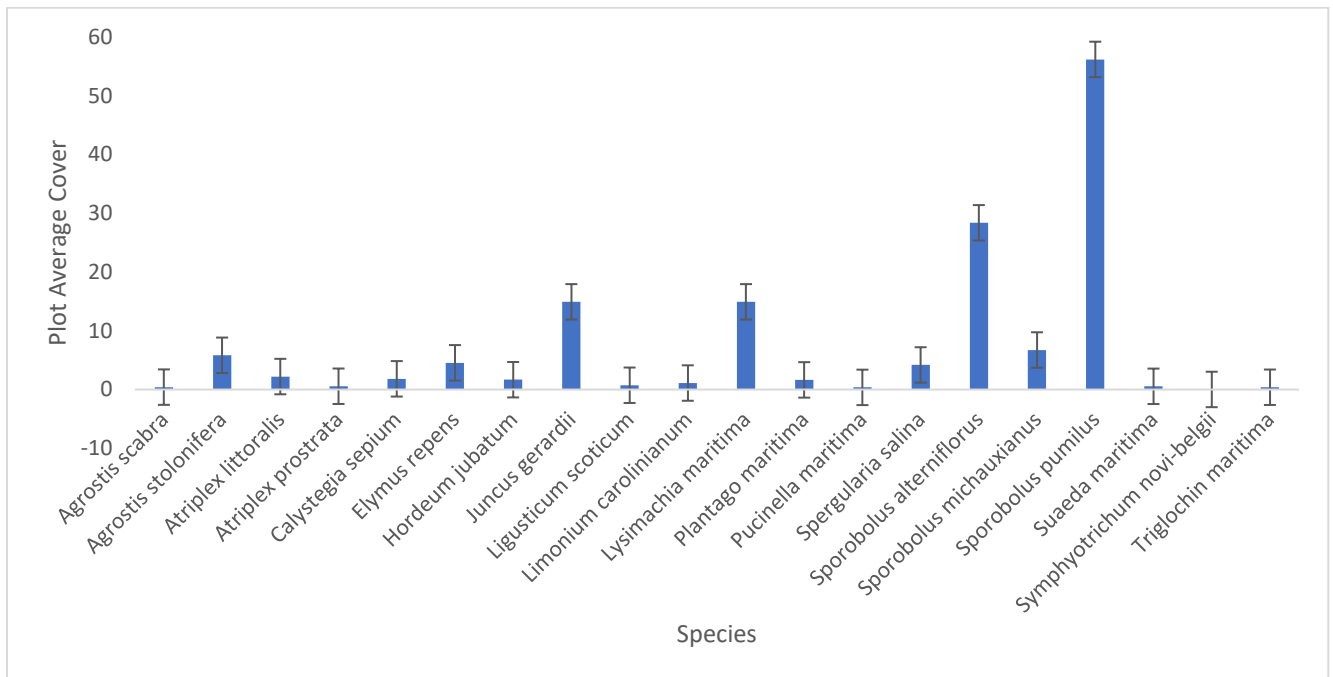


Figure 44. Plot average coverage at Shippagan Reference Site (SHP_R), with standard deviation bars.

4.2.1. Soil Nutrients

The main nutrients that were compared in this research are Nitrogen (N), Phosphorus pentoxide (P₂O₅) and Potassium oxide (K₂O) as shown in Table A10 in the Appendix. These three nutrients were selected as they play a critical role in plant growth, development, and physiology. A summary

of the maximum, minimum, median, Q1 and Q3 values for each increment (0-15 cm and 15-50 cm), is also shown. The top 15 cm layer has higher values in Nitrogen, and K_2O , at the reference site than at the study site: 0.17% and 536 kg/ha respectively. The low marsh and mid to high marsh zones at the reference site have the highest values of Nitrogen, P_2O_5 and K_2O , in the top 15 cm, compared to the study site. The highest Nitrogen percentage is 0.33% within the top 15 cm of the mid to high marsh zone at the reference site, while the study site has 0.16% Nitrogen within its top 15 cm at the mid to high marsh zone. The highest P_2O_5 value is 167.33 kg/ha, found in the mid to high marsh zone at the reference site within the top 15 cm layer, while the study site has 150 kg/ha for P_2O_5 . Lastly, the low marsh zone at the reference site has 822.67 kg/ha, while the study site has 270.00 kg/ha, all within the top 15 cm layer. This overall trend shows that within the top 15 cm layers, the reference site has high values of Nitrogen, P_2O_5 and K_2O , compared to the study site, and the bottom 15-50 cm layers at both sites (*Tables A7 and A8*). However, the 15-50 cm layers have much lower values compare to the top 15 cm layers. The shoreline zone has lower values at the reference site in the 15-50 cm layer, compared to the study site, although both sites generally have low values of Nitrogen, P_2O_5 and K_2O within the low marsh zone (*Tables A7 and A8*).

Results from the two-way ANOVA showed that there was no significant difference between the marsh zones and the sites, with all the nutrients tested (Table A10). The three main nutrients that were compared were Nitrogen, P_2O_5 , and K_2O . The changes in these nutrients as we advance along the marsh from the shoreline to low marsh, to mid to high marsh zones (0-15cm), showed that there was no statistically significant interaction between zone and site for the Nitrogen, P_2O_5 , and K_2O (*Table A10*).

The two exceptions were Nitrogen (15-50 cm), and Magnesium (15-50 cm). For Nitrogen (15-50 cm), the comparison between mid to high marsh and shoreline zones has a p-value of

0.0168, indicating a statistically significant difference (Table A10). The mid to high marsh zone had higher Nitrogen percentages, than the shoreline zones. However, there was no statistically significant difference between low marsh and mid to high marsh zones where the p-value is 0.3198, and low marsh and shoreline zones, where the p-value is 0.3124.

For Magnesium (15-50 cm), the comparison between low marsh and mid to high marsh zones has a p-value of 0.7016, which suggests no statistically significant difference, whereas the comparison between low marsh and shoreline zones has a p-value of 0.0356, suggesting a statistically significant difference. Higher Magnesium values were recorded in the low marsh zones, compared to the shoreline zones. When the mid to high marsh and shoreline zones were compared, a p-value of 0.1653 was obtained, suggesting no statistically significant difference.

4.3. Primary Productivity

The aboveground biomass excavated at each plot informs us of the primary productivity at each site. There was a total of 13 out of 25 plots found with aboveground biomass at SHP, compared to the 21 out of 25 plots at SHP_R (*Figure 45*). A total of 25 plots at each site were selected, with the intention of excavating aboveground biomass if present. The calculated aboveground biomass ($\text{g}\cdot\text{m}^{-2}$) mean at SHP was lower than at SHP_R, 28.54 $\text{g}\cdot\text{m}^{-2}$ and 44.77 $\text{g}\cdot\text{m}^{-2}$, respectively. The minimum recorded value was at SHP, 13.83 $\text{g}\cdot\text{m}^{-2}$, and the maximum recorded value was 80.8 at SHP_R $\text{g}\cdot\text{m}^{-2}$. There is a significant difference in the Q1, Q2 and Q3 (First quartile: Also known as Q1, or the lower quartile. Second quartile: Also known as Q2, or the median. Third quartile: Also known as Q3, or the upper quartile values) for both sites. SHP has 17.39 $\text{g}\cdot\text{m}^{-2}$, 26.20 $\text{g}\cdot\text{m}^{-2}$ and 35.40 $\text{g}\cdot\text{m}^{-2}$ respectively, while SHP_R has 29.59 $\text{g}\cdot\text{m}^{-2}$, 42.48 $\text{g}\cdot\text{m}^{-2}$ and 53.15 $\text{g}\cdot\text{m}^{-2}$ respectively. Each dataset has an outlier – the outlier value for SHP is 71.17 $\text{g}\cdot\text{m}^{-2}$ (which was found in the high marsh zone), while SHP_R has an outlier of 96.39 $\text{g}\cdot\text{m}^{-2}$ (which was found in

the low marsh zone). When the data set was combined for a more comprehensive analysis, the median recorded value was $24.23 \text{ g}\cdot\text{m}^{-2}$ while the mean was $26.22 \text{ g}\cdot\text{m}^{-2}$, both of which are lower than the separate median and mean values for each data set, SHP, and SHP_R. The P value for this analysis is 0.0000.

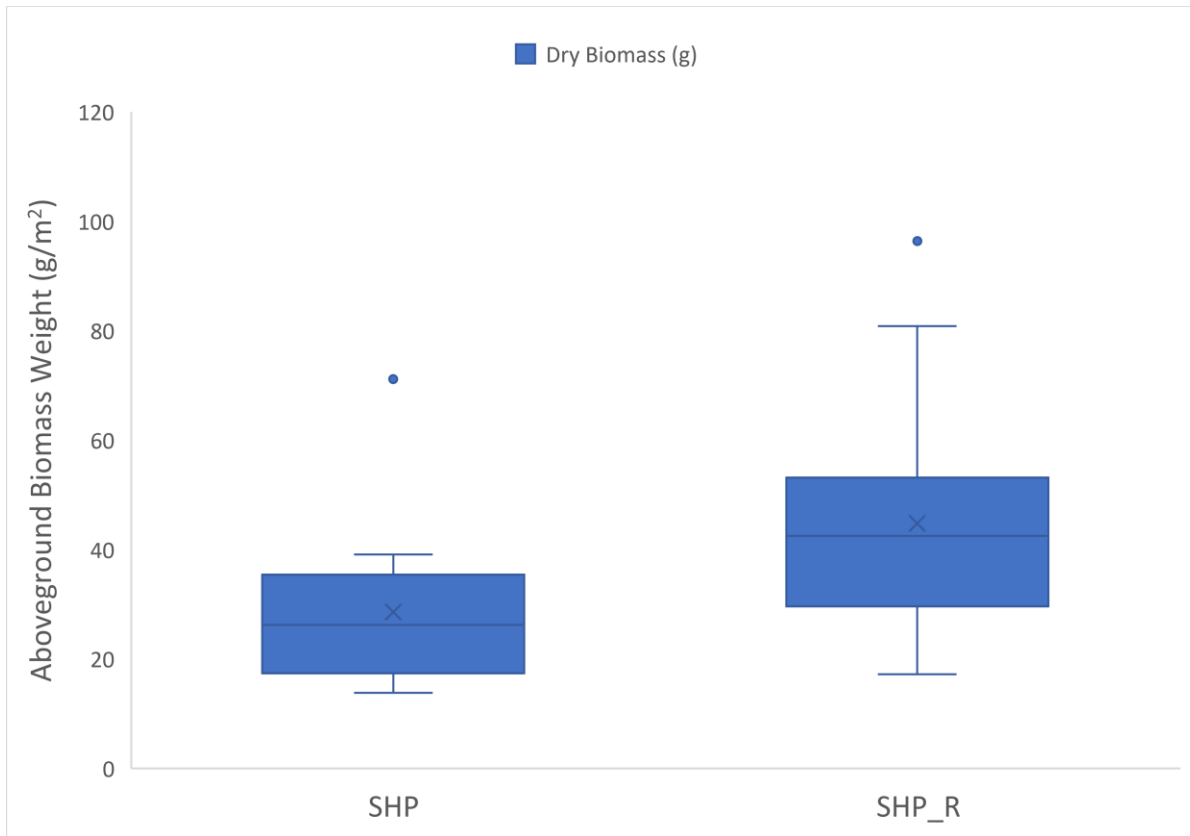


Figure 45. Average aboveground biomass at Shippagan Study Site (SHP) and Shippagan Reference Site (SHP_R).

4.4. Organic, Inorganic and Total Carbon

The graphs below show results from total carbon, inorganic carbon and organic carbon values calculated from the lab procedures. The procedure to determine inorganic carbon values is a simple mathematical calculation which involves subtracting organic carbon from the total carbon that was derived from the analysis. Figure 46 shows the total carbon per core in each marsh zone. The sediment cores were classified according to the marsh zones, shoreline, low marsh and mid to high

marsh zones. Overall, there was more total carbon, inorganic carbon, and organic carbon in the substrates at the reference site compared to the study site (*Figures 45 and 46*). The mean for total carbon from the study and the reference sites were derived, 25.09 g and 44.35 g respectively. The calculated medians for total carbon from the study and reference site were 0.25 g and 0.52 g, respectively.

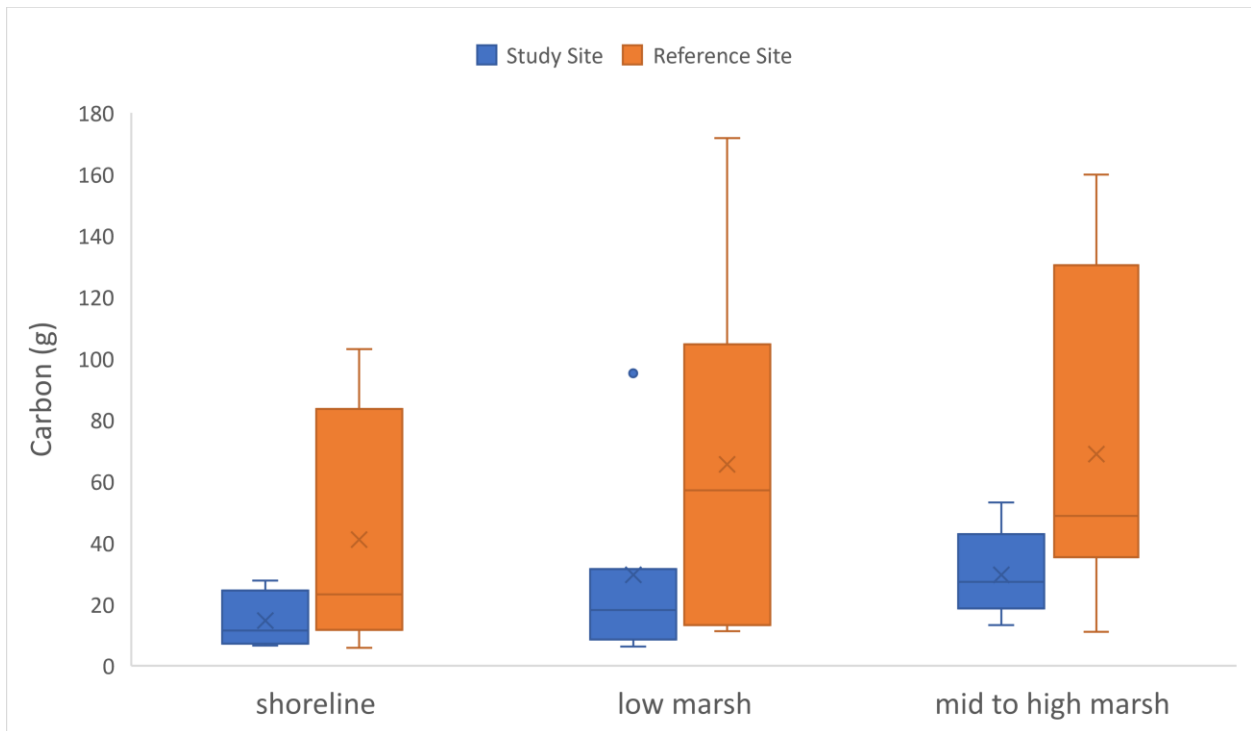


Figure 46. Total carbon at the Study and Reference Sites, within the shoreline, low marsh and mid to high marsh zones (x represents the mean within the data range (no statistically significant differences)).

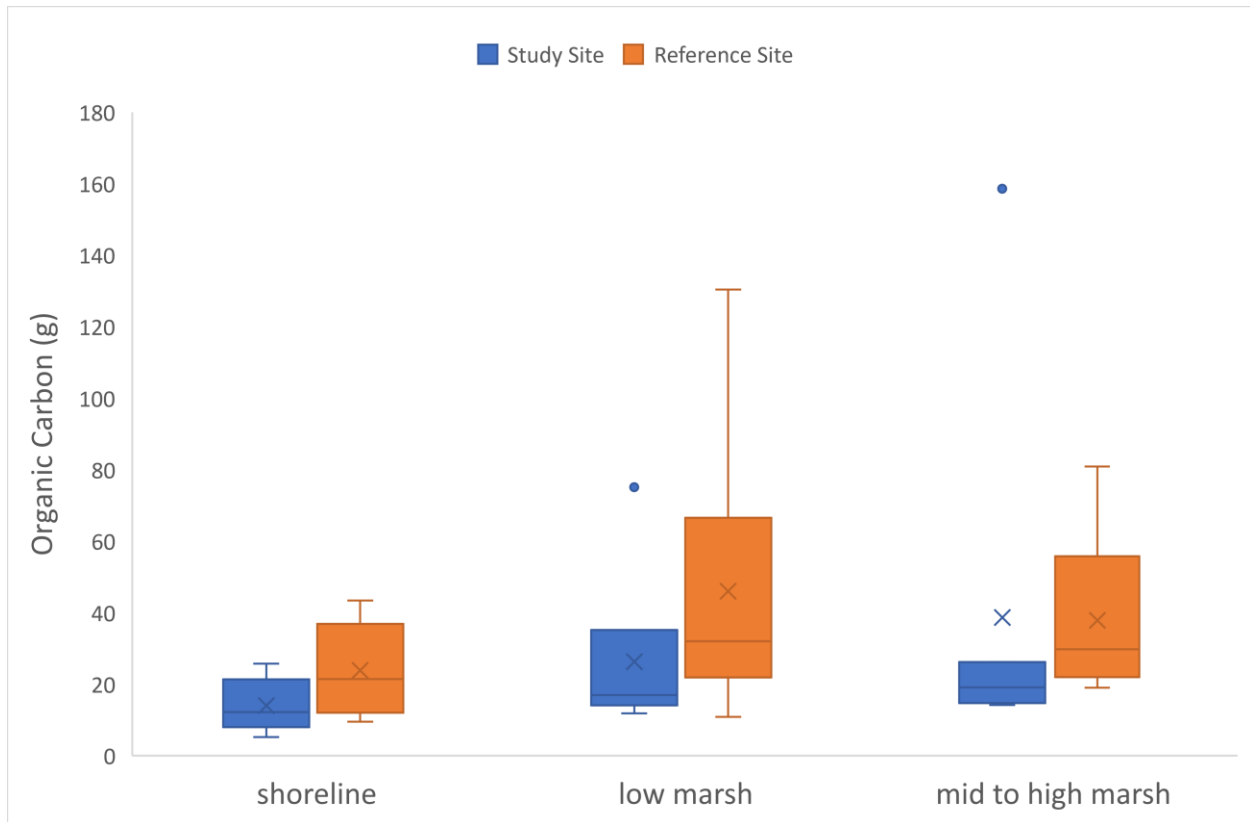


Figure 47. Organic carbon at the Study and Reference Sites, within the shoreline, low marsh and mid to high marsh zones (x represents the mean within the data range (statistically significant interaction)).

The organic carbon amounts have a unique pattern in that the low marsh zone has a wider range and overall, the largest amount of organic carbon compared to the rest of the zones (Figure 47). The minimum organic carbon amount recorded at the study site is 5.19 g, within the low marsh zone while the maximum carbon amount is 158.57 g (which is also an outlier) within the mid to high marsh zone. The following maximum carbon amount is 75.14 g within the low marsh zone. The reference site has a minimum carbon amount of 9.53 g within the shoreline zone, and the maximum carbon amount is 295.39 g within the low marsh zone. The mean values for organic carbon from the study site and reference site were 25.09 g and 62.69 g, respectively. The median values were 21.01 g and 47.82 g for the study and reference site, respectively.

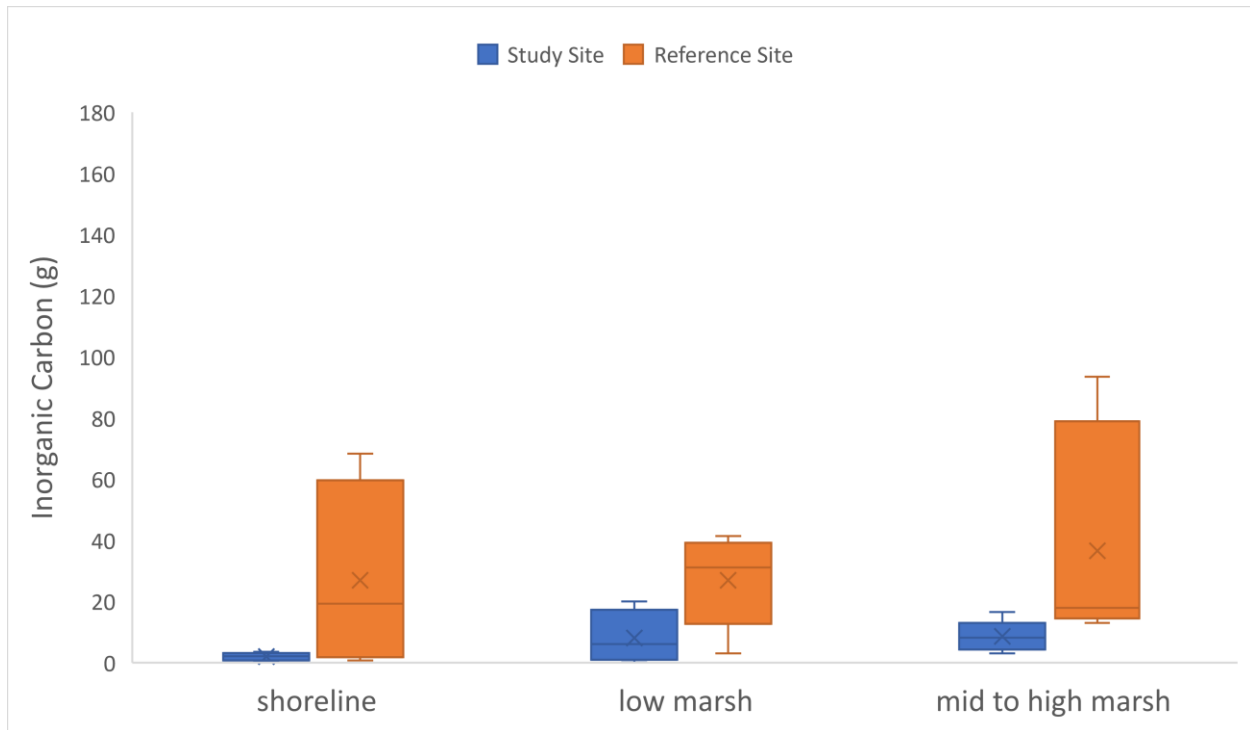


Figure 48. Inorganic carbon at the Study and Reference Sites, within the shoreline, low marsh and mid to high marsh zones (x represents the mean within the data range).

Overall, the inorganic carbon amounts at the study site (SHP) are much lower than the organic carbon values at the reference site (SHP_R). The minimum inorganic carbon amount recorded at the study site is 0.12 g, within the shoreline marsh zone while the maximum inorganic carbon amount is 20.03 g within the low marsh zone. However, the minimum inorganic carbon amount at the reference site is 0.74g within the shoreline zone, while the maximum inorganic carbon recorded is 78.91 g, found within the mid to high marsh zone. The mean values for inorganic carbon from the study site and reference site were 6.41 g and 31.15 g, respectively. The median values were 5.52 g and 31.19 g for the study and reference site, respectively.

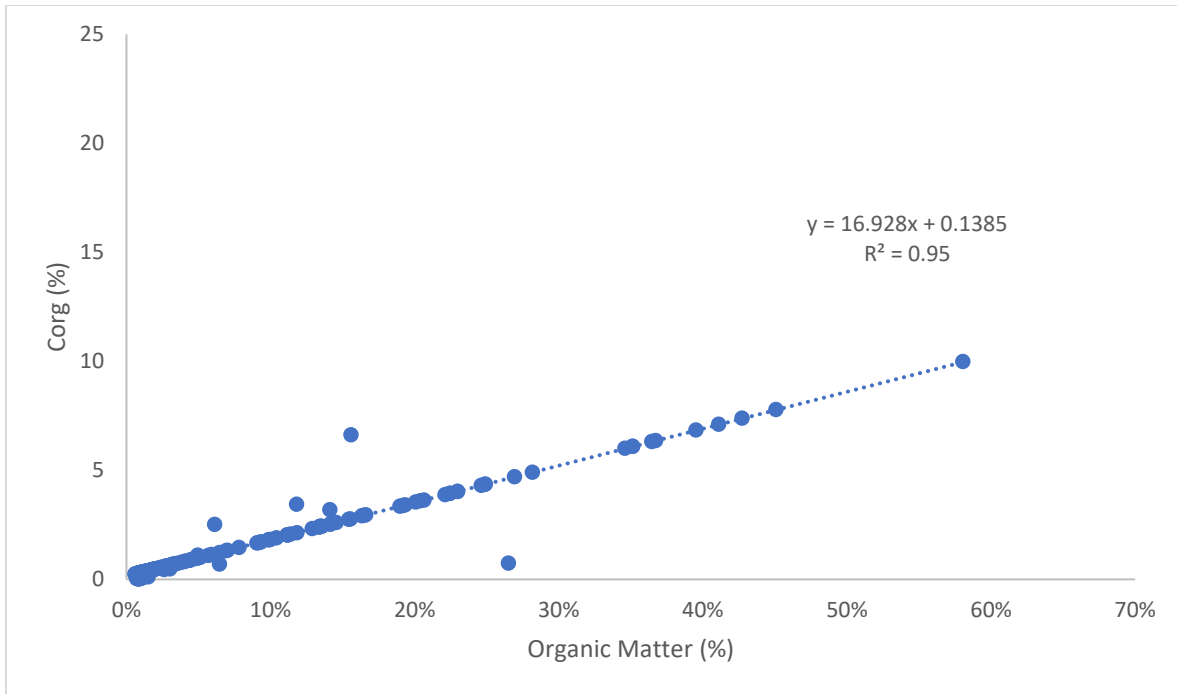


Figure 49. Percentage of Organic Carbon and Organic Matter from LOI at both the Reference and Study Sites.

Figure 49 shows the relationship between organic carbon and organic matter at both the Reference and Study sites. The equation was generated from data obtained from the lab and through extrapolation.

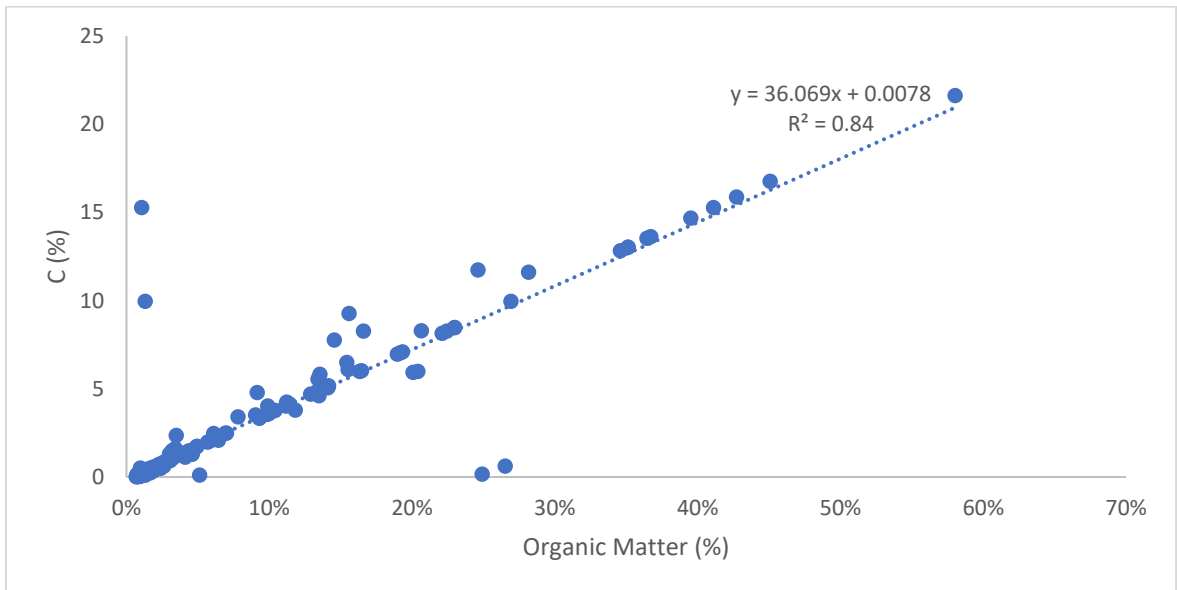


Figure 50. Percentage of Total Carbon and Organic Matter at both the Reference and Study Sites.

There is a linear relationship between the total carbon and the organic matter present at both sites and within a core. The R^2 value is 0.95 which is closer to 1 compared to the R^2 value of the total carbon and Organic Matter, which is 0.84. The data were analyzed using R. First, a Welch two-sample t-test was performed to determine the p-values for total carbon, organic carbon, and inorganic carbon. The p-value for total carbon was 0.0053, for organic carbon it was 0.0347, and for inorganic carbon, it was 0.0178. Next, a two-way ANOVA was conducted to analyze the changes in carbon content as we advance along the marsh from the shoreline to low marsh, and then to mid to high marsh areas. This analysis revealed that there was a statistically significant interaction between total carbon content and marsh zone ($F(5, 35) = 2.678$, p-value = 0.03758).

A separate two-way ANOVA test was performed to analyze the changes in organic carbon along the marsh. This test revealed that there was a statistically significant interaction between organic carbon content and marsh zone ($F(5, 35) = 2.732$, p-value = 0.0347). Finally, the changes in inorganic carbon within each marsh zone were analyzed. The results showed a statistically significant interaction between inorganic carbon content and marsh zone ($F(5, 23) = 3.458$, p-value = 0.0178).

4.5. Bulk Density, Organic, and Total Carbon changes with core depth

The changes in the bulk density, organic and total carbon can be observed with depth and by increment, within each marsh zone. The figures below show that the total carbon at the study site increases by marsh zone, with the mid to high marsh zone having the largest amounts of organic carbon and total carbon. The mid to high marsh zone has larger amounts of organic and total carbon within the 30-cm depth; we start to see a steady decrease in those values between the 30 and 50-cm depth. In contrast, the bulk density values increase consistently throughout the 50 cm depth. The shoreline and low marsh zone display low values of organic and total carbon, both graphs are

similar in magnitude and pattern within these zones. We do not expect to find large amounts of carbon in the shoreline and low marsh zones.

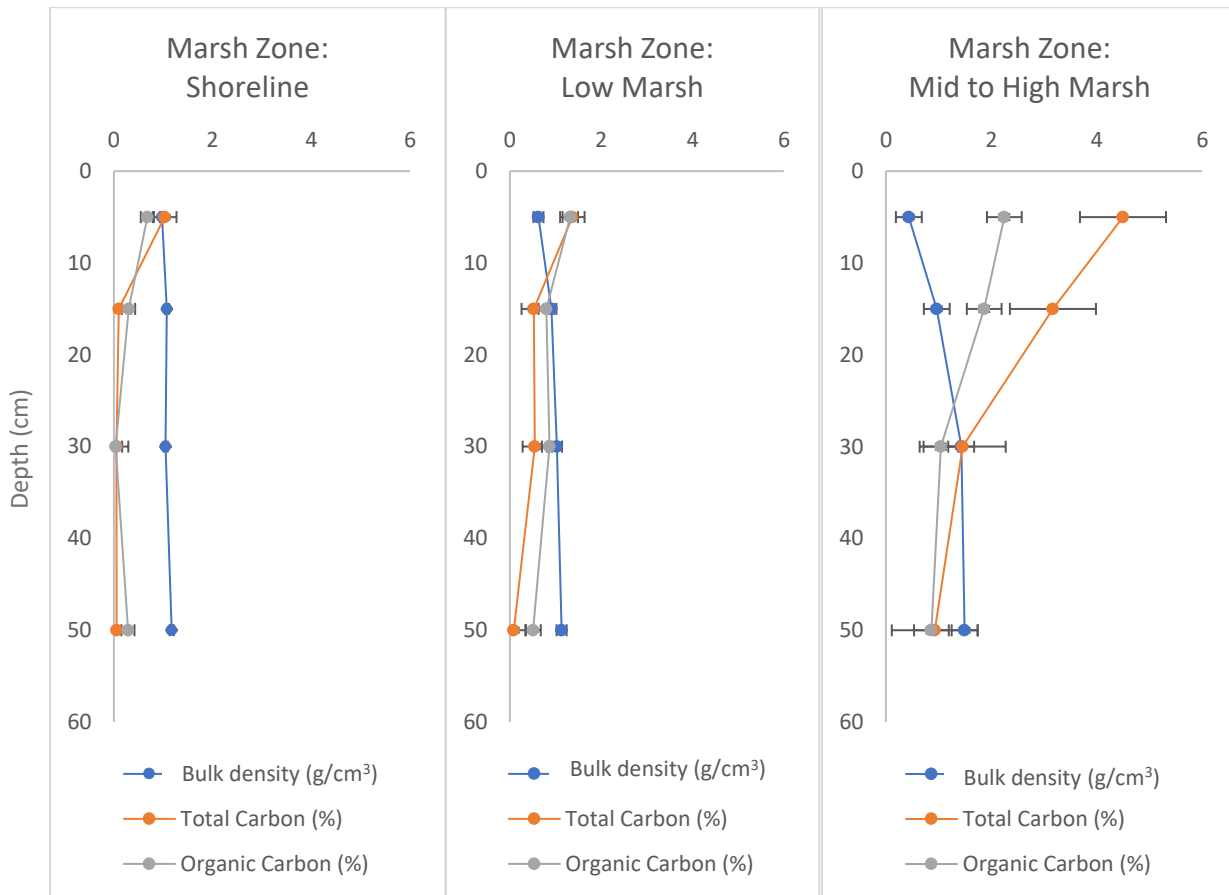


Figure 51. Changes with depth in bulk density, organic carbon, and total carbon for each marsh zone at the study site (SHP).

Overall, the total carbon, organic carbon and inorganic carbon values are much higher at the reference site than at the study site. The graphs below show the changes in the organic and total carbon content at the reference site. A clear pattern of increase can be observed as we advance from the shoreline zone to the low and mid to high marsh zone. The graphs also show that more carbon is stored within the 30 cm depth compared to the last 20 cm of the total 50 cm length of the cores. As we advance in depth, we see a steady decrease nearing 0 for the organic and total carbon.

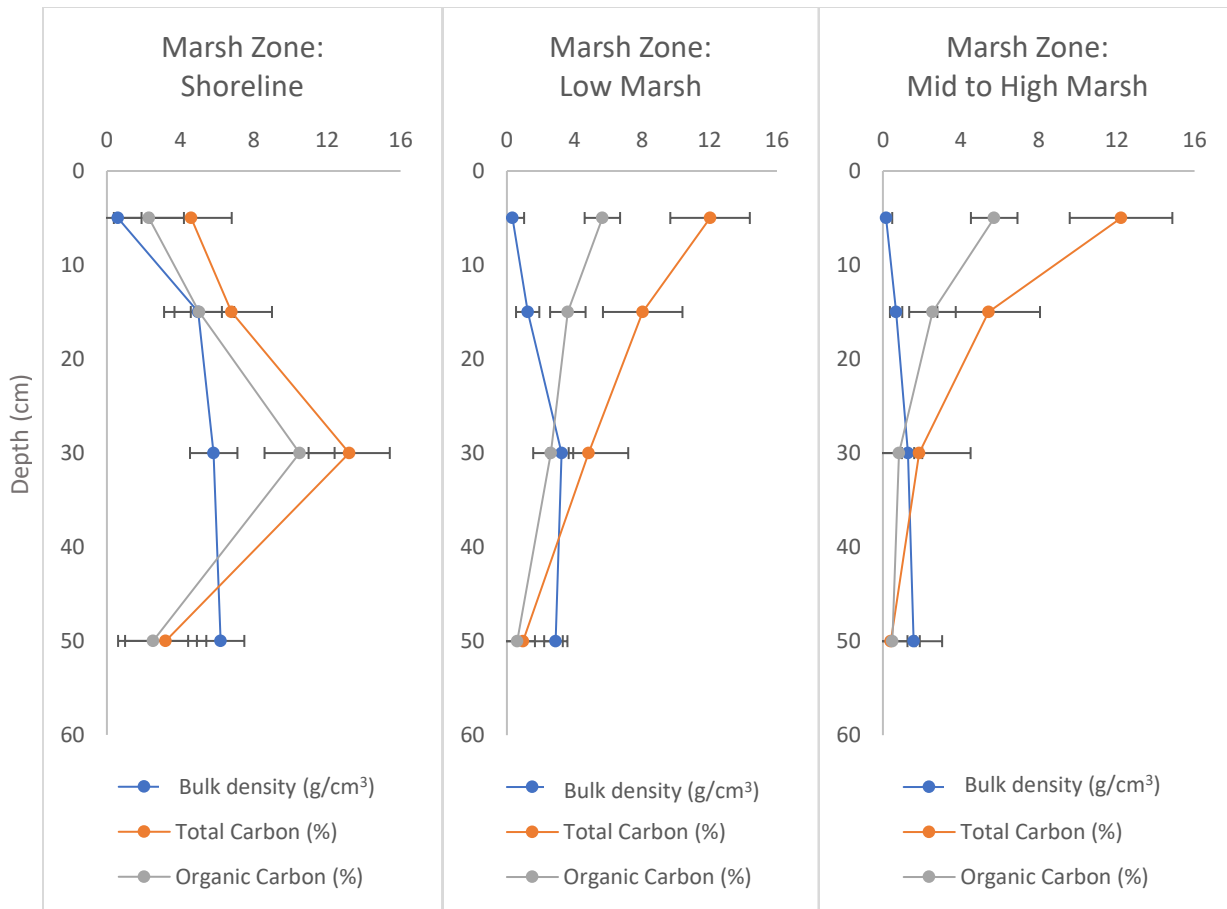


Figure 52. Changes with depth in bulk density, organic carbon, and total carbon for each marsh zone at the study site (SHP_R).

The general trend with changes in bulk density, organic and total carbon, is an increase within the first 30 cm, and a significant decrease as we go deeper into the 40 and 50 cm zone. This pattern can be observed at the reference site especially within the low and mid to high marsh zones. There is also sharp increase observed within the shoreline zone at the 30 cm depth, where the bulk density, total carbon and organic carbon peaked.

Chapter 5: Discussion

5.1. Research objectives and interpretation

The main objective of the research was to quantify the salt marsh functions that support the delivery of ecosystem services of an anthropogenically modified salt marsh and a natural salt marsh and compare how the functions of these ecosystem services might vary. I measured wave energy dissipation, habitat, primary productivity, and blue carbon. This research demonstrated that an anthropogenically modified salt marsh does support the delivery of ecosystem services, particularly wave energy dissipation. While the other salt marsh functions, specifically habitat and primary productivity, were better supported at the reference site, this research shows differences in the organic, inorganic, and total carbon values found at both sites. With the results obtained from the research, I was able to answer the initial research questions which were whether an anthropogenically modified salt marsh performs functions that support ecosystem services (wave energy dissipation, habitat, primary productivity, blue carbon), and how the ecosystem services of an anthropogenically modified salt marsh compare to those of a natural salt marsh.

The value of salt marsh ecosystem services can be understood through the quantification of their functions. This is essential when communicating the importance of salt marshes, both from an economic and conservation perspective. Quantifying the functions of ecosystem services at the study and reference sites (SHP and SHP_R) provided an in-depth understanding of how these ecosystem services are connected, and often dependent on each other.

5.2. Hydrology as a driver for salt marsh processes

A vital component that links these ecosystem services is hydrology. This is a key driver for all salt marsh processes in its structure and function. Ensuring optimal flow of water in and out of the site is also essential in salt marsh restoration, both directly and indirectly. Without appropriate

hydrology, we cannot expect a functional salt marsh (Allen, 2000; Byers & Chmura, 2014). Processes such as sedimentation, accretion, erosion, carbon sequestration and storage, nutrient uptake, water filtration, wave energy attenuation, and plant growth, are all facilitated by the presence of water and its movement (Allen, 2000; Byers & Chmura, 2014). The study site (SHP) has impeded water movement due to existing remnants of a wooden wall which was initially installed as a means of storm protection. An impediment in water flow in turn had an impact on the ecosystem services at the study site, which will be discussed within this chapter.

5.3.Wave energy dissipation

The presence of vegetation plays an active role in supporting wave energy dissipation. Wave energy dissipation is a function of a protective service that is dependent on other factors such as the wave height and water depth (Vuik et al., 2016). Wave attenuation occurs when large waves hit the bottom, and are subjected to bottom friction, forcing the wave to break upon impact with the bottom of the bed. Stem density and the physical plant properties also influence wave attenuation (Anderson & Smith, 2014; Maza et al., 2015; Lei & Nepf, 2019; Baker et al., 2022). The morphology of plants plays a vital role in attenuation, as plants that are more flexible are likely to bend and sway on the impact of an oncoming wave, reducing the drag force (van Veelen et al., 2020); in my study, *S. alterniflora* exhibited those characteristics at both the study and reference sites, within the low marsh area. Plant flexibility can play a significant role in wave attenuation, especially in hydrodynamic settings that can induce plant bending and motion. In literature, the highest wave attenuation was observed for plants with higher stiffness (Lei & Nepf, 2019; Paul et al., 2012). When regarded on a biomass basis, both flexible and rigid vegetation can lead to the same wave dissipation (Bouma et al., 2010; Maza et al., 2022). Where there is higher above-ground biomass, an increased wave energy dissipation is expected (Maza et al., 2015; Ondiviela et al.,

2014). I observed this trend within my dataset where the reference site had greater biomass than the study site, therefore a greater obscuration ratio, and in turn a greater wave attenuation at the reference site compared to the study site.

Where complete dissipation was reached and achieved, the impact of vegetation cannot be overlooked. For example, Events 1-3, show complete wave dissipation being reached, where the wave heights recorded are 0 by the time the waves reach RBR 4 – this is true for both the study and reference sites, however the reasons vary. Evidently, the presence of vegetation has a major impact at the reference site compared to the study site. As the waves travel along the transect, the vegetation behaves as an obstruction and provides a friction surface, reducing the wave heights to 0. The water depth values compared to the vegetation heights recorded show that the vegetation occupied the entire water column throughout those events hence the complete wave attenuation (*Table 6; Table 8*).

The reference site overall has much smaller waves due to the site being sheltered and having limited fetch. The similar values in maximum wave heights at RBR 1 and RBR 2 can be attributed to the fact that RBR 2 was deployed at the marsh edge and recorded similar wave values to the instrument in the open water. It is also important to consider that the distance between RBR 1 and RBR 2 was 3 m, which when there is no obstacle or any other form of obstruction, will lead to similar maximum wave heights being recorded at RBR 2. The maximum wave heights and water depth values recorded were different at each station. This was also early in the season where the marsh was fully vegetated. The reference site is a natural salt marsh which is fully vegetated, whereas the study site has only patches of vegetation cover due to disturbance. Undoubtedly, the rock sill at the study site provides a friction surface for oncoming waves to be dissipated, however, the rock sill does not occupy the entire water column (the rocks are approximately 0.3 m of an

average 1.1 m peak water level). The presence of rocks may explain why a longer distance is required for dissipation to occur – even then, the average wave reduction is not more than 32% within a 22 m distance. In contrast, the study site has an average wave reduction of 70% within 5 m of the transect (*Table 6*). The average wave reduction percentages used were obtained from Event 3, which was within the same period. The exponential wave decay constant (β) was 0.04 m^{-1} and 0.12 m^{-1} , for the study and reference sites, respectively, which depicts that vegetation characteristics and transect length have an impact on wave energy dissipation in our research.

In comparing the results from our study site (SHP) and the reference site (SHP_R) with existing literature, several key similarities and differences emerge. The study site (SHP) has a maximum water depth ranging from (1.32 to 1.76 meters) (*Table 8*) while Möller et al. (1999) presents a maximum water depth over the marsh platform of 1.39 meters, which is slightly higher than our recorded least value of maximum water depth. Additionally, the exponential wave decay constant (β) recorded in Möller et al. (1999) was 0.005 m^{-1} which is much lower compared to the exponential wave decay constants (β) at the study and reference sites in all events (study site: 0.02, 0.02, and 0.04 m^{-1} ; reference site 0.12 m^{-1}). When comparing the maximum significant wave heights, Möller (2006) reports maximum significant wave height of 0.32 m which is within the range observed at SHP (0.24 to 0.43 meters). However, Möller (2006) notably reports a transect length of 10 meters, which is shorter than the 22-meter transect utilized in our research. When we factor in the vegetation characteristics, Möller’s study has *Sporobolus anglicus*, and *Salicornia spp.*, species which are likely to have more surface area and provide more friction, resulting in a decrease maximum significant wave heights over a shorter distance (10 m), compared to the transect at SHP (22 m). The study site (SHP) has *S. alterniflorus* only (which means less surface area and less friction) within the transect – this could explain the decrease in maximum significant

wave heights over a 22 m distance. This means that the species morphology has an impact on the average wave height reduction, and how long the waves can travel before completely dissipating.

In comparing Möller (2006) with the reference site (SHP_R) in our research, there are significant parallels and distinctions that emerge. Möller (2006) reports a maximum water depth over the marsh platform of 0.70 meters, which is slightly higher than the range observed at SHP_R (0.34 to 0.54 meters). Additionally, there is a notable difference in the maximum significant wave height recorded by Möller (2006), which is 0.32 meters, while the range for SHP_R is 0.031 to 0.15 meters. Möller (2006) reports a transect length of 10 meters, which is twice as long as the 5-meter transect observed at SHP_R. However, the exponential wave decay constant (β) recorded in for Möller et al. (2006) was ranged from 0.012 – 0.019 m^{-1} , and 0.016 – 0.022 m^{-1} which is also much lower compared to the exponential wave decay constants (β) reference site (0.12 m^{-1}).

Table 8. Wave heights and water depths for field studies with similar vegetation species to those found in salt marshes in Canada, that quantify wave energy dissipation (modified from Table 1 in Tempest et al., 2015, and Table 1 in Vuik et al., 2016).

Publication	Vegetation Characteristics	Maximum water depth over marsh platform, h (m)	Maximum significant wave height, H_s (m)	Transect Length (m)	Average wave height reduction (%)	Exponential wave decay constant, β (m^{-1})
Jadhav et al. (2013)	<i>Sporobolus alterniflorus</i>	0.80	0.39			
Knutson et al. (1982)	<i>Sporobolus alterniflorus</i>	0.95	0.32*	10 20 30	65 87 94	0.105 0.102 0.094
Möller et al. (1999)	<i>Limonium vulgare</i> , <i>Aster tripolium</i> , <i>Atriplex portulacoides</i> , <i>Salicornia sp.</i> , <i>Spartina ap.</i> , <i>Sueda maritima</i> , <i>Plantago maritima</i> , <i>Puccinellia maritima</i>	1.39	0.58	180	61	0.005
Möller (2006)	<i>Sporobolus anglicus</i> , <i>Salicornia sp.</i>	0.70	0.32	10 10	15-20 11-17	0.016-0.022 0.012-0.019

Yang et al. (2012)	<i>Scirpus, Sporobolus alterniflorus</i>	1.61	0.73	51	79	0.031
Ysebaert et al. (2011)	<i>Sporobolus alterniflorus, Scirpus mariqueter</i>	1.86	0.64	>50	80	0.032
Vuik et al. (2016)	<i>Sporobolus anglicus,</i>	1.90	0.69	0.69	50	60 (h = 0.4) 20 (h > 0.8)
Vuik et al. (2016)	<i>Scirpus maritimus</i>	1.27	0.59	0.59	50	80 (h = 0.4) 50 (h = 0.8)
Wayne (1976)	<i>Sporobolus alterniflorus</i>			20	71	0.063
SHP (study site)	<i>Sporobolus alterniflorus</i>	1.32	0.24	22	15	0.02
		1.76	0.43	22	32	0.02
		1.54	0.27	22	27	0.04
SHP_R (reference site)	<i>Sporobolus alterniflorus, Sporobolus pumilus</i>	X	X	5	X	X
		0.34	0.031	5	5	X
		0.54	0.15	5	70	0.12

5.4. Vegetation cover, Primary productivity and Essential Nutrients

Salt marshes are known to support habitat for both plants and animals. In my research, having investigated the plant cover at each site, the presence of vegetation species and lack thereof can be attributed to many factors such as the soil nutrient content, variations in elevation, site disturbance, and most importantly, hydrology (Chang et al., 2016, Lyon and Lyon, 2011). The distribution of vegetation species is also due to edaphic factors such as the presence or absence of essential nutrients that promote plant growth (Broome et al., 1988, Levine et al., 1998). The distinct zonations that form within the salt marsh system are a combination of these contributory factors (Pennings and Bertness, 2001). Results from this research show that the key nutrients to plant growth are Nitrogen, P₂O₅, and K₂O, which are present at both the study and reference sites. Nitrogen plays a vital role as a component of amino acids (these are the building blocks of proteins) and of chlorophyll (Montgomery, 2021). A limitation in nitrogen prompts responses that lead to an increase in nitrogen uptake and utilization (Montgomery, 2021). Often, these responses can

involve structural or developmental changes such as changes in the morphology of roots (Montgomery, 2021). Root development may be restricted to conserve energy for survival or reproduction. In most cases, plants respond to limited nitrogen availability by creating synergistic relationships with nitrogen fixing bacteria roots (Montgomery, 2021). Phosphorus is also an important nutrient which is naturally present at relatively low levels in soils (Montgomery, 2021). It is vital for development, growth, and maintenance as it is a component of the nucleic acids DNA and RNA, and the energy storage molecule ATP and the phospholipids found in cell membranes (Montgomery, 2021). A phosphorus deficiency can result in an increase in phosphorus solubility by altering soil acidity through protein excretion (Montgomery, 2021). K_2O also plays an important role in plant growth and development. Potassium regulates osmotic pressure and balances cations and anions in the cytoplasm (Xu et al., 2020). Overall, Potassium affects the absorption and utilization of the other nutrients required by plants (Xu et al., 2020).

While the statistical tests reveal that there are no significant differences attributed to site, a few factors that may impact the essential nutrients (Nitrogen, P_2O_5 , and K_2O) explain the differences in biomass and primary productivity values. The sparse vegetation patterns observed at the study site (SHP), reflect its poor hydrology. Due to the existing wooden wall, which acts as a barrier to the salt marsh area, direction of water flow and movement is altered. In some instances, the water penetrates through the cracks and open crevices, however, due to this barrier, the marsh is not entirely flooded, specifically in the higher marsh area. This affects the growth of high marsh species such as *Sporobolus pumilis*, a species that thrives in the higher marsh area, with sufficient nutrients and adequate saturation (Pennings and Bertness, 2001). While nine species were detected at the study site (SHP), 20 species were detected at the reference site (SHP_R). This can be explained by the overall marsh health. The reference site (SHP_R), is a natural marsh that has not

encountered any disturbance to alter the species existence and distribution. However, the study site (SHP), has been affected by numerous anthropogenic changes at the site. The construction of the wooden wall altered the soil nutrient composition, and the flow patterns at the site which in turn altered the zonation pattern and the species composition at the site (Tables A7 and A8). The two dominant species *Sporobolus alterniflorus* and *Sporobolus pumilus*, which are significantly abundant at SHP and SHP_R reflect these impacts. The average plot cover for *Sporobolus alterniflorus* was equivalent between sites, whereas for *Sporobolus pumilus*, it exhibited a decrease between the sites. The reference site (SHP_R) had more cover of *Sporobolus pumilus*. *S. pumilus* takes longer to colonize a site and is not typically present within a high marsh zone in the first 1 – 3 years of restoration. At both sites, the shoreline zones presented lower Nitrogen values, however, where vegetation was present, in the low marsh, and especially the mid to high marsh zone, the nitrogen values are higher at both sites. A study carried out by Craft et al., (1991) at 10 different marshes, found nitrogen concentrations in estuarine marsh soils that ranged from 0 to 1.63%, which is a slightly wider range compared to the results obtained from our research (Table A7 and Table A8).

The other essential nutrients such as P_2O_5 and K_2O , range from 50 to 93 kg/ha and 251 to 735 kg/ha, respectively at the study site, however, the reference site values range from 19 to 167 kg/ha and 111 to 823 kg/ha, spread throughout the marsh zones. Overall, the reference site had a higher vegetation percent cover compared to the study site, this could be explained by the fact that plants can increase root biomass where soils are nutrient rich (Montgomery, 2021). Where there needs to be root modification, because of soil nutrient changes, this can affect the aboveground biomass. When the nutrients are limited, plants often shift energy away from shoots and toward roots as well as toward transport proteins that are involved in nutrient uptake (Montgomery, 2021).

However, when there is an abundance in nutrients and the roots are taking in healthy amounts of essential nitrate, the hormonal balance shifts and promoting more branching of shoots. Nitrate, which is composed of Nitrogen and Oxygen, is essential as it is used to produce proteins and other critical similar compounds (Montgomery, 2021).

The soil nutrient content significantly influences vegetation cover, subsequently impacting aboveground biomass values, and the overall primary productivity. In a study carried out on a salt marsh in the Yangtze Estuary, the average aboveground biomass recorded was $43 \text{ g}\cdot\text{m}^{-2}$ (Yuan et al., 2020). This value was closer to the average aboveground biomass value recorded for SHP_R ($44.77 \text{ g}\cdot\text{m}^{-2}$) and nearly twice as much as the average aboveground biomass recorded at SHP ($28.54 \text{ g}\cdot\text{m}^{-2}$) – however, the site conditions of the Yangtze Estuary were quite different compared to our study and reference site. When comparing the biomass values of the study site (SHP) to those recorded at the reference site (SHP_R), there is an evident pattern. The biomass values recorded at SHP were lower than those at SHP_R due to decreased vegetation cover resulting from marsh disturbance and alteration of flow patterns.

Another function that was quantified was habitat – with a focus on vegetation. Undoubtedly, there is a connection between primary productivity values and vegetation cover. Plants indirectly impact coastal hydrodynamics through the belowground contribution of decaying roots, enriching soil organic matter, leading to slower erosion rates in fine, organic-rich soils compared to mineral soils in wetlands (Gedan et al., 2011). Existing marsh vegetation stabilizes salt marshes by binding the soil with roots and reducing erosion rates, as highlighted by Feagan et al. (2009).

Belowground biomass is also important in these systems but was not sampled to preserve the vegetation at the already degraded study site. Aboveground biomass was more important in

this study as we were aiming to compare that data with the average plant percent cover which was sampled at the selected vegetation plots. Overall net primary productivity is measured by combining the above and belowground biomass and tracking the change over time. Productivity is a rate, whereas biomass is a state variable (indicative of conditions at a particular time). Marshes with vegetation have an increased capacity for accretion compared to those that are unvegetated (Shepard et al., 2011). In this study, I focused on the plant percent cover at each plot and the species present at the selected plots. The potential for measuring accretion can be explored in another study, building on the vegetation data I collected.

5.5. Blue Carbon

5.5.1. Total Carbon

The other ecosystem service that I quantified in this study is Blue Carbon – in which organic, inorganic, and total carbon values were analyzed. There are statistically significant differences found at both sites. The variation in the carbon amounts can be attributed to numerous factors. Firstly, as shown in *Figure 46*, the reference site has more total carbon per core compared to the study site. The total carbon increases as one advances from the shoreline to the high marsh zone. The increase in the total carbon amounts can be attributed to the presence of vegetation, which promotes primary productivity. The reference site has larger amounts of total carbon and overall, more vegetation percent cover. Secondly, the lower carbon amounts at the study site can be explained by the fact that the site has minimal to almost no vegetation cover in most areas. Since the sediment cores were collected adjacent to the vegetation plots, it would make sense that the shoreline has smaller amounts of total carbon as some of the plots had no vegetation cover at all. The increase in the carbon amounts as we advance into the marsh can also be attributed to the increase in vegetation cover.

5.5.2. Organic Carbon

When observing the trends in organic carbon, the low marsh zone has the largest amount of organic carbon for both sites (*Figure 47*). This is due to the inundation patterns that can be observed in the low marsh area. The high marsh zone is flooded periodically, however not as consistently as the low marsh zone. This is a microtidal zone, hence the vegetation within the low marsh zone is set out to thrive and outperform the vegetation in the shoreline (if any) and mid to high marsh zones. In a study carried out by Craft et al., (1991), organic carbon concentrations in estuarine marsh soils were found to be between 0.08% and 28 %. This is a much wider range compared to the 0 to 10% range of organic carbon at both the study and reference sites. In another study carried out on a salt marsh in Southern India, the organic carbon ranged from 0.03 to 3.81% (Kaviarasan et al. 2019). This range is much lower than the values we obtained in our research. In another study by Perera et al., (2022) where the variation of organic carbon with depth (50 cm) was assessed, the organic carbon values ranged from 0.5 to 3.8% at four different sites. This range of values is similar to those observed at the study site (SHP); however, the reference site (SHP_R), has a much wider range of values for the organic carbon.

When comparing the organic carbon values by marsh zone, there is a significant difference amongst the shoreline, low marsh and mid to high marsh values in our research. A study which investigated the organic carbon in the mangrove-salt marsh transition zones had different results compared to our research. Vaugh et al., (2019) recorded a range of 10.6–14.4% of organic carbon in the transition zone, 8.4–10.8% in the mangrove and 7.6–12.1% in the high marsh zone. For both the study and reference sites, the range of organic carbon is 0 – 2% and 0 – 7%, respectively within the high marsh zone. These ranges are much lower than what was observed by Vaugh et al., (2019). A primary explanation for that is the differences in vegetation species and flow patterns at the

Northern Florida sites. For example, the species composition included *Sporobolus alterniflorus* and *Batis maritima* (which was dominant in the transition zone between mangrove and salt marsh). Other salt marsh species that were found in the low marsh zone include *Spartina bakeri*, *Distichlis spicata*, *Salicornia virginica*, and *Sueda* spp., all of which are completely different from the low marsh species found at both our sites (SHP and SHP_R).

5.5.3. Inorganic Carbon

The inorganic carbon values follow a similar pattern to the organic and total carbon values, where the inorganic carbon increases as we advance within the salt marsh from the shoreline zone to the low marsh, to the mid to high marsh zone. This can be attributed to the presence of calcium carbonate shells within these marsh zones, especially along the shoreline at the reference site. However, there are smaller inorganic carbon values at the study site due to the removal and reconstruction of the wooden sea wall, which may have led to these shells being buried beyond a 50 cm depth over time. Another factor that could have contributed to the smaller values for the inorganic carbon content at the study site was the open area along the broken-down wooden wall, which promoted the movement of water through the shoreline, causing a shift in the sediment and destabilising any calcium carbonate shells that settled in that marsh zone.

Overall, the anthropogenically modified salt marsh performs functions that support ecosystem services. However, in comparing the quantity of the functions of these ecosystem services, the results from the research show that the anthropogenically modified salt marsh ecosystem services were compromised compared to those of the natural salt marsh. A natural salt marsh functions fully as the salt marsh processes are not hindered by any form of disturbance, hydrology, soil nutrient changes, which in turn affect primary productivity, vegetation cover and

the ability of the salt marsh to dissipate wave energy. The functions of ecosystem services are connected; hence the overall function of the entire ecosystem can be impacted by this connectivity.

While this research provides valuable insights into the comparison of functions of ecosystem services between anthropogenically modified and natural salt marshes, a few limitations must be acknowledged. When capturing images with the portable photo frame, the site conditions must be ideal (no rain, snow, wind, or any other weather element that may affect the quality of the images). This will ensure that the classification and product are accurate for the obscuration ratio calculations. In our research, one of the sampling days was extremely windy, hence we could not capture any images for the classification. Another limitation to this research was that I could not entirely assess the effectiveness of wave energy dissipation throughout the entire marsh. Wave energy dissipation is scale dependent; while I set up a transect to understand the wave energy and vegetation interactions within a part of the salt marsh, results could vary in another part of that same salt marsh. This is a challenge when there is a need to extrapolate findings to broader spatial extents.

Chapter 6: Conclusion and Future Recommendations

The research in the present thesis has shown that anthropogenically modified salt marshes can perform functions that support ecosystem services. It also shows that natural salt marshes are vital as they support ecosystem services at a much higher potential compared to the marshes that have been disturbed or degraded. Quantifying the functions of the ecosystem services offered by anthropogenically modified salt marshes pre-restoration is a key component in ensuring the success of a restoration project. Numerical values generated from these studies are essential to not overestimate or underestimate the success of a restoration project.

In my research, I found that the anthropogenically modified salt marsh supports vegetation species and primary productivity, has the ability to sequester carbon just as the natural salt marsh, and it can dissipate wave energy. There are many factors that can affect how salt marshes support ecosystem services, including the presence of vegetation cover at a site, and existing barriers play a role in wave breaking and affect oncoming waves from reaching the mainland. Other factors that may lead to the difference in the primary productivity of each site include the soil type and the nutrients present in the soil. The reference site was found to have higher primary productivity due to its diverse vegetation species and the extent of the vegetation cover at each plot, compared to the study site which had only patches of vegetation and a less diverse list of species present. In turn, the carbon and total carbon at the reference site was found to be higher than at the study site. The salt marsh at the reference site is not disturbed or degraded, and the carbon that is sequestered has not been affected by human changes at the site such as the construction of the sea wall. However, the study site has been affected by numerous changes in an effort to protect the area from storm surges.

Future recommendations include an extended monitoring program at the modified salt marsh site to monitor the trajectory of restoration. Now that the sill has finally been constructed (Summer 2023) after lengthy delays, post construction data will need to be obtained to see if the restored marsh eventually ecologically aligns with the natural salt marsh. Extended monitoring is a crucial aspect when it comes to salt marsh restoration as it provides valuable data on dynamic changes in vegetation, sediment deposition, and hydrodynamic conditions. This allows for a comprehensive understanding of the ecosystem's evolution and how the trajectory of restoration has progressed. By implementing extended monitoring, we can ensure that the assessment of restoration benefits and the ecosystem service benefits are not overestimated. If any issues emerge, the restoration strategies can be revised, or adaptive monitoring can be implemented.

This research raised some interesting questions about the overestimation and underestimation of functions of ecosystem services post-restoration, whereby a shifting baseline exists due to environmental processes. While these environmental processes play a vital role in shaping the resilience of the salt marsh ecosystem during restoration, it also presents challenges in accurately estimating the functions of ecosystem services - this can affect the integrity or credibility of the research. One way to combat this challenge is to sample at different times of the year, to have a wholesome representation of the site under different conditions, ensuring an enriched dataset.

An interesting avenue for research would be the use of baseline data to further investigate marsh viability pre- and post- storms. With living shorelines, or vegetated marshes, there is also a need to investigate the use of selected vegetation species for marsh plantings in restoration projects.

This research addressed whether anthropogenically modified salt marshes perform functions that support ecosystem services. The empirical data collected are essential for climate change adaptation and mitigation studies that will inform policymaking and decisions on coastal protection and restoration. Understanding how these coastal systems function through site-specific data allows for the development of tailored adaptation strategies. The findings will be instrumental in guiding policymaking for coastal protection and restoration, ensuring that strategies are grounded in empirical evidence. The data will also support the planning and assessment of restoration projects, ensuring accurate evaluations of ecosystem services. Key takeaways from this research include the importance of understanding that natural salt marshes better support functions of ecosystem services compared to anthropogenically modified salt marshes. The empirical data obtained are vital for creating site-specific adaptation and restoration strategies. Additionally, extended monitoring is necessary for precise assessment of salt marshes and adaptive management of restoration projects. Lastly, recognizing and accounting for environmental processes is valuable to avoid the over or under estimation of ecosystem services provided by salt marshes.

References:

- Act, C. E. A. (2013). Fisheries and Oceans Canadian Environmental Assessment Act. Project Effects Determination Report.
- Anderson, M. E., & Smith, J. M. (2014). Wave attenuation by flexible, idealized salt marsh vegetation. *Coastal Engineering (Amsterdam)*, 83, 82–92.
- Allen, J. R. (2000). Morphodynamics of Holocene salt marshes: a review sketch from the Atlantic and Southern North Sea coasts of Europe. *Quaternary Science Reviews*, 19(12), 1155-1231.
- Allen, J. R., & Pye, K. (Eds.). (1992). *Saltmarshes: morphodynamics, conservation and engineering significance*. Cambridge University Press.
- Baker, S., Murphy, E., Cornett, A., & Knox, P. (2022). Experimental study of wave attenuation across an artificial salt marsh. *Frontiers in Built Environment*, 8, 893664.
- Berman, M., Baztan, J., Kofinas, G., Vanderlinden, J. P., Chouinard, O., Huctin, J. M., ... & Thomson, K. (2020). Adaptation to climate change in coastal communities: findings from seven sites on four continents. *Climatic Change*, 159, 1-16.
- Bertness, M. D., Crain, C., Holdredge, C., & Sala, N. (2008). Eutrophication and consumer control of New England salt marsh primary productivity. *Conservation Biology*, 22(1), 131-139.
- Bertness, M. D., Crain, C., Holdredge, C., & Sala, N. (2008). Eutrophication and consumer control of New England salt marsh primary productivity. *Conservation Biology*, 22(1), 131-139.
- Big Shippagan Lighthouse* (no date) *LighthouseFriends*. Available at: <https://www.lighthousefriends.com/light.asp?ID=1238> (Accessed: April 5, 2023).
- Blott, S. J., & Pye, K. (2001). GRADISTAT: a grain size distribution and statistics package for the analysis of unconsolidated sediments. *Earth surface processes and Landforms*, 26(11), 1237-1248.
- Bouma, T. J., De Vries, M. B., Low, E., Peralta, G., Tánčzos, I. V., van de Koppel, J., & Herman, P. M. J. (2005). Trade-offs related to ecosystem engineering: A case study on stiffness of emerging macrophytes. *Ecology*, 86(8), 2187-2199.
- Brand, E., Ramaekers, G., & Lodder, Q. (2022). Dutch experience with sand nourishments for dynamic coastline conservation—An operational overview. *Ocean & Coastal Management*, 217, 106008.
- Bridges, T., King, J., Simm, J. D., Beck, M., Collins, G., Lodder, Q., & Mohan, R. (2021). *International guidelines on natural and nature-based features for flood risk management*. USACE.
- Bridges, T. S., Burks-Copes, K. A., Bates, M. E., Collier, Z. A., Fischenich, J. C., Piercy, C. D., ... & Vuxton, E. A. (2015). *Use of natural and nature-based features (NNBF) for coastal resilience*. Vicksburg: US Army Engineer Research and Development Center, Environmental Laboratory, Coastal and Hydraulics Laboratory. Broome, S. W., Craft, C.

- B., & Burchell, M. R. (2019). Tidal marsh creation. In *Coastal Wetlands* (pp. 789-816). Elsevier.
- Brondízio, E. S., Settele, J., Diaz, S., & Ngo, H. T. (2019). Global assessment report on biodiversity and ecosystem services of the Intergovernmental Science-Policy Platform on Biodiversity and Ecosystem Services.
- Byers, S. C., Mills, E. L., & Stewart, P. L. (1978). A comparison of methods of determining organic carbon in marine sediments, with suggestions for a standard method. *Hydrobiologia*, *58*(1), 43-47.
- Byers, S. E., & Chmura, G. L. (2014). Observations on shallow subsurface hydrology at Bay of Fundy macrotidal salt marshes. *Journal of Coastal Research*, *30*(5), 1006-1016.
- Chang, E. R., Veeneklaas, R. M., Bakker, J. P., Daniels, P., & Esselink, P. (2016). What factors determined restoration success of a salt marsh ten years after deembankment? *Applied Vegetation Science*, *19*(1), 66–77. <https://doi.org/10.1111/avsc.12195>
- Coleman, B. D., Mares, M. A., Willig, M. R., & Hsieh, Y. H. (1982). Randomness, area, and species richness. *Ecology*, *63*(4), 1121-1133.
- Cornett, A., Provan, M., Nistor, I., & Drouin, A. (2013). Modelling Coastal Processes At Shippagan Gully Inlet, New Brunswick, Canada.
- Craft, C. B., Seneca, E. D., & Broome, S. W. (1991). Loss on ignition and Kjeldahl digestion for estimating organic carbon and total nitrogen in estuarine marsh soils: calibration with dry combustion. *Estuaries*, *14*, 175-179.
- Darby, F. A., & Turner, R. E. (2008). Below-and aboveground *Spartina alterniflora* production in a Louisiana salt marsh. *Estuaries and Coasts*, *31*(1), 223-231.
- Dasgupta, P., & Treasury, H. M. (2022). The economics of biodiversity: the Dasgupta review. *Odisha Economic Journal*, *54*(2), 170-176.
- Davis, J. L., Currin, C. A., O'Brien, C., Raffenburg, C., & Davis, A. (2015). Living shorelines: coastal resilience with a blue carbon benefit. *PloS one*, *10*(11), e0142595.
- Davidson-Arnott, R., Bauer, B., & Houser, C. (2019). Chapter 9: Coastal Dunes and Aeolian Processes. *Introduction to Coastal Processes and Geomorphology*, (2nd ed.,, pp. 280-342). Cambridge University Press.
- Dawe, N. K., & White, E. R. (1982). Some aspects of the vegetation ecology of the Little Qualicum River estuary, British Columbia. *Canadian Journal of Botany*, *60*(8), 1447-1460.
- Denny, M. (2021). Wave-Energy Dissipation: Seaweeds and Marine Plants Are Ecosystem Engineers. *Fluids*, *6*(4), 151.
- de Schipper, M. A., Ludka, B. C., Raubenheimer, B., Luijendijk, A. P., & Schlacher, T. A. (2021). Beach nourishment has complex implications for the future of sandy shores. *Nature Reviews Earth & Environment*, *2*(1), 70-84.

- Desplanque, C., & Mossman, D. J. (2004). Tides and their seminal impact on the geology, geography, history, and socio-economics of the Bay of Fundy, eastern Canada. *Atlantic Geology*, 40(1), 1–65. <https://doi.org/10.4138/729>
- De Vriend, H. J., van Koningsveld, M., Aarninkhof, S. G., de Vries, M. B., & Baptist, M. J. (2015). Sustainable hydraulic engineering through building with nature. *Journal of Hydro-environment research*, 9(2), 159-171.
- Duarte, C. M., Losada, I. J., Hendriks, I. E., Mazarrasa, I., & Marbà, N. (2013). The role of coastal plant communities for climate change mitigation and adaptation. *Nature climate change*, 3(11), 961-968.
- Ellenberg, D., & Mueller-Dombois, D. (1974). *Aims and methods of vegetation ecology* (p. 547). New York: Wiley.
- Ellis, K., J. Graham, J. Kickbush, and T.M. Bowron. (2021). Shippagan Gully Dredging and Breakwater Construction Project: Conservation Offsetting and Monitoring Plan – FINAL DRAFT. Report No. 47. Halifax, Nova Scotia. Prepared for Department of Fisheries and Oceans – Small Craft Harbours Branch Maritimes and Gulf Regions. p147
- Environment Canada. 2015a. Canadian Climate Normals 1981-2010. Bathurst Climate Station, New Brunswick. Accessed May 13, 2016 at: http://climate.weather.gc.ca/climate_normals/results_1981_2010_e.html?searchType=stnName&txtStationName=Bathurst&searchMethod=contains&txtCentralLatMin=0&txtCentralLatSec=0&txtCentralLongMin=0&txtCentralLongSec=0&stnID=6916&dispBack=1
- Folk, R. L., & Ward, W. C. (1957). Brazos River bar [Texas]; a study in the significance of grain size parameters. *Journal of sedimentary research*, 27(1), 3-26.
- Eyquem, J. L. 2021. Rising Tides and Shifting Sands: Combining Natural and Grey Infrastructure to Protect Canada's Coastal Communities. Intact Centre on Climate Adaptation, University of Waterloo.
- Feagin, R. A., Lozada-Bernard, S. M., Ravens, T. M., Möller, I., Yeager, K. M., & Baird, A. H. (2009). Does vegetation prevent wave erosion of salt marsh edges? *Proceedings of the National Academy of Sciences*, 106(25), 10109–10113. <https://doi.org/10.1073/pnas.48.10.1728>
- Fletemeyer, J., Hearin, J., Haus, B., & Sullivan, A. (2018). The impact of sand nourishment on beach safety. *Journal of Coastal Research*, 34(1), 1-5.
- Foster-Martinez, M. R., Lacy, J. R., Ferner, M. C., & Variano, E. A. (2018). Wave attenuation across a tidal marsh in San Francisco Bay. *Coastal Engineering*, 136, 26-40.
- Garzon, J. L., Miesse, T., & Ferreira, C. M. (2019). Field-based numerical model investigation of wave propagation across marshes in the Chesapeake Bay under storm conditions. *Coastal Engineering*, 32- 46.
- Gedan, K. B., Kirwan, M. L., Wolanski, E., Barbier, E. B., & Silliman, B. R. (2011). The present and future role of coastal wetland vegetation in protecting shorelines: answering recent challenges to the paradigm. *Climatic change*, 106(1), 7-29.

- Gittman, R. K., Peterson, C. H., Currin, C. A., Joel Fodrie, F., Piehler, M. F., & Bruno, J. F. (2016). Living shorelines can enhance the nursery role of threatened estuarine habitats. *Ecological Applications*, 26(1), 249-263.
- Gittman, R. K., Popowich, A. M., Bruno, J. F., & Peterson, C. H. (2014). Marshes with and without sills protect estuarine shorelines from erosion better than bulkheads during a Category 1 hurricane. *Ocean & Coastal Management*, 102, 94-102.
- Greenan, B.J.W., James, T.S., Loder, J.W., Pepin, P., Azetsu-Scott, K., Ianson, D., Hamme, R.C., Gilbert, D., Tremblay, J-E., Wang, X.L. and Perrie, W. (2019): Changes in oceans surrounding Canada; Chapter 7 in (eds.) Bush and Lemmen, *Canada's Changing Climate Report*; Government of Canada, Ottawa, Ontario, p. 343–423.
- Hardisky, M. A., Daiber, F. C., Roman, C. T., & Klemas, V. (1984). Remote sensing of biomass and annual net aerial primary productivity of a salt marsh. *Remote Sensing of Environment*, 16(2), 91-106.
- Hutchinson, I. (1982). Vegetation–environment relations in a brackish marsh, Lulu Island, Richmond, BC. *Canadian Journal of Botany*, 60(4), 452-462.
- Intergovernmental Panel on Climate Change (IPCC). (2022). *Climate change 2022: Impacts, adaptation, and vulnerability. Contribution of Working Group II to the Sixth Assessment Report of the Intergovernmental Panel on Climate Change* (H.-O. Pörtner, D. C. Roberts, M. Tignor, E. S. Poloczanska, K. Mintenbeck, A. Alegría, M. Craig, S. Langsdorf, S. Löschke, V. Möller, A. Okem, & B. Rama, Eds.). Cambridge University Press. <https://doi.org/10.1017/9781009325844>
- Jadhav, R.S., Chen, Q., & Smith, J.M. (2013). Spectral distribution of wave energy dissipation by salt marsh vegetation. *Coastal Engineering*, 77, 99-107.
- John, B. M., Shirlal, K. G., & Rao, S. (2015). Effect of artificial sea grass on wave attenuation-an experimental investigation. *Aquatic Procedia*, 4, 221-226.
- Kaviarasan, T., Dahms, H. U., Gokul, M. S., Henciya, S., Muthukumar, K., Shankar, S., & Arthur James, R. (2019). Seasonal Species Variation of Sediment Organic Carbon Stocks in Salt Marshes of Tuticorin Area, Southern India. *Wetlands (Wilmington, N.C.)*, 39(3), 483–494. <https://doi.org/10.1007/s13157-018-1094-6>.
- Kirwan, M. L., & Murray, A. B. (2008). Ecological and morphological response of brackish tidal marshland to the next century of sea level rise: Westham Island, British Columbia. *Global and Planetary Change*, 60(3-4), 471-486.
- Lei, J., & Nepf, H. (2019). Blade dynamics in combined waves and current. *Journal of Fluids and Structures*, 87, 137-149.
- Leonardi, N., Ganju, N. K., & Fagherazzi, S. (2016). A linear relationship between wave power and erosion determines salt-marsh resilience to violent storms and hurricanes. *Proceedings of the National Academy of Sciences*, 113(1), 64-68.
- Levine, J. M., Brewer, J. S., & Bertness, M. D. (1998). Nutrients, competition and plant zonation in a New England salt marsh. *Journal of Ecology*, 86(2), 285–292. <https://doi.org/10.1046/j.1365-2745.1998.00253.x>

- Luternauer, J. L., Atkins, R. J., Moody, A. I., Williams, H. E., & Gibson, J. W. (1995). Salt marshes. In *Developments in Sedimentology* (Vol. 53, pp. 307-332). Elsevier.
- Lyon, J. G., & Lyon, L. K. (2011). *Wetland identification and deliniation* (2nd ed.). CRC Press.
- Macreadie, P. I., Hughes, A. R., & Kimbro, D. L. (2013). Loss of 'blue carbon' from coastal salt marshes following habitat disturbance. *PloS one*, 8(7), e69244.
- Marani, M., D'Alpaos, A., Lanzoni, S., & Santalucia, M. (2011). Understanding and predicting wave erosion of marsh edges. *Geophysical Research Letters*, 38(21).
- Maza, M., Lara, J. L., & Losada, I. J. (2015). A coupled model of submerged vegetation under oscillatory flow using Navier-Stokes equations. *Coastal Engineering*, 98, 43-57.
- McLeod, E., Chmura, G. L., Bouillon, S., Salm, R., Björk, M., Duarte, C. M., ... & Silliman, B. R. (2011). A blueprint for blue carbon: toward an improved understanding of the role of vegetated coastal habitats in sequestering CO₂. *Frontiers in Ecology and the Environment*, 9(10), 552-560.
- Météoblue.com. No Date. Wind-Rose Diagrams for Lamèque area. Accessed February 27, 2018 at: www.météoblue.com.
- Michener, W. K., Blood, E. R., Bildstein, K. L., Brinson, M. M., & Gardner, L. R. (1997). Climate change, hurricanes and tropical storms, and rising sea level in coastal wetlands. *Ecological applications*, 7(3), 770-801.
- Mitsch, W. J., & Gosselink, J. G. (1993). *Wetlands* (Second edn). Van Nostrand Reinhold, New York, NY; 1993. 672 pp. (ISBN 0-442-00805-8)
- Möller, I., Spencer, T., French, J. R., Leggett, D. J., & Dixon, M. (1999). Wave Transformation Over Salt Marshes: A Field and Numerical Modelling Study from North Norfolk, England. *Estuarine, Coastal and Shelf Science*, 49(3), 411-426.
- Möller, I. (2006). Quantifying saltmarsh vegetation and its effect on wave height dissipation: Results from a UK East coast saltmarsh. *Estuarine, Coastal and Shelf Science*, 69(3), 337-351.
- Montgomery, B. L. (2021). *Lessons from plants*. Harvard University Press.
- Murphy, E., Cornett, A., van Proosdij, D., & Mulligan, R. P. (Eds.) (2024). *Nature-Based Infrastructure for Coastal Flood and Erosion Risk Management – A Canadian Design Guide*. ISBN 978-0- 660-71886-6.
- Nellemann, C., & Corcoran, E. (Eds.). (2009). *Blue carbon: the role of healthy oceans in binding carbon: a rapid response assessment*. UNEP/Earthprint.
- Neumeier, U. (2005). Quantification of vertical density variations of salt-marsh vegetation. *Estuarine, Coastal and Shelf Science*, 63(4), 489-496.
- Neves, J. P., Ferreira, L. F., Simões, M. P., & Gazarini, L. C. (2007). Primary production and nutrient content in two salt marsh species, *Atriplex portulacoides* L. and *Limoniastrum monopetalum* L., in southern Portugal. *Estuaries and Coasts*, 30, 459-468.

- Norström, A. V., Agarwal, B., Balvanera, P., Baptiste, B., Bennett, E. M., Brondízio, E., ... & Spierenburg, M. (2022). The programme on ecosystem change and society (PECS)—a decade of deepening social-ecological research through a place-based focus. *Ecosystems and People*, 18(1), 598-608.
- Ngulube, M.D. (2021). The Wave Dissipation Potential of *Spartina alterniflora* in the Bay of Fundy. [Honors thesis, Saint Mary's University, Patrick Power Library]. Retrieved from: <https://library2.smu.ca/handle/01/29565>
- Nicholls, R. J., Wong, P. P., Burkett, V., Woodroffe, C. D., & Hay, J. (2008). Climate change and coastal vulnerability assessment: scenarios for integrated assessment. *Sustainability Science*, 3, 89-102.
- O'Connor, M. I., Violin, C. R., Anton, A., Ladwig, L. M., & Piehler, M. F. (2011). Salt marsh stabilization affects algal primary producers at the marsh edge. *Wetlands Ecology and Management*, 19(2), 131-140.
- Osborne, P. D., van Proosdij, D., & Camarena, A. (2024). "Chapter 8 – Sediment-Based Solutions." In Murphy, E., Cornett, A., van Proosdij, D., & Mulligan, R. P. (Eds.) Nature-Based Infrastructure for Coastal Flood and Erosion Risk Management – A Canadian Design Guide. ISBN 978-0-660-71886-6.
- Osland, M. J., Enwright, N., Day, R. H., & Doyle, T. W. (2013). Winter climate change and coastal wetland foundation species: salt marshes vs. mangrove forests in the southeastern United States. *Global change biology*, 19(5), 1482-1494.
- Paul, M., & Amos, C. L. (2011). Spatial and seasonal variation in wave attenuation over *Zostera noltii*. *Journal of Geophysical Research: Oceans*, 116(C8).
- Peet, R. K., Wentworth, T. R., & White, P. S. (1998). A flexible, multipurpose method for recording vegetation composition and structure. *Castanea*, 262-274.
- Pennings, S. C., & Bertness, M. D. (2001). Salt marsh communities. In M. D. Bertness, S. D. Gaines, & M. E. Hay (Eds.), *Marine community ecology* (pp. 289–316). <https://doi.org/10.1016/j.scitotenv.2022.153313>
- Perera, N., Lokupitiya, E., Halwatura, D., & Udagedara, S. (2022). Quantification of blue carbon in tropical salt marshes and their role in climate change mitigation. *The Science of the Total Environment*, 820, 153313–153313. <https://doi.org/10.1016/j.scitotenv.2022.153313>
- Pilskaln, C. H., & Paduan, J. B. (1992). Laboratory techniques for the handling and geochemical analysis of water column particulate and surface sediment samples. *Monterey Bay Aquarium Research Institute (MBARI) Technical Report*, 92-9.
- Provan, M., Logan, S., Nistor, I., Cornett, A., & Drouin, A. (2018). Field and numerical investigations of the morpho-hydrodynamic processes of the tidal inlet at Shippagan Gully, New Brunswick, Canada. *Coastal Engineering Journal*, 60(4), 400-422.
- Provan, M., Nistor, I., Cornett, A., & Drouin, A. (2014). Hydrodynamic And Morphologic Modeling of Alternative Design Scenarios For Shippagan Gully, New Brunswick Canada. *Coastal Engineering Proceedings*, (34), 30-30.

- Rabinowitz, T. R. M., & Andrews, J. (2022). Valuing the salt marsh ecosystem: Developing ecosystem accounts. Environment Accounts and Statistics Analytical and Technical Paper Series. *Statistics Canada Catalogue*, (16-001).
- Raposa. (2008). Early Ecological Responses to Hydrologic Restoration of a Tidal Pond and Salt Marsh Complex in Narragansett Bay, Rhode Island. *Journal of Coastal Research*, 10055(10055), 180–192. <https://doi.org/10.2112/SI55-015>
- Rahman, H. T., Sherren, K., & Van Proosdij, D. (2019). Institutional innovation for nature-based coastal adaptation: lessons from salt marsh restoration in Nova Scotia, Canada. *Sustainability*, 11(23), 6735.
- Reed, G., Fox, S., Littlechild, D., McGregor, D., Lewis, D., Popp, J., Wray, K., Kassi, N., Ruben, R., Morales, S. and Lonsdale, S. (2024). For Our Future: Indigenous Resilience Report. Ottawa, Ontario.
- Ravens, T. M., Thomas, R. C., Roberts, K. A., & Santschi, P. H. (2009). Causes of salt marsh erosion in Galveston Bay, Texas. *Journal of Coastal Research*, 25(2), 265-272.
- Richards, C. L., Pennings, S. C., & Donovan, L. A. (2005). Habitat range and phenotypic variation in salt marsh plants. *Plant Ecology*, 176, 263-273.
- Robinson, S. L., & Lundholm, J. T. (2012). Ecosystem services provided by urban spontaneous vegetation. *Urban Ecosystems*, 15(3), 545-557.
- Sales Jr, R. F. M. (2009). Vulnerability and adaptation of coastal communities to climate variability and sea-level rise: Their implications for integrated coastal management in Cavite City, Philippines. *Ocean & Coastal Management*, 52(7), 395-404.
- Schwimmer, R. A. (2001). Rates and processes of marsh shoreline erosion in Rehoboth Bay, Delaware, USA. *Journal of Coastal Research*, 672-683.
- Scyphers, S. B., Beck, M. W., Furman, K. L., Haner, J., Keeler, A. G., Landry, C. E., ... & Grabowski, J. H. (2020). Designing effective incentives for living shorelines as a habitat conservation strategy along residential coasts. *Conservation Letters*, 13(5), e12744.
- Shepard, C. C., Crain, C. M., & Beck, M. W. (2011). The protective role of coastal marshes: a systematic review and meta-analysis. *PloS one*, 6(11), e27374.
- Stronkhorst, J., Huisman, B., Giardino, A., Santinelli, G., & Santos, F. D. (2018). Sand nourishment strategies to mitigate coastal erosion and sea level rise at the coasts of Holland (The Netherlands) and Aveiro (Portugal) in the 21st century. *Ocean & Coastal Management*, 156, 266-276.
- Sutton-Grier, A. E., Wowk, K., & Bamford, H. (2015). Future of our coasts: The potential for natural and hybrid infrastructure to enhance the resilience of our coastal communities, economies and ecosystems. *Environmental Science & Policy*, 51, 137-148.
- Tempest, J., Möller, I., & Spencer, T. (2015). A review of plant-flow interactions on salt marshes: the importance of vegetation structure and plant mechanical characteristics. *WIREs Water*, 2, 669-681.

- Tiner, R. W. (2005). In search of swampland: A wetland sourcebook and field guide (2nd ed.). Rutgers University Press.
- van der Meulen, F., IJff, S., & van Zetten, R. (2023). Nature-based solutions for coastal adaptation management, concepts and scope, an overview. *Nordic Journal of Botany*, 2023(1), e03290.
- van Proosdij, D., Stolle, J., Markov, A., & Caldera, G. (2024). “Chapter 9 - VegetationBased Solutions.” In Murphy, E., Cornett, A., van Proosdij, D., & Mulligan, R. P. (Eds.) Nature-Based Infrastructure for Coastal Flood and Erosion Risk Management – A Canadian Design Guide. ISBN 978-0- 660-71886-6.
- Vaughn, D. R., Bianchi, T. S., Shields, M. R., Kenney, W. F., & Osborne, T. Z. (2020). Increased Organic Carbon Burial in Northern Florida Mangrove-Salt Marsh Transition Zones. *Global Biogeochemical Cycles*, 34(5). <https://doi.org/10.1029/2019GB006334>
- Vouk, I. & Eyquem, J. L. (2024). “Chapter 3 – Existing Guidance.” In Murphy, E., Cornett, A., van Proosdij, D., & Mulligan, R. P. (Eds.) Nature-Based Infrastructure for Coastal Flood and Erosion Risk Management – A Canadian Design Guide. ISBN 978-0-660-71886-6.
- Vouk, I., Pilechi, V., Provan, M., & Murphy, E. (2021). Nature-based solutions for coastal and riverine flood and erosion risk management. *Canadian Standards Association*.
- Vuik, V., Jonkman, S. N., Borsje, B. W., & Suzuki, T. (2016). Nature-based flood protection: The efficiency of vegetated foreshores for reducing wave loads on coastal dikes. *Coastal Engineering (Amsterdam)*, 116, 42–56. <https://doi.org/10.1016/j.coastaleng.2016.06.001>
- Weliky, K., Suess, E., Ungerer, C. A., Muller, P. J., & Fischer, K. (1983). Problems with accurate carbon measurements in marine sediments and particulate matter in seawater: A new approach 1. *Limnology and Oceanography*, 28(6), 1252-1259.
- Wollenberg, J. T., Ollerhead, J., & Chmura, G. L. (2018). Rapid carbon accumulation following managed realignment on the Bay of Fundy. *Plos one*, 13(3), e0193930.
- Xu, X., Du, X., Wang, F., Sha, J., Chen, Q., Tian, G., ... & Jiang, Y. (2020). Effects of potassium levels on plant growth, accumulation and distribution of carbon, and nitrate metabolism in apple dwarf rootstock seedlings. *Frontiers in Plant Science*, 11, 534048.
- Ysebaert, T., Yang, S., Zhang, L., He, Q., Bouma, T., & Herman, P. (2011). Wave attenuation by two contrasting ecosystem engineering salt marsh macrophytes in the intertidal pioneer zone. *Wetlands (Wilmington, N.C.)*, 31(6), 1043-1054.
- Yuan, Y., Li, X., Jiang, J., Xue, L., & Craft, C. B. (2020). Distribution of organic carbon storage in different salt-marsh plant communities: A case study at the Yangtze Estuary. *Estuarine, Coastal and Shelf Science*, 243, 106900.

Appendix

List of Tables:

Table A1: Pictures of sediment cores at SHP and SHP_R

Figure A1: Summary of bulk density, total carbon, and organic carbon for each sediment core by marsh zone at each site.

Figure A2: Average stem height and stem density at each RBR station, at SHP and SHP_R.

Table A2: Point IDs and surveyed locations of vegetation plots and sediment cores.

Table A3: P- values calculated for each Welch two sample t-test.

Table A4: No. of events, maximum wave heights and date.

Table A5: Average maximum and significant wave height throughout the deployment at each station combined.

Table A6: Soil nutrient analysis data

Table A7: Summary of soil nutrients per increment and marsh zone at Study Site (SHP)

Table A8: Summary of soil nutrients per increment and marsh zone at Reference Site (SHP_R)

Table A9: Grain size analysis data

Table A10: ANOVA tests: Nutrient Analysis Summary

Table A11: Nutrient Analysis Summary Q1, Q2, and Q3.

Table A12: Nutrient Analysis Summary (standard deviations).



SHP_C09

- Mid-marsh
- Top 5 cm OM
- Sand



Medium Sand
Poorly Sorted
Very Coarse Skewed
Leptokurtic



SHP_RC14

- Low marsh
- Top 5 cm OM
- 5 – 10 cm sand
- 10+ silt

Coarse Sand
Poorly Sorted
Very Coarse Skewed
Platykurtic

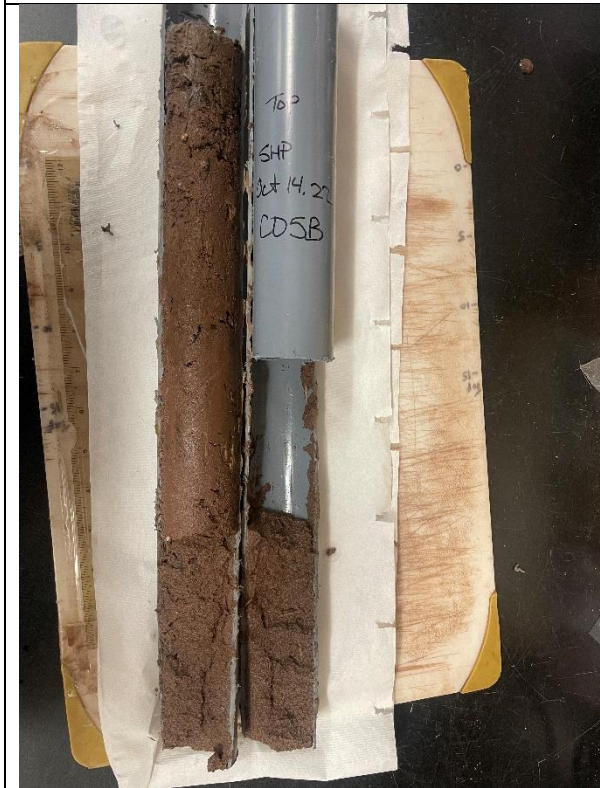
 <p>A photograph of a soil core sample labeled SHP_C02. The core is a dark brown, fine-grained material, approximately 15 cm long, held in a white plastic sleeve. The sleeve is marked with a ruler on the left side. The core is placed on a wooden board with a ruler on the right side. A yellow box of Glad paper towels is visible in the bottom right corner.</p>	<p>SHP_C02</p> <ul style="list-style-type: none"> • Low marsh • Sand throughout
 <p>A photograph of a soil core sample labeled SHP_RC15. The core is a dark brown, fine-grained material, approximately 15 cm long, held in a white plastic sleeve. The sleeve is marked with a ruler on the left side. The core is placed on a wooden board with a ruler on the right side. A yellow box of Glad paper towels is visible in the bottom right corner. The sleeve is labeled with 'Top', 'SHP RC15', 'V-131', and 'Bottom'.</p>	<p>SHP_RC15</p> <ul style="list-style-type: none"> • Mid-marsh



SHP_RC18

- Low marsh

Medium Sand
Poorly Sorted
Very Coarse Skewed
Very Leptokurtic



SHP_C05B

- Mid-marsh

Medium Sand
Moderately Sorted
Very Coarse Skewed
Extremely Leptokurtic



SHP_C04

- Shoreline

Medium Sand
Well Sorted
Symmetrical
Very Leptokurtic



SHP_RC23

- Low marsh

Coarse Sand
Poorly Sorted
Very Coarse Skewed
Leptokurtic



SHP_RC18

- Low marsh

Medium Sand
Poorly Sorted
Very Coarse Skewed
Very Leptokurtic



SHP_C25

- Mid-marsh
- Sand in lower half

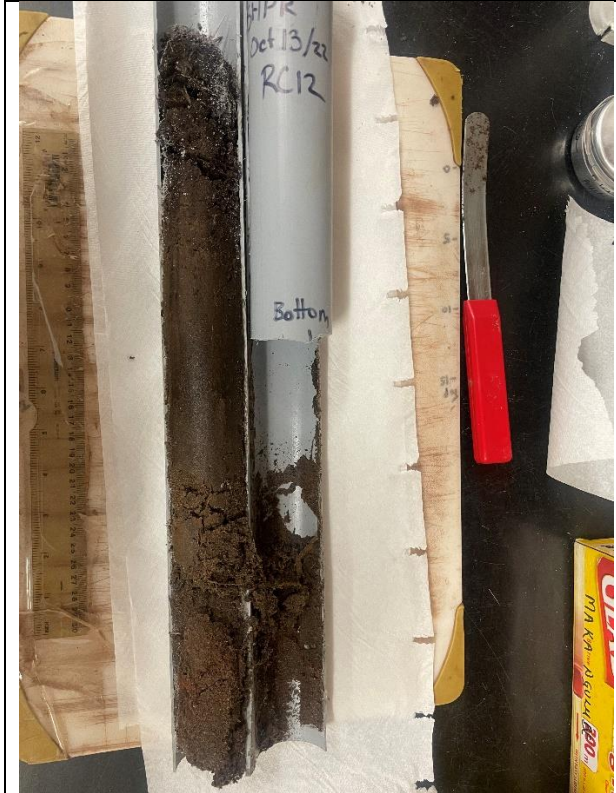
Medium Sand
Poorly Sorted
Very Coarse Skewed
Leptokurtic



SHP_C17

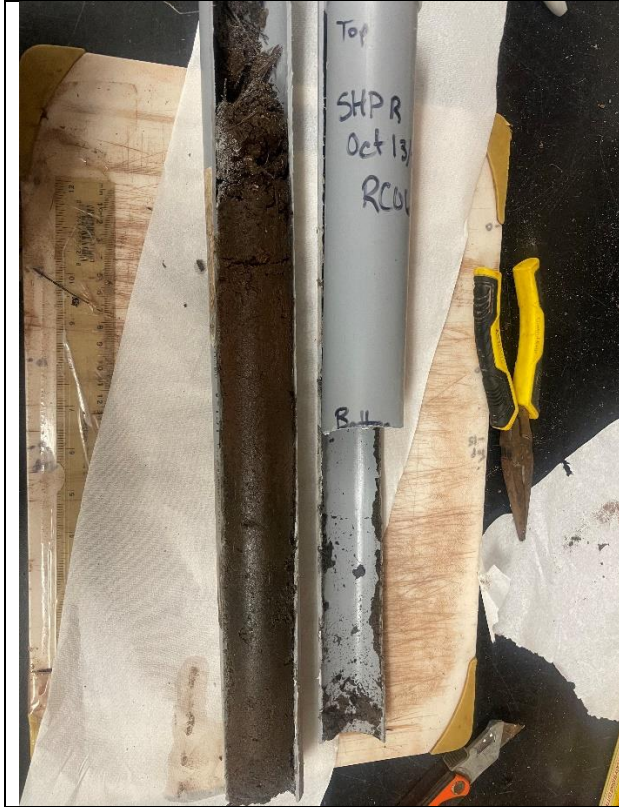
- Low marsh

Medium Sand
Moderately Sorted
Very Coarse Skewed
Extremely Leptokurtic



SHP_RC12

Medium Sand
Poorly Sorted
Very Coarse Skewed
Mesokurtic



SHP_RC06

- Low marsh



SHP_C12

- Mid-marsh

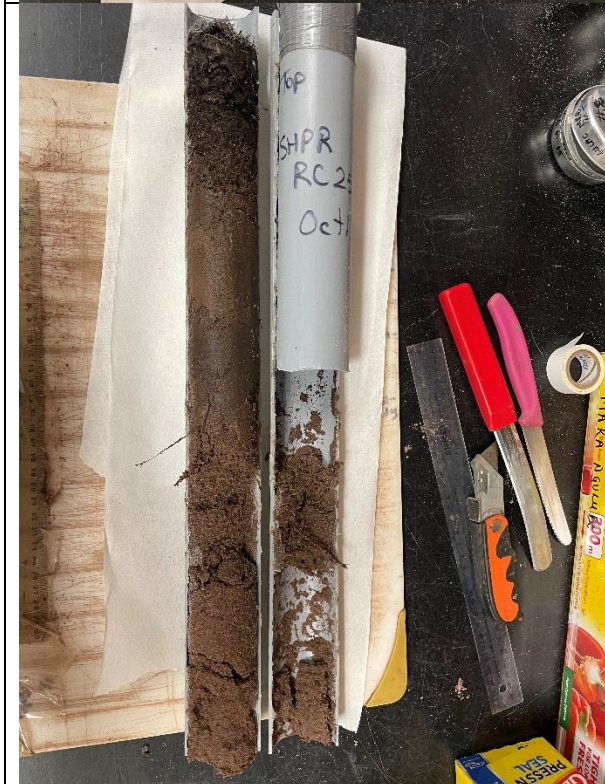
Fine Sand
Moderately Well Sorted
Fine Skewed
Mesokurtic



SHP_C24

- Mid-marsh

Coarse Sand
Poorly Sorted
Very Coarse Skewed
Platykurtic



SHP_RC25

- Mid-marsh

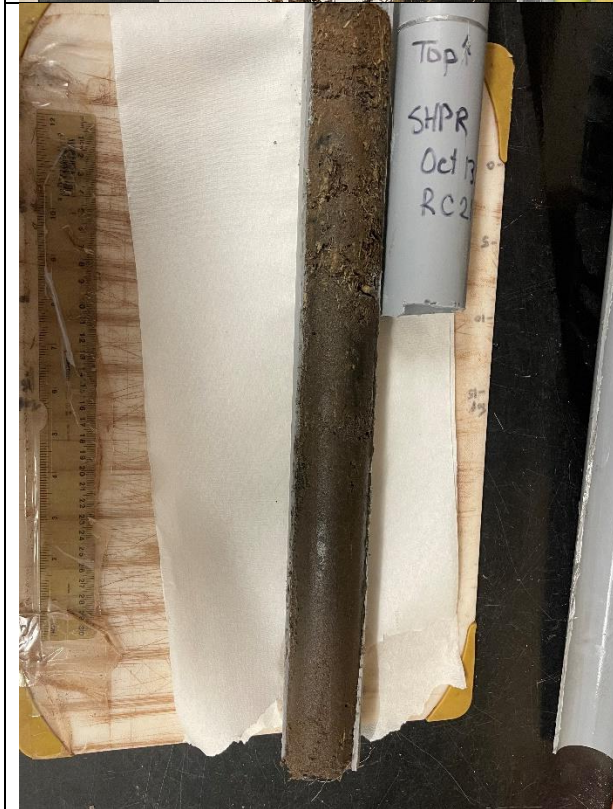
Medium Sand
Moderately Sorted
Fine Skewed
Leptokurtic



SHP_RC22

- Shoreline

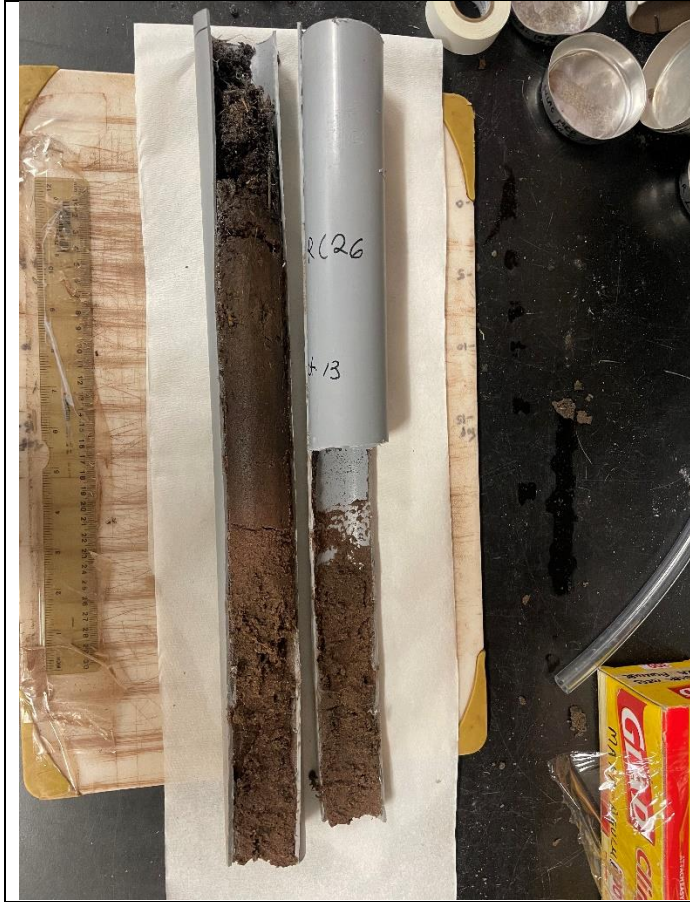
Medium Sand
Poorly Sorted
Very Coarse Skewed
Platykurtic



SHP_RC21

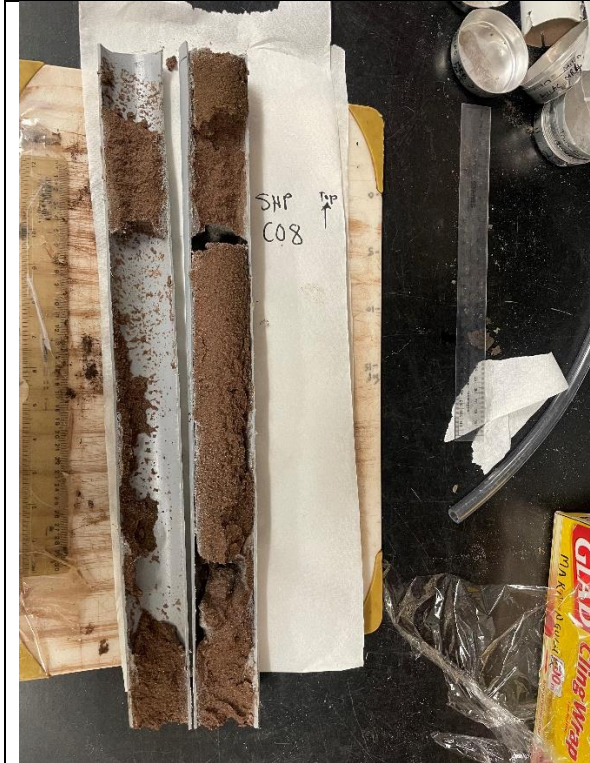
- Shoreline

Medium Sand
Poorly Sorted
Coarse Skewed
Extremely Leptokurtic



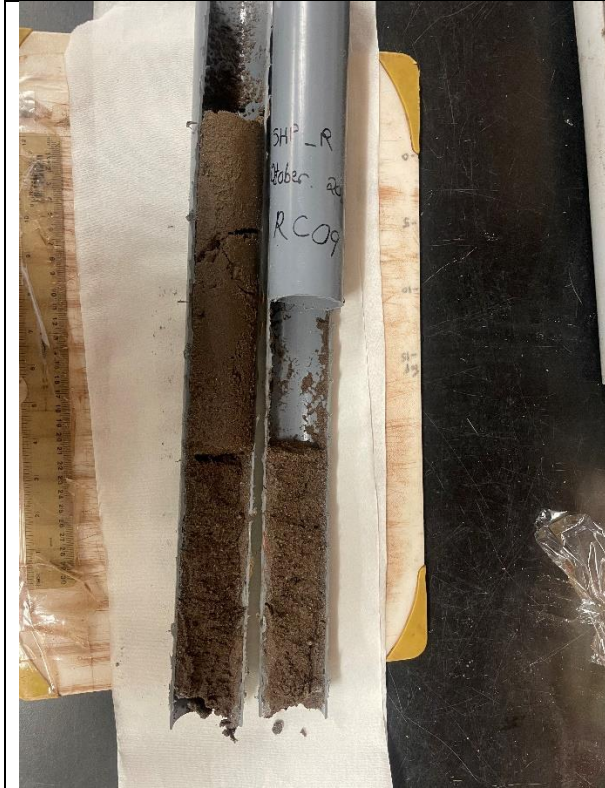
SHP_RC26

- Mid-marsh



SHP_C08

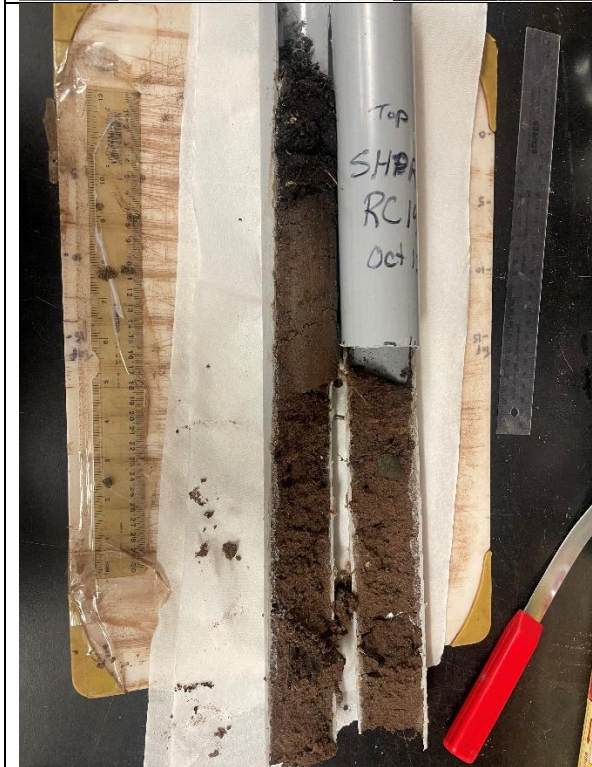
- Shoreline
- Sandy



SHP_RC09

- Mid-marsh
- Sandy

Medium Sand
Poorly Sorted
Coarse Skewed
Very Leptokurtic



SHP_RC19

- Mid-marsh



SHP_C05

- Mid-marsh

Medium Sand
Moderately Sorted
Very Coarse Skewed
Extremely Leptokurtic



SHP_C20

- Shoreline

Medium Sand
Moderately Sorted
Symmetrical
Extremely Leptokurtic



SHP_RC16

- Mid-marsh



SHP_C22

- Mid-marsh



SHP_C18

- Low marsh
- Sandy throughout



SHP_RC13

- Low marsh

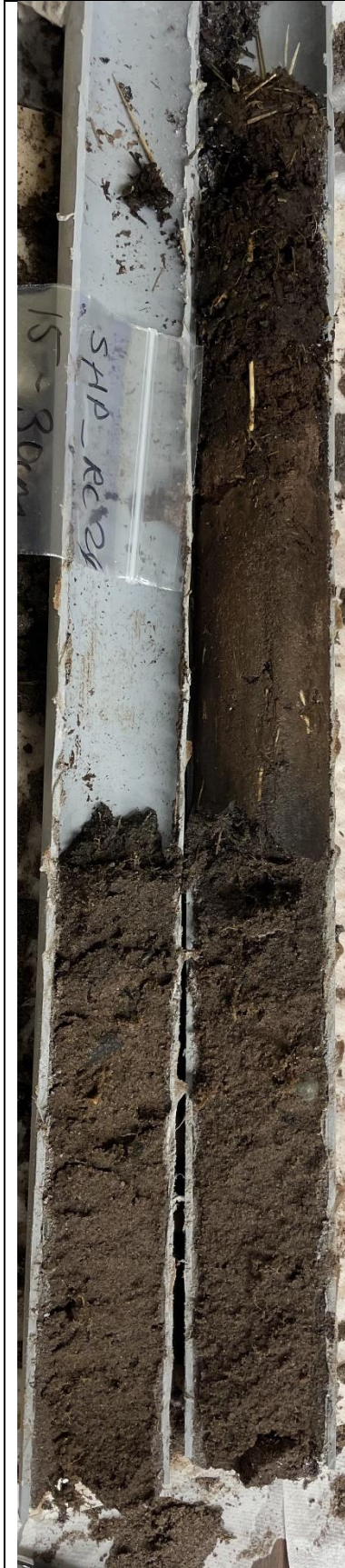
Fine Sand
Moderately Well Sorted
Fine Skewed
Mesokurtic



SHP_RC08

- Mid-marsh

Fine Sand
Moderately Well Sorted
Fine Skewed
Platykurtic



SHP_RC24

- Low marsh

Medium Sand
Poorly Sorted
Coarse Skewed
Very Leptokurtic



SHP_RC11

- Mid-marsh

Medium Sand
Poorly Sorted
Coarse Skewed
Very Leptokurtic



SHP_RC18

- Low marsh

Medium Sand
Poorly Sorted
Very Coarse Skewed
Very Leptokurtic



SHP_C16

- Shoreline
- Sandy throughout

Medium Sand
Moderately Sorted
Very Coarse Skewed
Leptokurtic



SHP_C13

- Low marsh
- Sandy throughout

Medium Sand
Moderately Sorted
Symmetrical
Extremely Leptokurtic



SHP_C23

- Low marsh
- Sandy throughout

Medium Sand
Poorly Sorted
Coarse Skewed
Extremely Leptokurtic



SHP_C21

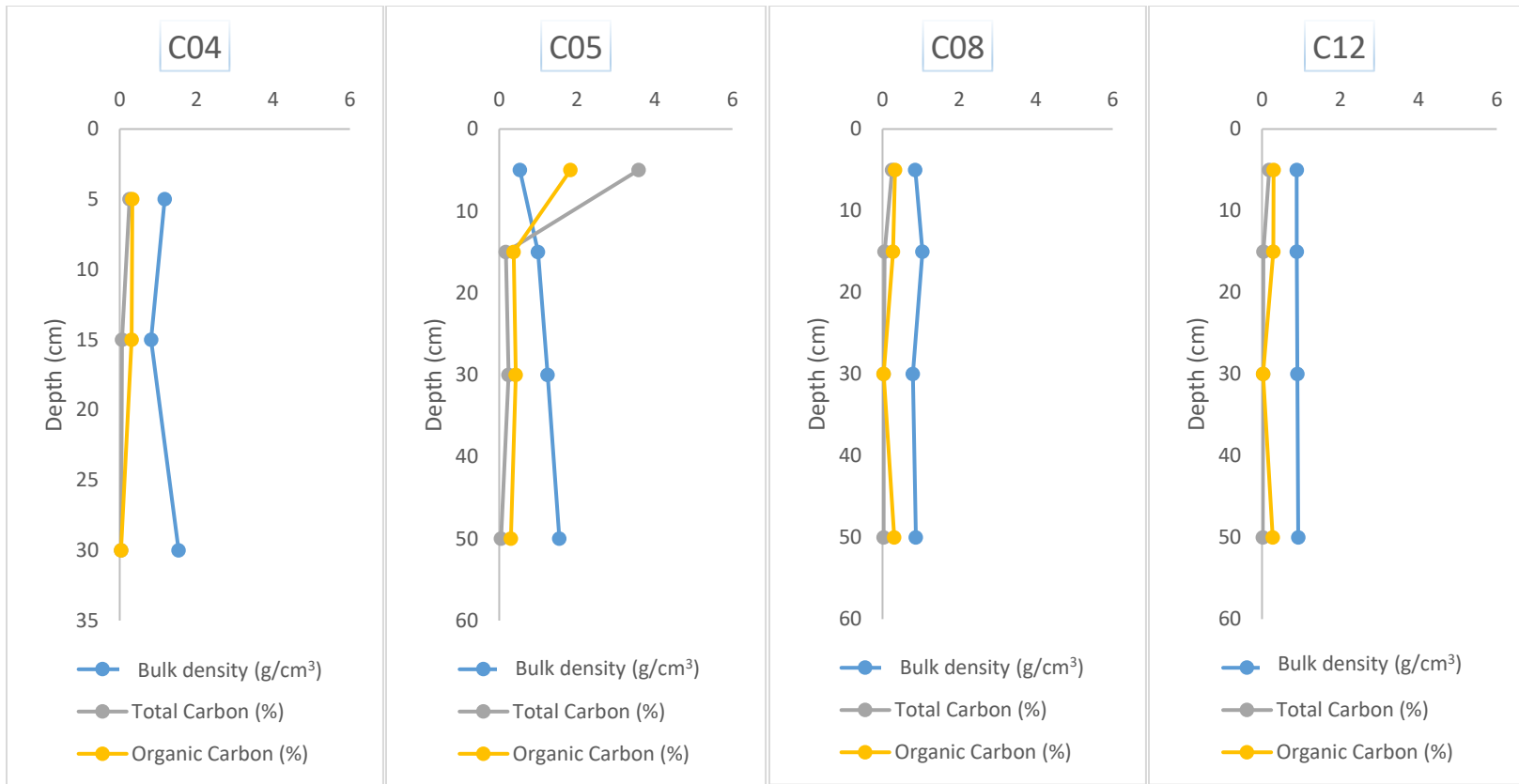
- Mid-marsh



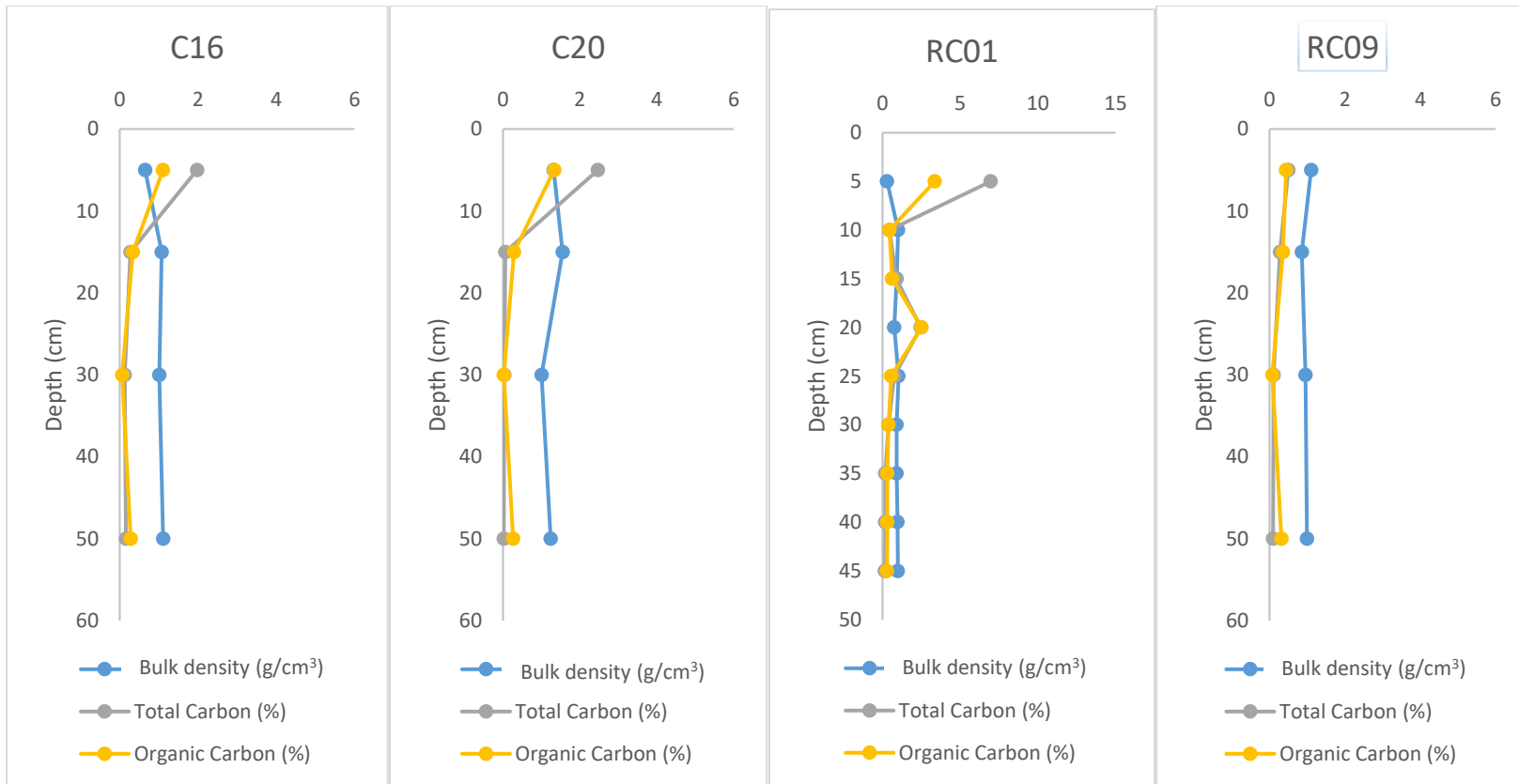
SHP_RC01

- Shoreline

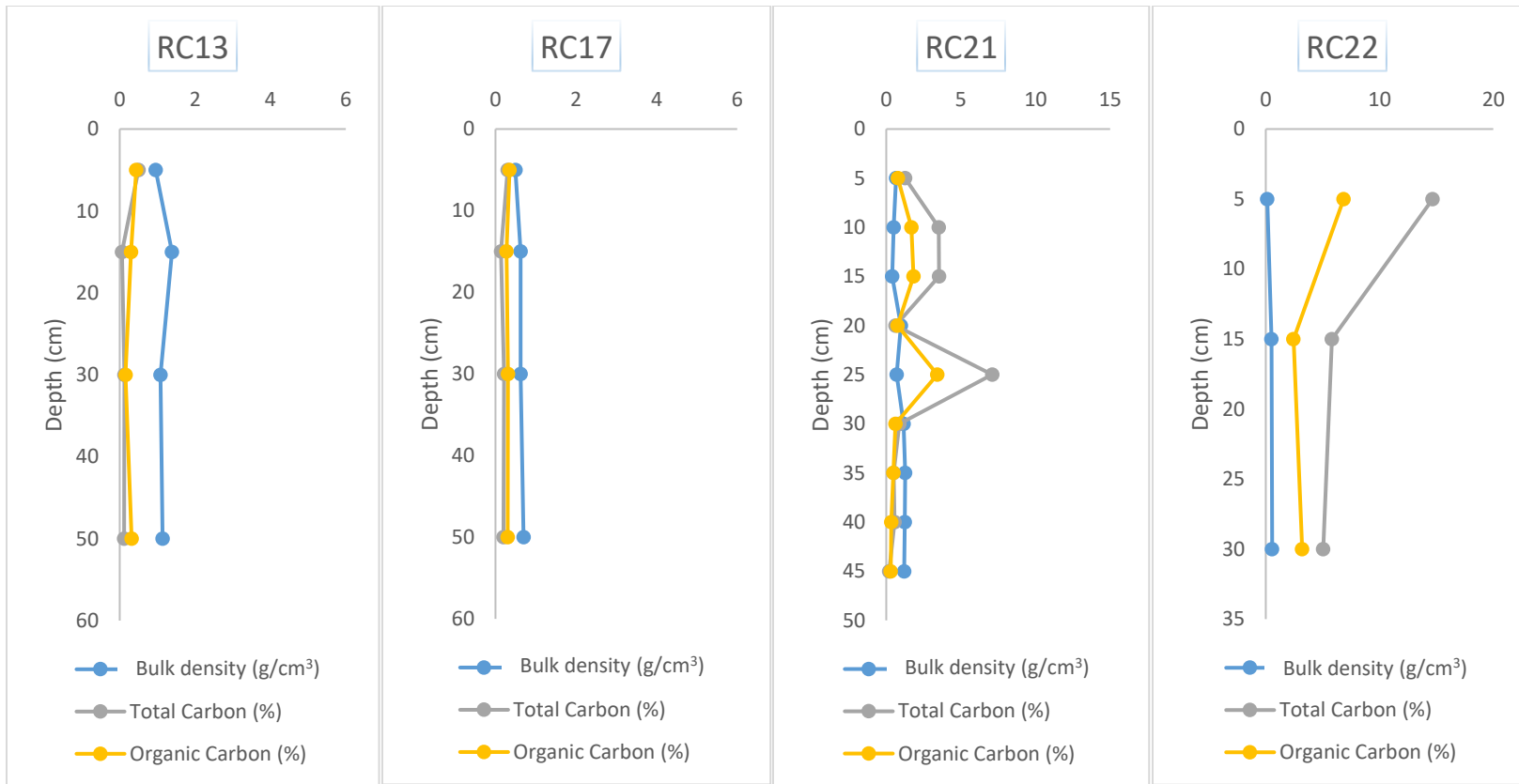
Medium Sand
Moderately Sorted
Very Coarse Skewed
Very Leptokurtic



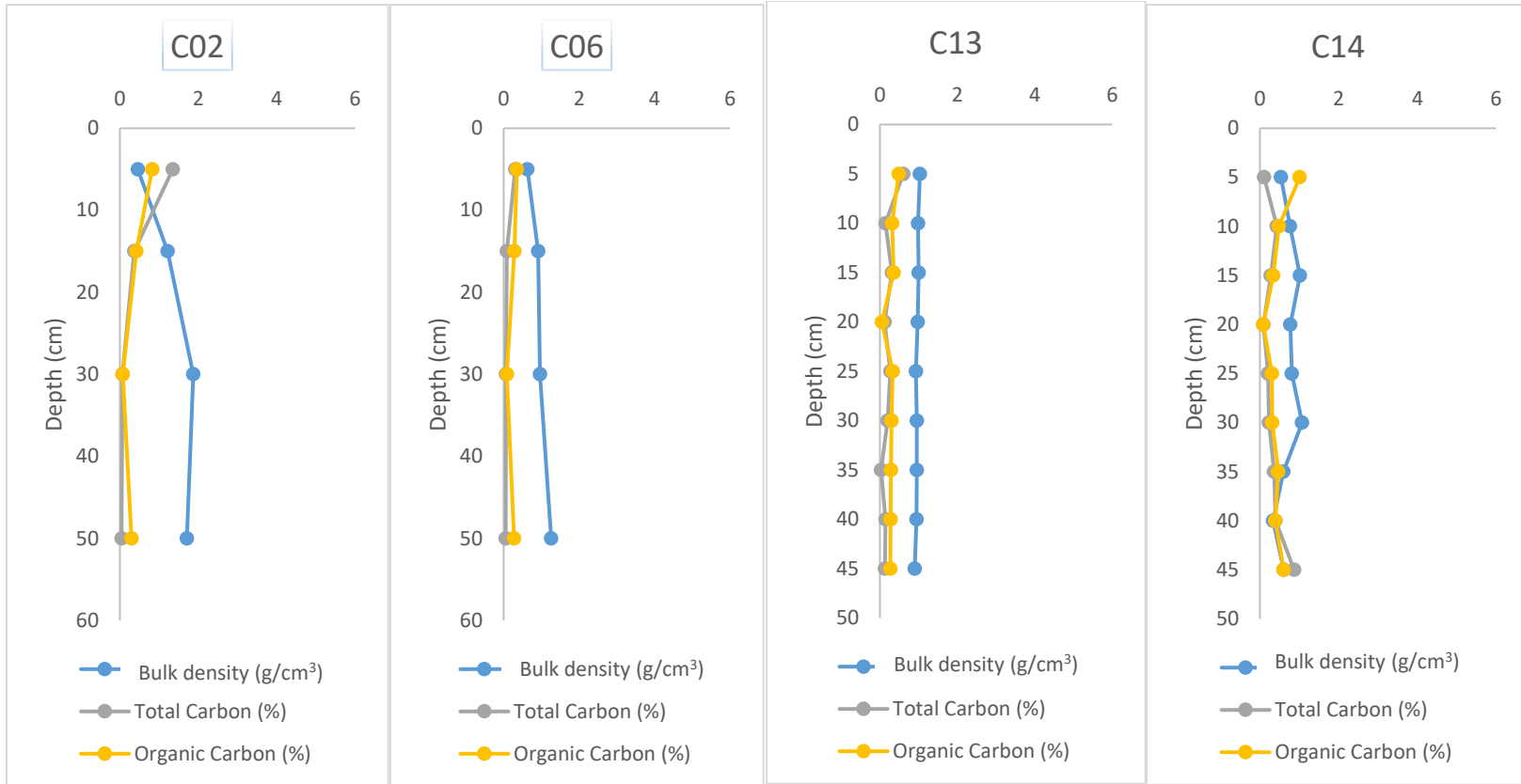
MARSH ZONE: SHORELINE



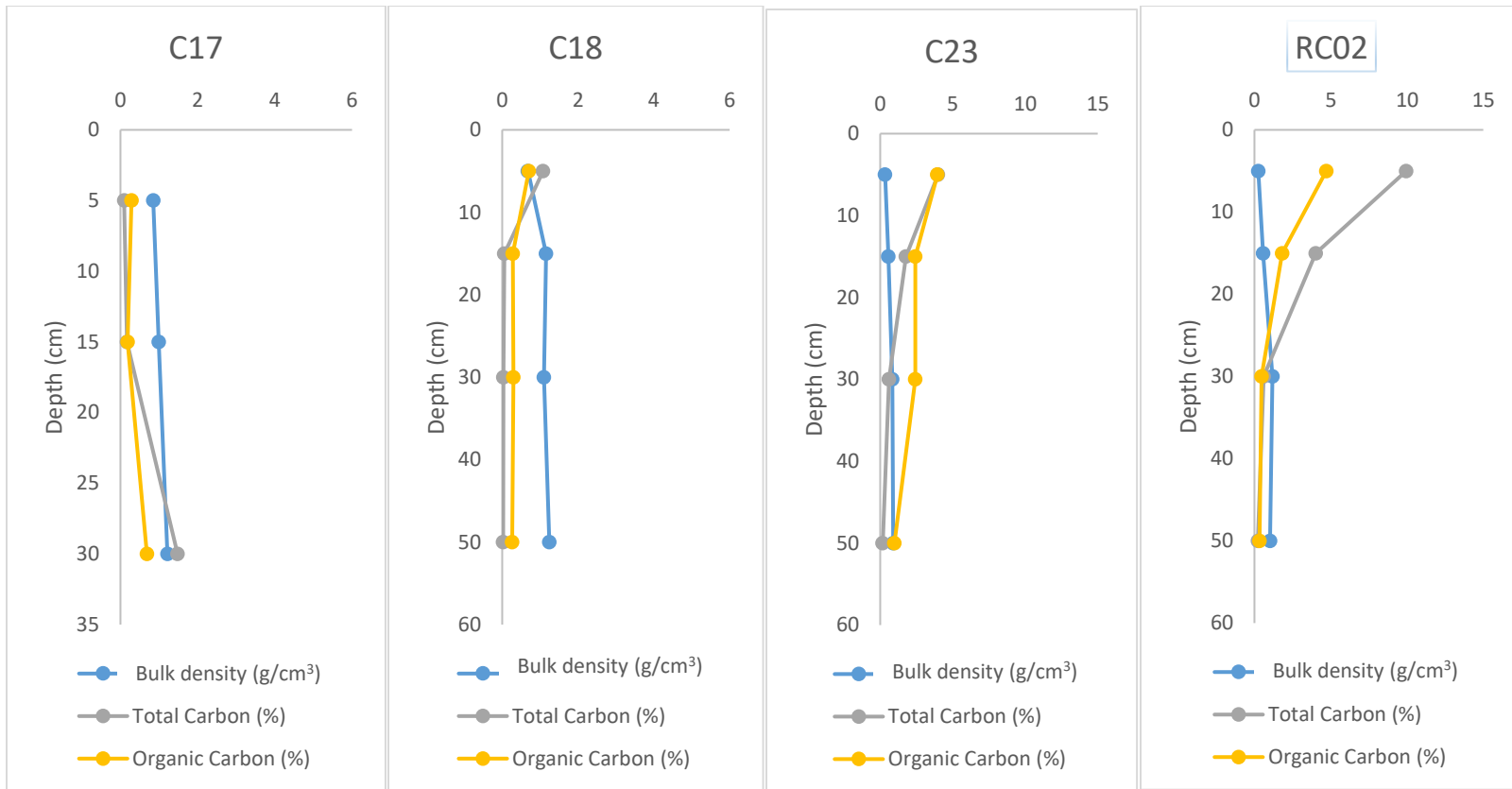
MARSH ZONE: SHORELINE



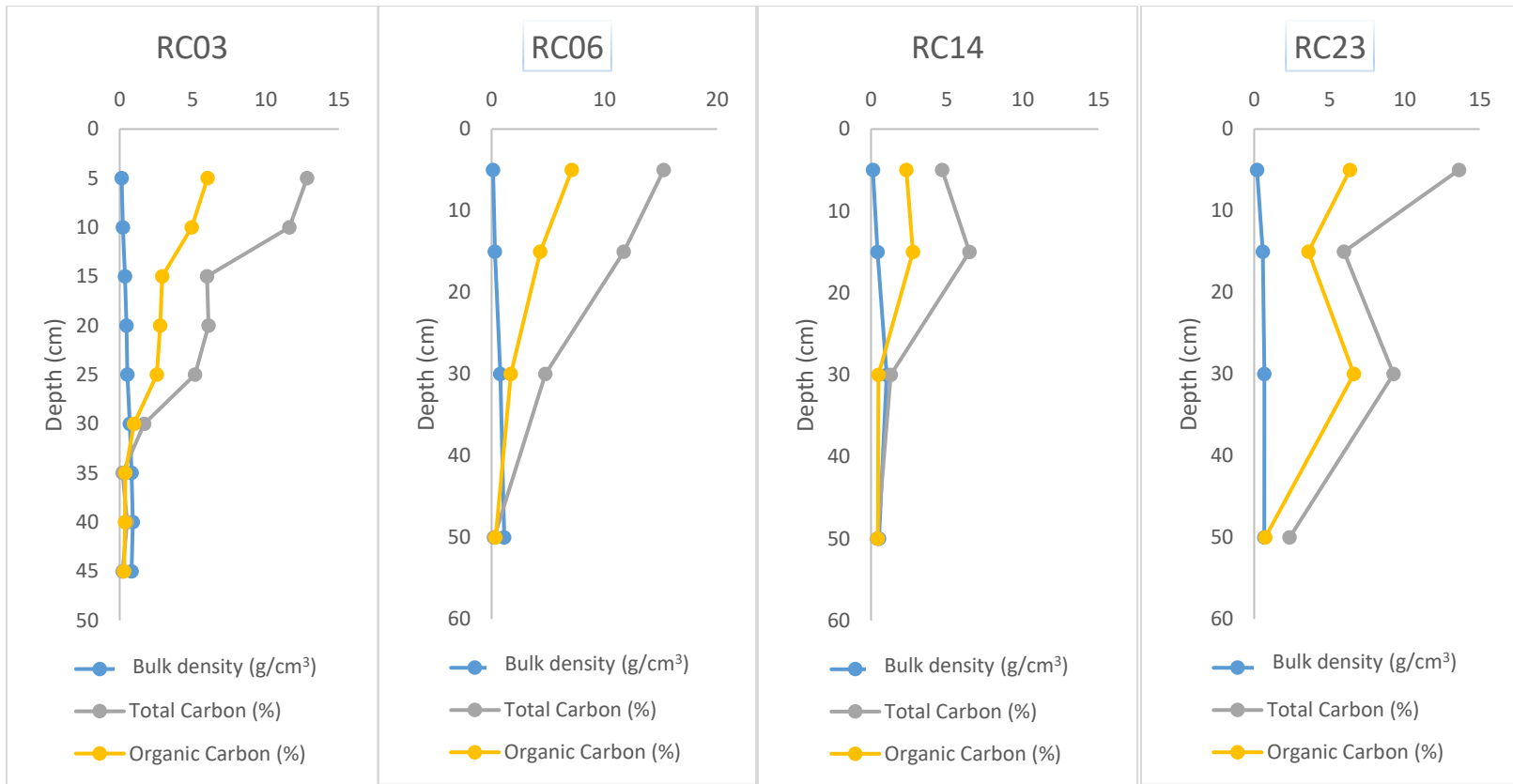
MARSH ZONE: SHORELINE



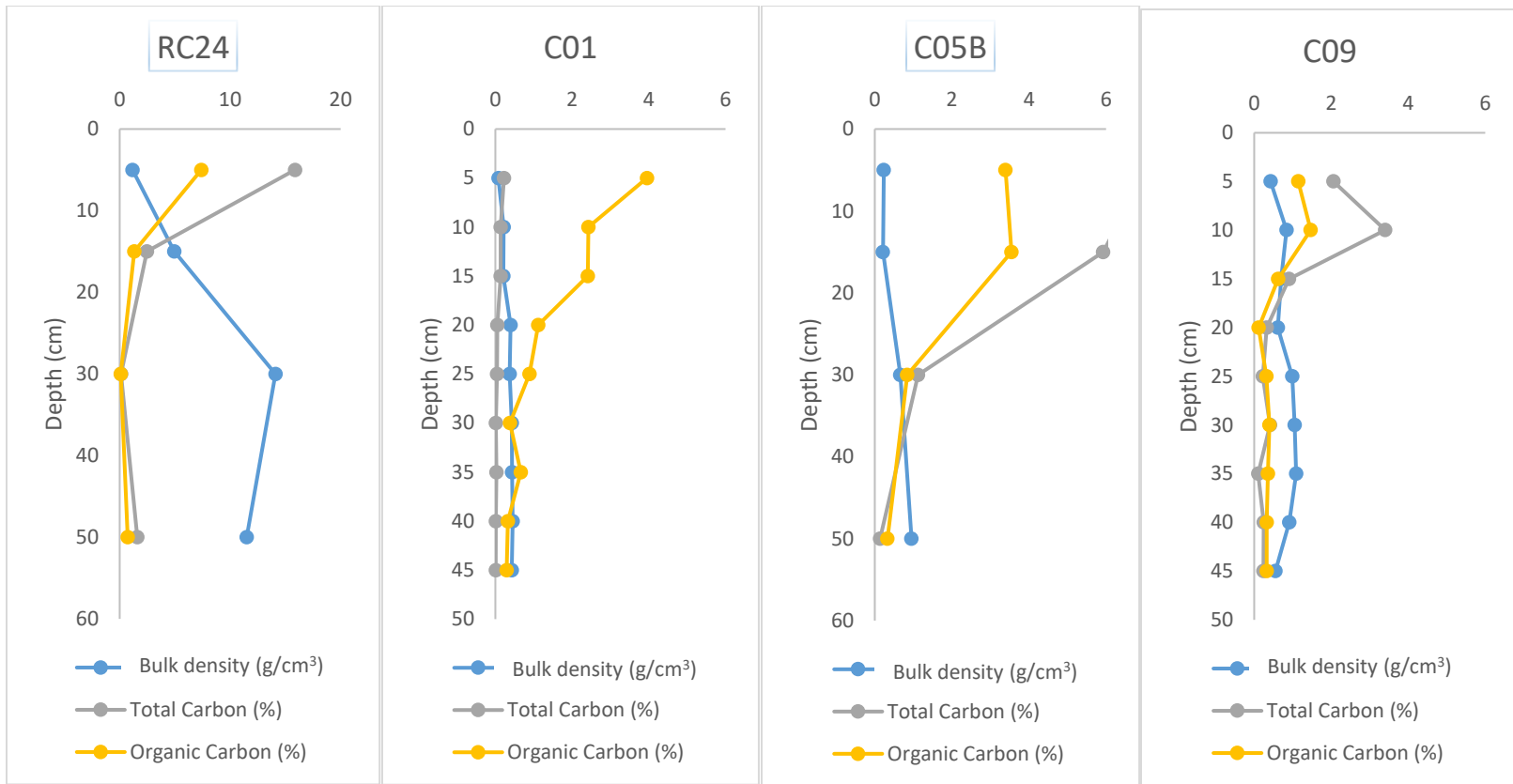
MARSH ZONE: LOW MARSH



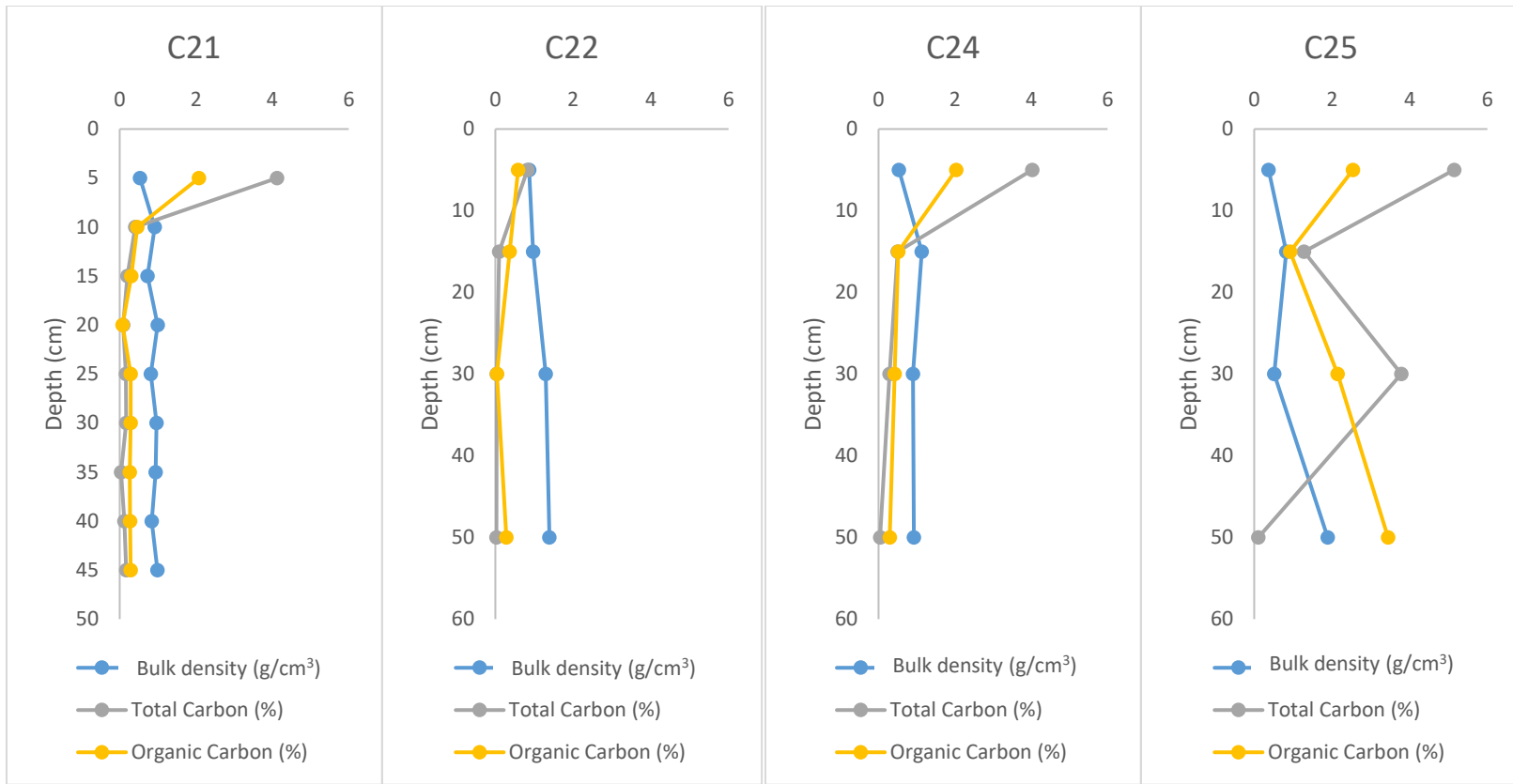
MARSH ZONE: LOW MARSH



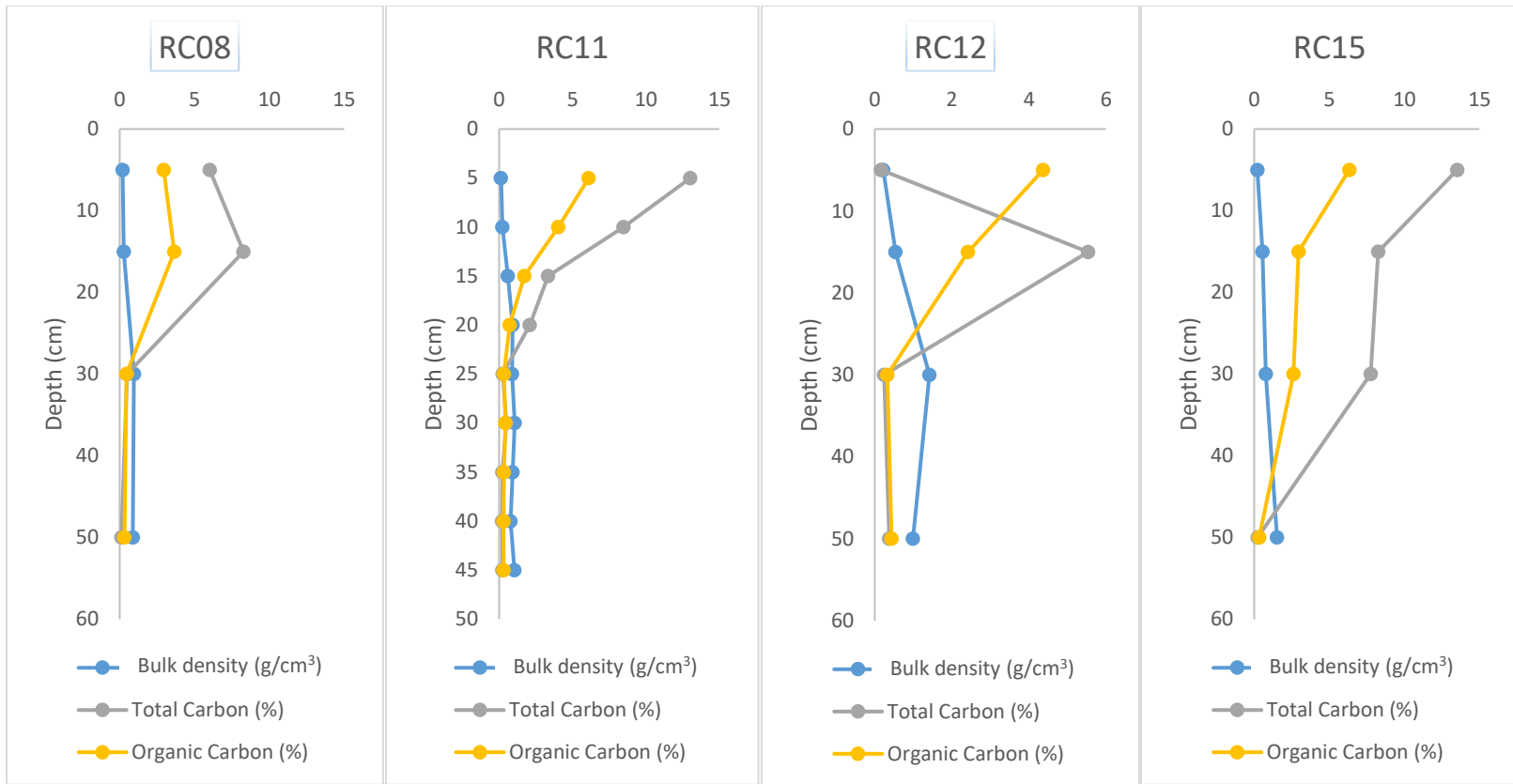
MARSH ZONE: LOW MARSH



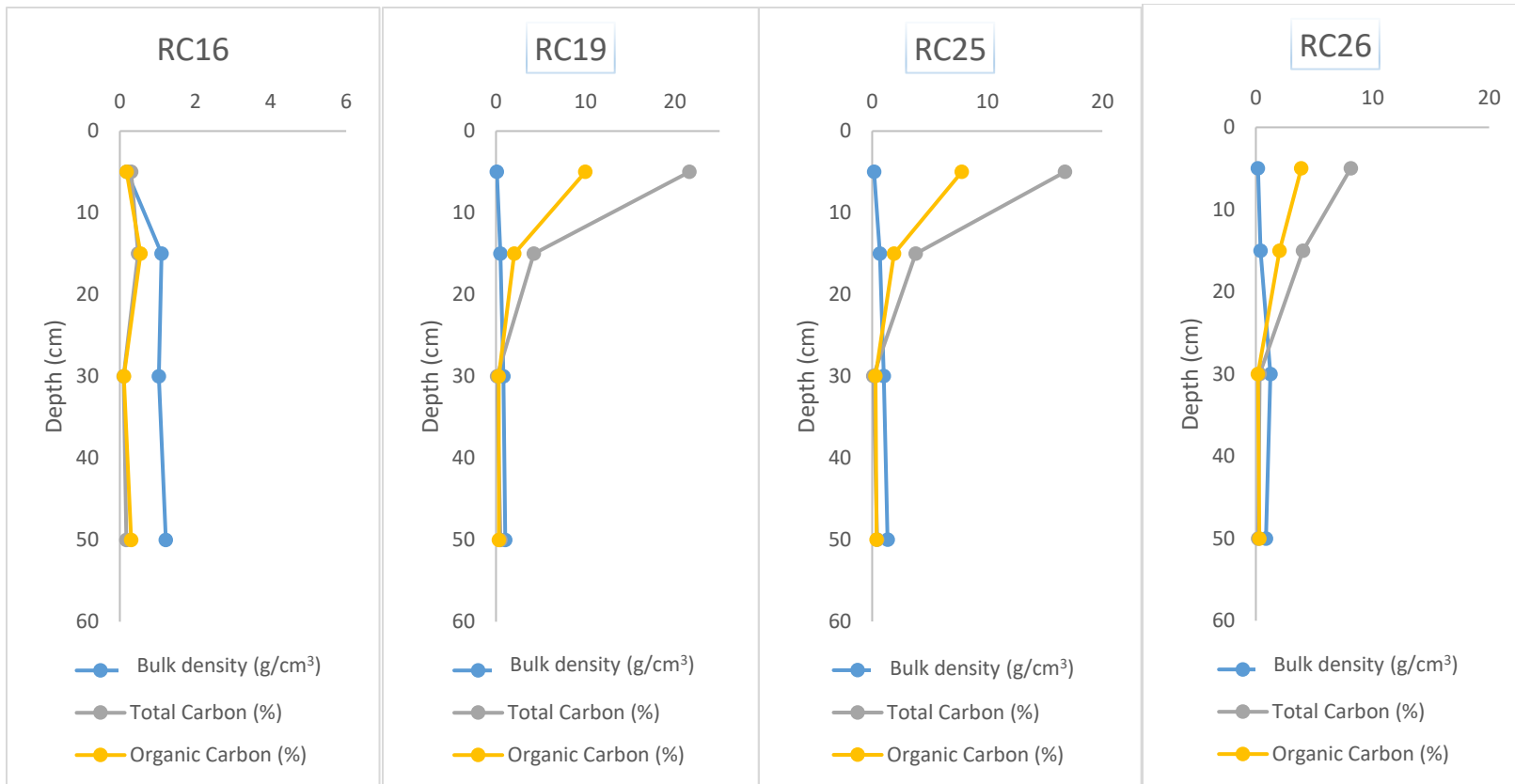
MARSH ZONE: MID TO HIGH MARSH



MARSH ZONE: MID TO HIGH MARSH



MARSH ZONE: MID TO HIGH MARSH



MARSH ZONE: MID TO HIGH MARSH

Figure A1: Summary of bulk density, total carbon, and organic carbon for each sediment core by marsh zone at each site.

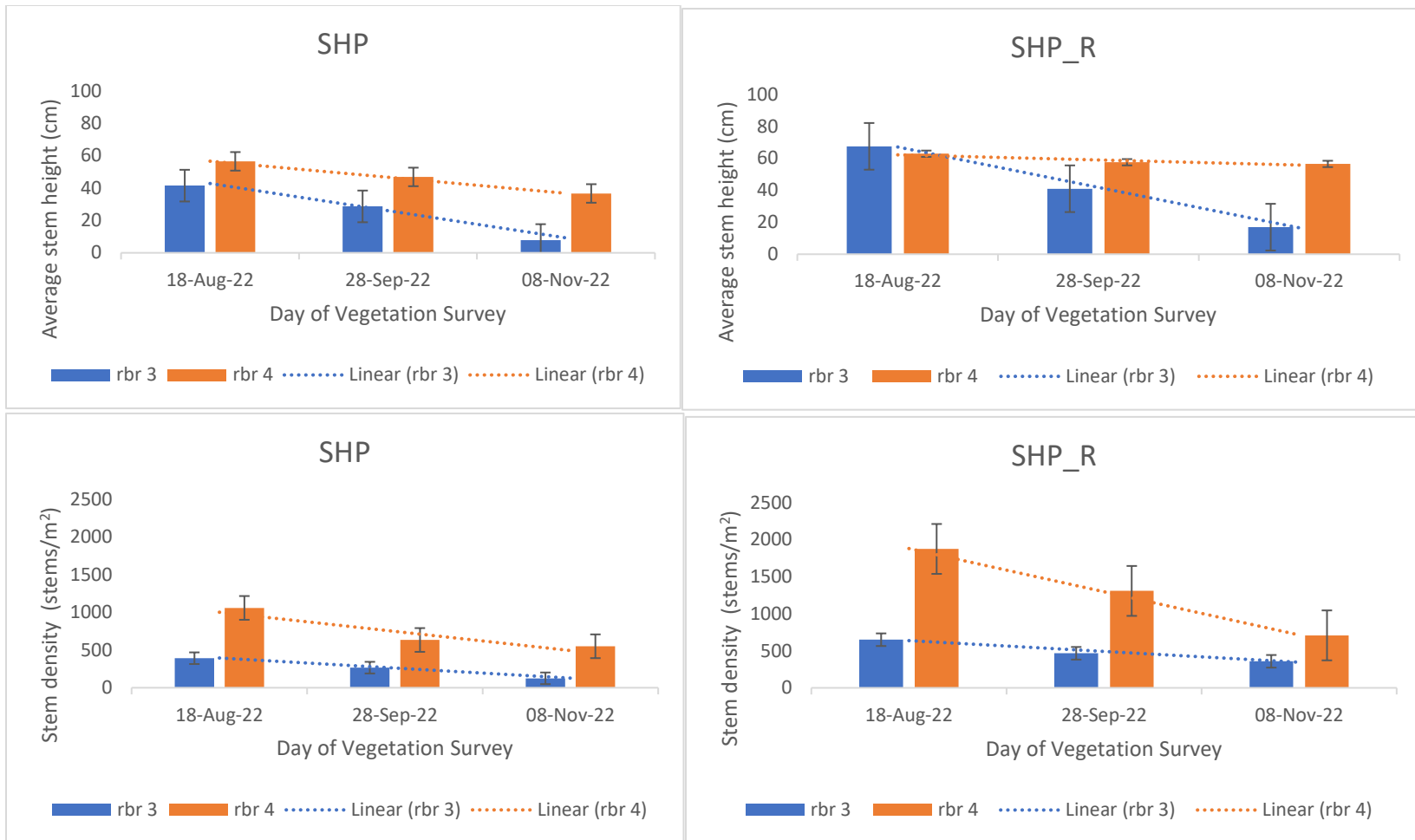


Figure A2: Average stem height and stem density at each RBR station, at SHP and SHP_R.

Table A2: Point IDs and surveyed locations of vegetation plots and sediment cores (CD)

Vegetation Stations				Sediment Cores			
PtID	X	Y	OHeight	PtID	X	Y	OHeight
W_02	375511.5	5286921	1.159	C22	375525.3	5286915	1.085
SW_03	375508.7	5286931	0.976	C23	375521.6	5286926	1.102
MS_04	375505.9	5286941	0.459	C21	375517.4	5286907	1.133
SW_07	375496	5286928	1.008	C01	375515	5286914	1.043
MS_08	375492.8	5286937	0.371	C04	375506.7	5286941	0.479
SW_11	375485.2	5286925	0.944	C08	375493.3	5286936	0.491
MS_12	375482.5	5286935	0.369	C12	375482.8	5286934	0.459
SW_15	375473.8	5286922	0.985	C16	375471.4	5286929	0.471
MS_16	375470.7	5286931	0.35	C20	375460.9	5286922	0.732
SW_19	375463	5286918	1.056	C02	375512.2	5286921	1.133
MS_20	375459.4	5286928	0.361	C06	375499.9	5286921	1.442
W_18	375466.6	5286911	1.153	C10	375487.7	5286918	1.553
W_17	375470.2	5286904	1.54	C14	375478.9	5286915	1.456
W_14	375478.1	5286915	1.357	C18	375467.6	5286911	1.162
W_13	375481.5	5286907	1.103	C17	375471.2	5286904	1.472
W_10	375489.3	5286918	1.464	C13	375482.4	5286908	1.163
W_09	375492.1	5286911	1.175	C09	375493.1	5286911	1.198
W_06	375499	5286920	1.439	C25	375495.8	5286903	1.145
W_05	375502.1	5286913	1.135	C24	375506.1	5286906	1.146
W_01	375514.1	5286914	0.98	C05b	375503.3	5286904	1.135
W21	375516.7	5286906	1.141	RC01	365155.1	5278043	-0.084
W22	375524.4	5286915	1.11	RC02	365162	5278039	0.029
W23	375520.8	5286925	1.092	RC03	365168.5	5278035	0.007
W24	375505.1	5286906	1.109	RC06	365164.9	5278043	0.024
W25	375494.8	5286903	1.129	RC08	365178.5	5278035	0.039
R01	365154.3	5278042	-0.153	RC11	365174.3	5278043	0.068
R02	365161.3	5278039	-0.095	RC12	365181.5	5278039	0.096
R03	365168	5278034	-0.093	RC14	365170.1	5278052	0.067
R04	365174.9	5278030	-0.043	RC15	365177.3	5278047	0.039
R08	365177.9	5278034	-0.091	RC16	365184.2	5278043	0.101
R07	365170.9	5278038	-0.064	RC18	365173.2	5278056	0.061
R06	365164.1	5278043	-0.049	RC19	365180.1	5278051	0.093
R05	365157	5278046	-0.278	RC24	365173.7	5278061	0.093
R09	365159.8	5278050	-0.448	RC25	365180.8	5278057	0.088
R10	365166.8	5278047	0.072	RC21	365144	5278043	-0.265
R11	365173.6	5278043	-0.027	RC22	365154.4	5278037	-0.047
R12	365180.6	5278038	-0.065	RC23	365164.6	5278032	-0.09
R13	365162.5	5278055	-0.431	RC09	365160.6	5278051	-0.466

R14	365169.6	5278051	-0.008		RC13	365162.9	5278055	-0.42
R15	365176.5	5278047	-0.048		RC17	365165.8	5278059	-0.436
R16	365183.4	5278043	0.038		RC26	365187.5	5278053	0.046
R17	365165.3	5278059	-0.444					
R18	365172.4	5278055	-0.011					
R19	365179.2	5278051	0.057					
R20	365186.2	5278047	0.111					

Table A3: P- values calculated for each Welch two sample t-test

Site	Parameter	P-value
SHP; SHP_R	Plot average cover	0.6523
	Plant community composition	0.009
SHP; SHP_R	Top 2 dominant species	<i>S. alterniflorus</i> : 0.3667 <i>S. pumilus</i> : 0.0423

Table A4: No. of events and date.

SHP		SHP_R	
Event 1	Aug 27 – Sept 9, 2022	Event 1	Aug 16 – Sept 5, 2022
Event 2	Sept 15 – Sept 19, 2022	Event 2	Sept 14 – Oct 4, 2022
Event 3	Sept 22 – Oct 5, 2022	Event 3	Oct 6- Oct 12, 2022
Event 4	Oct 8 – Oct 15, 2022	Event 4	Oct 25 – Nov 5, 2022
Event 5	Oct 25 – Nov 5, 2022	n/a	

Table A5: Average maximum and significant wave height throughout the deployment at each station combined.

	rbr 1	rbr 2	rbr 3	rbr 4
Average Maximum Wave Height (m)	0.044	0.020	0.003	0.002
Average Significant Wave Height (m)	0.024	0.010	0.004	0.001

Table A6: Soil nutrients present for each core that was processed.

Lab #	2305702-001			2305702-002			2305702-003			2305702-004		
Sample ID	SHP C09 0-15			SHP C09 15-50			SHP C01 0-15			SHP C01 15-50		
Crop to be Grown	Unknown			Unknown			Unknown			Unknown		
Parameter	Analysis		Rating	Analysis		Rating	Analysis		Rating	Analysis		Rating
Carbon (%)	1.64			0.11			3.85			0.39		
Nitrogen (%)	0.15			< 0.02			0.39			0.03		
P2O5 (kg/ha)	160			70			214			138		
K2O (kg/ha)	646			286			1142			410		
Calcium (kg/ha)	876			260			1604			478		
Magnesium (kg/ha)	1340			538			2232			826		
Sodium (kg/ha)	7372			3976			11746			4894		
Sulfur (kg/ha)	562			300			838			432		
Aluminum (ppm)	265			124			411			201		
Boron (ppm)	21.10			1.80			45.50			6.20		
Copper (ppm)	0.90			0.30			1.50			0.60		
Iron (ppm)	176			108			171			85		
Manganese (ppm)	140			33			74			<3		
Zinc (ppm)	2.00			0.70			2.60			1.10		
Salt (mmhos/cm)	8.350			5.150			9.530			6.730		
Required Nutrient (kg/ha)	N	P2O5	K2O	N	P2O5	K2O	N	P2O5	K2O	N	P2O5	K2O

Lab #	2305702-005			2305702-006			2305702-007			2305702-008		
Sample ID	SHP C25 0-15			SHP C25 15-50			SHP C04 0-15			SHP C04 15-50		
Crop to be Grown	Unknown			Unknown			Unknown			Unknown		
Parameter	Analysis	Rating		Analysis	Rating		Analysis	Rating		Analysis	Rating	
Carbon (%)	1.41			0.51			< 0.02			0.13		
Nitrogen (%)	0.13			0.05			< 0.02			< 0.02		
P2O5 (kg/ha)	144			80			76			36		
K2O (kg/ha)	862			478			300			248		
Calcium (kg/ha)	874			462			402			258		
Magnesium (kg/ha)	1390			946			672			594		
Sodium (kg/ha)	7328			6280			4808			4182		
Sulfur (kg/ha)	604			766			378			328		
Aluminum (ppm)	257			202			<100			<100		
Boron (ppm)	40.40			5.40			2.30			1.40		
Copper (ppm)	0.90			0.50			0.40			0.20		
Iron (ppm)	153			122			65			41		
Manganese (ppm)	57			<3			12			<3		
Zinc (ppm)	1.60			5.70			1.00			0.60		
Salt (mmhos/cm)	7.440			7.670			5.910			5.860		
Required Nutrient (kg/ha)	N	P2O5	K20	N	P2O5	K20	N	P2O5	K20	N	P2O5	K20
Lab #	2305702-009			2305702-010			2305702-011			2305702-012		
Sample ID	SHP C05B 0-15			SHP C05B 15-50			SHP RC23 0-15			SHP RC23 15-50		
Crop to be Grown	Unknown			Unknown			Unknown			Unknown		
Parameter	Analysis	Rating		Analysis	Rating		Analysis	Rating		Analysis	Rating	
Carbon (%)	5.24			0.43			7.97			4.41		
Nitrogen (%)	0.47			0.04			0.71			0.40		
P2O5 (kg/ha)	214			104			192			<32		
K2O (kg/ha)	1356			410			1048			562		
Calcium (kg/ha)	1690			422			1140			1002		
Magnesium (kg/ha)	2954			762			2426			1778		
Sodium (kg/ha)	15718			4976			14148			9992		
Sulfur (kg/ha)	1108			434			1718			3296		
Aluminum (ppm)	373			193			298			256		
Boron (ppm)	73.30			6.40			12.50			11.70		
Copper (ppm)	1.70			0.40			0.40			<0.1		
Iron (ppm)	253			51			165			897		
Manganese (ppm)	167			6			<3			7		
Zinc (ppm)	3.20			0.80			2.80			3.20		
Salt (mmhos/cm)	10.590			6.280			15.960			9.370		
Required Nutrient (kg/ha)	N	P2O5	K20	N	P2O5	K20	N	P2O5	K20	N	P2O5	K20

Lab #	2305702-013			2305702-014			2305702-015			2305702-016		
Sample ID	SHP RC18 0-15			SHP RC18 15-50			SHP C20 0-15			SHP C20 15-50		
Crop to be Grown	Unknown			Unknown			Unknown			Unknown		
Parameter	Analysis	Rating		Analysis	Rating		Analysis	Rating		Analysis	Rating	
Carbon (%)	2.83			0.41			0.06			< 0.02		
Nitrogen (%)	0.27			0.03			< 0.02			< 0.02		
P2O5 (kg/ha)	144			82			64			42		
K2O (kg/ha)	776			308			250			242		
Calcium (kg/ha)	1108			324			908			234		
Magnesium (kg/ha)	1890			672			588			566		
Sodium (kg/ha)	9514			4462			4176			4290		
Sulfur (kg/ha)	610			710			310			322		
Aluminum (ppm)	194			134			<100			<100		
Boron (ppm)	9.90			1.80			2.20			1.30		
Copper (ppm)	0.30			0.30			0.40			0.30		
Iron (ppm)	191			228			94			37		
Manganese (ppm)	3			<3			67			6		
Zinc (ppm)	1.10			1.20			1.30			0.80		
Salt (mmhos/cm)	8.860			6.170			4.914			4.683		
Required Nutrient (kg/ha)	N	P2O5	K2O	N	P2O5	K2O	N	P2O5	K2O	N	P2O5	K2O
Lab #	2305702-017			2305702-018			2305702-019			2305702-020		
Sample ID	SHP C05 0-15			SHP C05 15-50			SHP C16 0-15			SHP C16 15-50		
Crop to be Grown	Unknown			Unknown			Unknown			Unknown		
Parameter	Analysis	Rating		Analysis	Rating		Analysis	Rating		Analysis	Rating	
Carbon (%)	0.71			0.15			0.30			0.07		
Nitrogen (%)	0.08			< 0.02			0.03			< 0.02		
P2O5 (kg/ha)	122			86			72			54		
K2O (kg/ha)	504			268			288			162		
Calcium (kg/ha)	598			228			488			304		
Magnesium (kg/ha)	1066			472			508			282		
Sodium (kg/ha)	6266			2976			2550			1592		
Sulfur (kg/ha)	546			240			188			106		
Aluminum (ppm)	228			132			157			<100		
Boron (ppm)	6.60			2.20			11.30			1.80		
Copper (ppm)	0.80			0.40			0.50			0.40		
Iron (ppm)	186			77			157			165		
Manganese (ppm)	135			14			152			111		
Zinc (ppm)	1.50			0.60			2.30			2.00		
Salt (mmhos/cm)	7.870			5.420			2.691			1.772		
Required Nutrient (kg/ha)	N	P2O5	K2O	N	P2O5	K2O	N	P2O5	K2O	N	P2O5	K2O

Lab #	2305702-021			2305702-022			2305702-023			2305702-024		
Sample ID	SHP C08 0-15			SHP C08 15-50			SHP C06 0-15			SHP C06 15-50		
Crop to be Grown	Unknown			Unknown			Unknown			Unknown		
Parameter	Analysis	Rating	Analysis	Rating	Analysis	Rating	Analysis	Rating	Analysis	Rating		
Carbon (%)	0.07		0.03		0.14		0.06					
Nitrogen (%)	< 0.02		< 0.02		< 0.02		< 0.02					
P2O5 (kg/ha)	68		36		72		66					
K2O (kg/ha)	278		246		196		210					
Calcium (kg/ha)	362		806		230		238					
Magnesium (kg/ha)	640		594		372		388					
Sodium (kg/ha)	4344		3990		2110		2458					
Sulfur (kg/ha)	322		298		154		178					
Aluminum (ppm)	103		<100		116		105					
Boron (ppm)	2.20		1.50		2.60		2.40					
Copper (ppm)	0.50		0.30		0.40		1.20					
Iron (ppm)	79		56		95		101					
Manganese (ppm)	53		20		70		68					
Zinc (ppm)	1.30		0.60		1.60		1.90					
Salt (mmhos/cm)	5.510		5.550		2.517		3.637					
Required Nutrient (kg/ha)	N	P2O5	K2O	N	P2O5	K2O	N	P2O5	K2O			

Lab #	2305702-025			2305702-026			2305702-027			2305702-028		
Sample ID	SHP RC14 0-15			SHP RC14 15-50			SHP RC26 0-15			SHP RC26 15-50		
Crop to be Grown	Unknown			Unknown			Unknown			Unknown		
Parameter	Analysis	Rating	Analysis	Rating	Analysis	Rating	Analysis	Rating				
Carbon (%)	3.64		1.39		2.31		0.15					
Nitrogen (%)	0.33		0.13		0.20		< 0.02					
P2O5 (kg/ha)	116		108		196		74					
K2O (kg/ha)	508		410		590		260					
Calcium (kg/ha)	960		604		1064		248					
Magnesium (kg/ha)	1442		932		1606		552					
Sodium (kg/ha)	6390		4484		7182		3402					
Sulfur (kg/ha)	676		824		488		278					
Aluminum (ppm)	170		184		210		<100					
Boron (ppm)	7.10		4.60		7.70		1.50					
Copper (ppm)	0.30		0.20		0.30		0.10					
Iron (ppm)	221		339		174		55					
Manganese (ppm)	5		<3		5		<3					
Zinc (ppm)	1.40		1.10		1.70		0.40					
Salt (mmhos/cm)	8.240		5.850		7.930		5.230					
Required Nutrient (kg/ha)	N	P2O5	K2O	N	P2O5	K2O	N	P2O5	K2O			

Lab #	2305702-029			2305702-030			2305702-031			2305702-032		
Sample ID	SHP RC15 0-15			SHP RC15 15-50			SHP C02 0-15			SHP C02 15-50		
Crop to be Grown	Unknown			Unknown			Unknown			Unknown		
Parameter	Analysis	Rating		Analysis	Rating		Analysis	Rating		Analysis	Rating	
Carbon (%)	2.62			0.66			0.24			< 0.02		
Nitrogen (%)	0.26			0.05			0.03			< 0.02		
P2O5 (kg/ha)	198			52			128			52		
K2O (kg/ha)	758			282			364			264		
Calcium (kg/ha)	1146			430			602			256		
Magnesium (kg/ha)	2036			728			896			590		
Sodium (kg/ha)	10304			4004			4214			3996		
Sulfur (kg/ha)	746			964			354			322		
Aluminum (ppm)	247			151			241			<100		
Boron (ppm)	11.10			2.70			10.60			2.10		
Copper (ppm)	0.30			0.10			0.80			0.20		
Iron (ppm)	183			321			227			77		
Manganese (ppm)	<3			<3			202			51		
Zinc (ppm)	0.80			0.60			3.00			1.10		
Salt (mmhos/cm)	10.960			5.850			5.650			5.640		
Required Nutrient (kg/ha)	N	P2O5	K2O	N	P2O5	K2O	N	P2O5	K2O	N	P2O5	K2O
Lab #	2305702-033			2305702-034			2305702-035			2305702-036		
Sample ID	SHP C17 0-15			SHP C17 15-50			SHP RC25 0-15			SHP RC25 15-50		
Crop to be Grown	Unknown			Unknown			Unknown			Unknown		
Parameter	Analysis	Rating		Analysis	Rating		Analysis	Rating		Analysis	Rating	
Carbon (%)	0.09			0.10			5.90			0.14		
Nitrogen (%)	< 0.02			< 0.02			0.53			< 0.02		
P2O5 (kg/ha)	104			104			188			78		
K2O (kg/ha)	236			276			778			246		
Calcium (kg/ha)	642			384			1418			284		
Magnesium (kg/ha)	456			546			2202			500		
Sodium (kg/ha)	2822			3686			9314			3340		
Sulfur (kg/ha)	196			272			606			252		
Aluminum (ppm)	117			134			206			100		
Boron (ppm)	3.60			4.20			11.20			1.30		
Copper (ppm)	0.80			0.60			0.40			0.10		
Iron (ppm)	110			117			167			64		
Manganese (ppm)	87			78			<3			<3		
Zinc (ppm)	2.90			1.90			1.60			< 0.20		
Salt (mmhos/cm)	2.381			4.244			9.740			4.113		
Required Nutrient (kg/ha)	N	P2O5	K2O	N	P2O5	K2O	N	P2O5	K2O	N	P2O5	K2O

Lab #	2305702-037			2305702-038			2305702-039			2305702-040		
Sample ID	SHP RC22 0-25			SHP C24 0-15			SHP C24 15-50			SHP RC02 0-15		
Crop to be Grown	Unknown			Unknown			Unknown			Unknown		
Parameter	Analysis	Rating	Analysis	Rating	Analysis	Rating	Analysis	Rating	Analysis	Rating		
Carbon (%)	2.69		1.36		0.29		5.99					
Nitrogen (%)	0.25		0.14		0.02		0.57					
P2O5 (kg/ha)	76		184		76		220					
K2O (kg/ha)	646		764		320		912					
Calcium (kg/ha)	944		864		320		1380					
Magnesium (kg/ha)	1502		1480		626		2258					
Sodium (kg/ha)	7594		8478		3920		11164					
Sulfur (kg/ha)	2262		672		438		1194					
Aluminum (ppm)	257		277		145		259					
Boron (ppm)	11.70		15.00		3.50		18.60					
Copper (ppm)	<0.1		0.90		0.50		0.50					
Iron (ppm)	609		169		70		252					
Manganese (ppm)	15		97		<3		12					
Zinc (ppm)	1.90		1.80		1.40		2.30					
Salt (mmhos/cm)	8.770		9.130		6.240		2.310					
Required Nutrient (kg/ha)	N	P2O5	K2O	N	P2O5	K2O	N	P2O5	K2O	N	P2O5	K2O

Lab #	2305702-041			2305702-042			2305702-043			2305702-044		
Sample ID	SHP RC02 15-50			SHP RC21 0-15			SHP RC21 15-50			SHP RC13 0-15		
Crop to be Grown	Unknown			Unknown			Unknown			Unknown		
Parameter	Analysis	Rating	Analysis	Rating	Analysis	Rating	Analysis	Rating	Analysis	Rating		
Carbon (%)	1.33		0.96		0.38		0.13					
Nitrogen (%)	0.14		0.10		0.04		< 0.02					
P2O5 (kg/ha)	106		78		38		66					
K2O (kg/ha)	508		426		222		374					
Calcium (kg/ha)	728		494		312		354					
Magnesium (kg/ha)	1206		846		550		764					
Sodium (kg/ha)	6812		5418		3280		5128					
Sulfur (kg/ha)	1340		1082		1390		780					
Aluminum (ppm)	217		162		140		126					
Boron (ppm)	7.00		4.30		2.20		2.30					
Copper (ppm)	0.20		0.20		<0.1		0.10					
Iron (ppm)	365		294		590		233					
Manganese (ppm)	3		4		12		<3					
Zinc (ppm)	1.70		1.00		1.00		1.20					
Salt (mmhos/cm)	8.030		3.749		5.550		5.400					
Required Nutrient (kg/ha)	N	P2O5	K2O	N	P2O5	K2O	N	P2O5	K2O	N	P2O5	K2O

Lab #	2305702-045			2305702-046			2305702-047		
Sample ID	SHP RC13 15-50			SHP C18 0-15			SHP C18 15-50		
Crop to be Grown	Unknown			Unknown			Unknown		
Parameter	Analysis		Rating	Analysis		Rating	Analysis		Rating
Carbon (%)	0.04			0.10			< 0.02		
Nitrogen (%)	< 0.02			< 0.02			< 0.02		
P2O5 (kg/ha)	48			74			58		
K2O (kg/ha)	320			276			242		
Calcium (kg/ha)	300			436			244		
Magnesium (kg/ha)	660			618			504		
Sodium (kg/ha)	4664			4254			3948		
Sulfur (kg/ha)	704			338			294		
Aluminum (ppm)	111			109			<100		
Boron (ppm)	1.10			7.00			1.40		
Copper (ppm)	<0.1			0.30			0.30		
Iron (ppm)	148			121			82		
Manganese (ppm)	<3			71			30		
Zinc (ppm)	0.70			1.10			0.70		
Salt (mmhos/cm)	5.730			6.330			6.420		
Required Nutrient (kg/ha)	N	P2O5	K2O	N	P2O5	K2O	N	P2O5	K2O

Table A7: Summary of soil nutrients per increment and marsh zone at Study Site (SHP)

Nitrogen (%)	P2O5 (kg/ha)	K2O (kg/ha)	Calcium (kg/ha)	Magnesium (kg/ha)	Sodium (kg/ha)	Sulfur (kg/ha)	Aluminum (ppm)	Boron (ppm)	Copper (ppm)	Iron (ppm)	Manganese (ppm)	Zinc (ppm)	Salt (mmhos/cm)
shoreline 0-15													
0.04	82.50	333.00	567.50	741.50	4898.50	389.00	132.75	3.33	0.53	106.00	66.75	1.28	5.87
shoreline 15-50													
0.02	50	251	381.5	556.5	3859.5	297	108	1.6	0.3	52.75	10.75	0.65	5.37825
low marsh 0 -15													
0.025	116	300	622	676	3531.5	275	179	7.1	0.8	168.5	144.5	2.95	4.0155
low marsh 15-50													
0.02	78.00	270.00	320.00	568.00	3841.00	297.00	117.00	3.15	0.40	97.00	64.50	1.50	4.94
mid to high 0-15													
0.158	150	735.6	833.2	1437.6	8078.8	623.2	246.4	27.34	0.88	153.6	71.4	1.68	7.808
mid to high 15-50													
0.032	93.6	380.8	449.6	1398.4	4112.8	415.4	144.7	4.06	14.36	73.8	9.28	2.908	5.628

Table A8: Summary of soil nutrients per increment and marsh zone at Reference Site (SHP_R)

Nitrogen (%)	P2O5 (kg/ha)	K2O (kg/ha)	Calcium (kg/ha)	Magnesium (kg/ha)	Sodium (kg/ha)	Sulfur (kg/ha)	Aluminum (ppm)	Boron (ppm)	Copper (ppm)	Iron (ppm)	Manganese (ppm)	Zinc (ppm)	Salt (mmhos/cm)
shoreline 0-15													
0.18	77.00	536.00	719.00	1174.00	6506.00	1672.00	209.50	8.00	0.15	451.50	9.50	1.45	6.26
shoreline 15-50													
0.03	19.00	111.00	156.00	275.00	1640.00	695.00	70.00	1.10	0.05	295.00	6.00	0.50	2.78
low marsh 0 -15													
0.54	176.00	822.67	1160.00	2042.00	10567.33	1196.00	242.33	12.73	0.40	212.67	6.67	2.17	8.84
low marsh 15-50													
0.22	82.00	493.33	778.00	1305.33	7096.00	1820.00	219.00	7.77	0.17	533.67	4.33	2.00	7.75
mid to high 0-15													
0.33	167.33	681.33	1174.67	1893.33	8669.33	676.00	207.67	9.80	0.33	190.33	3.67	1.27	9.65
mid to high 15-50													
0.03	68.00	262.67	320.67	593.33	3582.00	498.00	117.00	1.83	0.10	146.67	3.00	0.40	5.06

Table A9: Grain size analysis data (from Gradistat - statistics classification (e.g. medium sand) are from Folk and Ward).

SAMPLE STATISTICS

	C09	RC03	C24	RC01
ANALYST AND DATE:	Maka Ngulube, 06-02-2024	.	.	.
SIEVING ERROR:	-0.2%	-0.1%	-16.9%	14.7%
SAMPLE TYPE:	Trimodal, Poorly Sorted	Polymodal, Poorly Sorted	Bimodal, Poorly Sorted	Trimodal, Poorly Sorted
TEXTURAL GROUP:	Gravelly Sand	Sandy Gravel	Gravelly Sand	Gravelly Sand
SEDIMENT NAME:	Very Fine Gravelly Medium Sand	Sandy Very Fine Gravel	Very Fine Gravelly Medium Sand	Very Fine Gravelly Medium Sand
MEAN (\bar{x}_v):	649.6	959.6	824.8	456.5
SORTING (σ_v):	698.3	969.5	874.6	537.8
SKEWNESS (Sk_v):	1.859	0.756	1.166	2.908
KURTOSIS (K_v):	4.917	1.661	2.488	10.54
MEAN (\bar{x}_s):	437.4	533.5	501.0	318.8
SORTING (σ_s):	2.198	2.948	2.532	2.051
SKEWNESS (Sk_s):	1.035	0.371	0.776	1.243
KURTOSIS (K_s):	3.194	1.630	2.157	4.613
MEAN (\bar{x}_p):	1.193	0.907	0.997	1.649
SORTING (σ_p):	1.136	1.560	1.340	1.036
SKEWNESS (Sk_p):	-1.035	-0.371	-0.776	-1.243
KURTOSIS (K_p):	3.194	1.630	2.157	4.613
MEAN (M_{ci}):	460.7	506.4	571.8	298.4
SORTING (σ_{ci}):	2.204	3.034	2.615	2.120
SKEWNESS (Sk_{ci}):	0.602	0.447	0.638	0.235
KURTOSIS (K_{ci}):	1.426	0.585	0.818	1.696
MEAN (M_{si}):	1.118	0.982	0.806	1.745
SORTING (σ_{si}):	1.140	1.601	1.387	1.084
SKEWNESS (Sk_{si}):	-0.602	-0.447	-0.638	-0.235
KURTOSIS (K_{si}):	1.426	0.585	0.818	1.696
MEAN:	Medium Sand	Coarse Sand	Coarse Sand	Medium Sand
SORTING:	Poorly Sorted	Poorly Sorted	Poorly Sorted	Poorly Sorted
SKEWNESS:	Very Coarse Skewed	Very Coarse Skewed	Very Coarse Skewed	Coarse Skewed
KURTOSIS:	Leptokurtic	Very Platykurtic	Platykurtic	Very Leptokurtic
MODE 1 (μm):	302.5	302.5	302.5	302.5
MODE 2 (μm):	605.0	2400.0	2400.0	152.5
MODE 3 (μm):	2400.0	152.5		605.0
MODE 1 (ϕ):	1.747	1.747	1.747	1.747
MODE 2 (ϕ):	0.747	-1.243	-1.243	2.737
MODE 3 (ϕ):	-1.243	2.737		0.747
D ₁₀ (μm):	252.9	149.0	252.4	142.4
D ₅₀ (μm):	320.6	328.5	323.3	292.9
D ₉₀ (μm):	2127.0	2506.5	2413.6	701.8
(D ₉₀ / D ₁₀) (μm):	8.409	16.82	9.563	4.927
(D ₉₀ - D ₁₀) (μm):	1874.1	2357.5	2161.2	559.4
(D ₇₅ / D ₂₅) (μm):	2.207	8.065	4.124	1.955
(D ₇₅ - D ₂₅) (μm):	333.7	1859.7	865.1	168.9
D ₁₀ (ϕ):	-1.089	-1.326	-1.271	0.511
D ₅₀ (ϕ):	1.641	1.606	1.629	1.772
D ₉₀ (ϕ):	1.983	2.747	1.986	2.812
(D ₉₀ / D ₁₀) (ϕ):	-1.821	-2.072	-1.562	5.504
(D ₉₀ - D ₁₀) (ϕ):	3.072	4.072	3.257	2.301
(D ₇₅ / D ₂₅) (ϕ):	2.603	-1.773	-9.666	1.631
(D ₇₅ - D ₂₅) (ϕ):	1.142	3.012	2.044	0.967
% GRAVEL:	12.2%	30.4%	22.7%	6.1%
% SAND:	87.8%	69.6%	77.3%	93.9%
% MUD:	0.0%	0.0%	0.0%	0.0%
% V COARSE GRAVEL:	0.0%	0.0%	0.0%	0.0%
% COARSE GRAVEL:	0.0%	0.0%	0.0%	0.0%
% MEDIUM GRAVEL:	0.0%	0.0%	0.0%	0.0%
% FINE GRAVEL:	0.0%	0.0%	0.0%	0.0%
% V FINE GRAVEL:	12.2%	30.4%	22.7%	6.1%
% V COARSE SAND:	6.8%	2.8%	3.9%	3.5%
% COARSE SAND:	13.7%	8.0%	8.4%	11.4%
% MEDIUM SAND:	59.2%	39.6%	56.6%	52.7%
% FINE SAND:	7.5%	17.7%	8.0%	25.2%
% V FINE SAND:	0.6%	1.5%	0.4%	1.0%
% V COARSE SILT:	0.0%	0.0%	0.0%	0.0%
% COARSE SILT:	0.0%	0.0%	0.0%	0.0%
% MEDIUM SILT:	0.0%	0.0%	0.0%	0.0%
% FINE SILT:	0.0%	0.0%	0.0%	0.0%
% V FINE SILT:	0.0%	0.0%	0.0%	0.0%
% CLAY:	0.0%	0.0%	0.0%	0.0%

C02	RC17	RC11	RC02	C14
1.2%	0.2%	0.7%	1.3%	1.3%
Bimodal, Moderately Well Sorted Slightly Gravelly Sand	Bimodal, Moderately Well Sorted Slightly Gravelly Sand	Polymodal, Poorly Sorted Gravelly Sand	Polymodal, Poorly Sorted Gravelly Sand	Trimodal, Moderately Sorted Gravelly Sand
Slightly Very Fine Gravelly Medium Sand	Slightly Very Fine Gravelly Medium Sand	Very Fine Gravelly Medium Sand	Very Fine Gravelly Medium Sand	Very Fine Gravelly Medium Sand
402.5	272.8	523.8	790.4	532.5
380.8	233.1	649.7	862.4	581.9
3.977	6.573	2.287	1.204	2.514
19.92	56.63	6.768	2.653	8.171
325.7	232.7	333.7	457.9	379.1
1.710	1.596	2.262	2.694	2.024
1.512	1.303	1.209	0.625	1.242
7.019	7.246	3.786	2.082	4.344
1.618	2.103	1.583	1.127	1.399
0.774	0.674	1.177	1.430	1.017
-1.512	-1.303	-1.209	-0.625	-1.242
7.019	7.246	3.786	2.082	4.344
338.6	230.9	306.5	484.4	373.8
1.623	1.518	2.222	2.977	1.915
0.400	-0.232	0.280	0.457	0.516
3.460	0.804	1.661	0.835	1.715
1.562	2.115	1.706	1.046	1.420
0.698	0.603	1.152	1.574	0.938
-0.400	0.232	-0.280	-0.457	-0.516
3.460	0.804	1.661	0.835	1.715
Medium Sand	Fine Sand	Medium Sand	Medium Sand	Medium Sand
Moderately Well Sorted	Moderately Well Sorted	Poorly Sorted	Poorly Sorted	Moderately Sorted
Very Coarse Skewed Extremely Leptokurtic	Fine Skewed Platykurtic	Coarse Skewed Very Leptokurtic	Very Coarse Skewed Platykurtic	Very Coarse Skewed Very Leptokurtic
302.5	302.5	302.5	302.5	302.5
152.5	152.5	152.5	2400.0	605.0
		2400.0	152.5	152.5
1.747	1.747	1.747	1.747	1.747
2.737	2.737	2.737	-1.243	0.747
		-1.243	2.737	2.737
168.9	135.6	141.0	147.7	171.0
301.1	261.5	291.0	317.1	310.8
626.7	343.7	1356.7	2384.6	1201.2
3.709	2.535	9.619	16.14	7.025
457.7	208.1	1215.7	2236.8	1030.2
1.277	2.015	2.034	4.268	1.925
73.82	156.3	177.0	847.5	249.5
0.674	1.541	-0.440	-1.254	-0.265
1.732	1.935	1.781	1.657	1.686
2.565	2.883	2.826	2.759	2.548
3.805	1.871	-6.421	-2.201	-9.633
1.891	1.342	3.266	4.013	2.812
1.227	1.599	1.673	-13.298	2.000
0.353	1.011	1.024	2.094	0.945
2.5%	0.8%	9.6%	21.0%	7.6%
97.5%	99.2%	90.4%	79.0%	92.4%
0.0%	0.0%	0.0%	0.0%	0.0%
0.0%	0.0%	0.0%	0.0%	0.0%
0.0%	0.0%	0.0%	0.0%	0.0%
0.0%	0.0%	0.0%	0.0%	0.0%
0.0%	0.0%	0.0%	0.0%	0.0%
2.5%	0.8%	9.6%	21.0%	7.6%
4.0%	1.0%	4.2%	5.8%	5.3%
9.8%	3.5%	8.5%	9.2%	13.6%
71.7%	51.3%	48.8%	43.6%	62.0%
11.4%	42.9%	28.2%	19.3%	10.9%
0.5%	0.4%	0.7%	1.2%	0.6%
0.0%	0.0%	0.0%	0.0%	0.0%
0.0%	0.0%	0.0%	0.0%	0.0%
0.0%	0.0%	0.0%	0.0%	0.0%
0.0%	0.0%	0.0%	0.0%	0.0%
0.0%	0.0%	0.0%	0.0%	0.0%
0.0%	0.0%	0.0%	0.0%	0.0%

RC01	C05B	C22	RC12	RC26
0.6%	0.7%	1.3%	0.8%	0.4%
Trimodal, Moderately Sorted	Unimodal, Moderately Sorted	Bimodal, Poorly Sorted	Polymodal, Poorly Sorted	Bimodal, Moderately Sorted
Slightly Gravelly Sand	Gravelly Sand	Gravelly Sand	Gravelly Sand	Slightly Gravelly Sand
ghtly Very Fine Gravelly Medium Sa	Very Fine Gravelly Medium Sand	Very Fine Gravelly Medium Sand	Very Fine Gravelly Medium Sand	ghtly Very Fine Gravelly Medium Sa
350.7	544.8	460.3	625.0	382.9
335.6	649.0	526.6	738.9	460.3
4.455	2.309	2.954	1.793	3.636
26.10	6.719	10.80	4.580	15.79
280.8	368.9	331.6	381.3	279.4
1.762	2.082	1.963	2.436	1.914
1.148	1.574	1.426	0.951	1.545
5.456	4.709	5.295	2.888	6.002
1.832	1.439	1.592	1.391	1.840
0.817	1.058	0.973	1.284	0.936
-1.148	-1.574	-1.426	-0.951	-1.545
5.456	4.709	5.295	2.888	6.002
278.2	358.9	303.6	382.7	243.7
1.732	1.880	2.009	2.576	1.743
0.008	0.543	0.240	0.393	-0.069
0.988	4.657	4.121	1.025	1.316
1.846	1.478	1.720	1.386	2.037
0.792	0.911	1.006	1.365	0.802
-0.008	-0.543	-0.240	-0.393	0.069
0.988	4.657	4.121	1.025	1.316
Medium Sand	Medium Sand	Medium Sand	Medium Sand	Fine Sand
Moderately Sorted	Moderately Sorted	Poorly Sorted	Poorly Sorted	Moderately Sorted
Symmetrical	Very Coarse Skewed	Coarse Skewed	Very Coarse Skewed	Symmetrical
Mesokurtic	Extremely Leptokurtic	Extremely Leptokurtic	Mesokurtic	Leptokurtic
302.5	302.5	302.5	302.5	302.5
152.5		152.5	152.5	152.5
605.0			2400.0	
1.747	1.747	1.747	1.747	1.747
2.737		2.737	2.737	2.737
0.747			-1.243	
140.6	175.1	152.4	143.7	138.8
284.4	302.8	297.8	302.8	278.8
595.9	1394.6	1038.0	2183.0	602.0
4.238	7.965	6.809	15.19	4.337
455.3	1219.5	885.6	2039.3	463.2
1.983	1.277	1.311	3.212	2.015
165.9	74.15	80.99	396.7	166.1
0.747	-0.480	-0.054	-1.126	0.732
1.814	1.724	1.747	1.723	1.843
2.830	2.514	2.714	2.799	2.849
3.789	-5.239	-50.397	-2.485	3.891
2.083	2.994	2.767	3.925	2.117
1.626	1.228	1.252	3.116	1.631
0.987	0.352	0.391	1.684	1.011
1.8%	9.9%	5.8%	13.5%	4.2%
98.2%	90.1%	94.2%	86.5%	95.8%
0.0%	0.0%	0.0%	0.0%	0.0%
0.0%	0.0%	0.0%	0.0%	0.0%
0.0%	0.0%	0.0%	0.0%	0.0%
0.0%	0.0%	0.0%	0.0%	0.0%
0.0%	0.0%	0.0%	0.0%	0.0%
1.8%	9.9%	5.8%	13.5%	4.2%
2.2%	4.6%	4.8%	4.9%	2.3%
12.1%	2.9%	7.1%	11.1%	7.4%
53.8%	71.8%	64.7%	45.3%	52.3%
29.8%	10.5%	16.9%	24.7%	33.3%
0.4%	0.3%	0.8%	0.6%	0.4%
0.0%	0.0%	0.0%	0.0%	0.0%
0.0%	0.0%	0.0%	0.0%	0.0%
0.0%	0.0%	0.0%	0.0%	0.0%
0.0%	0.0%	0.0%	0.0%	0.0%
0.0%	0.0%	0.0%	0.0%	0.0%
0.0%	0.0%	0.0%	0.0%	0.0%

RC08	RC16	C20	RC24	C12
1.3%	0.5%	0.9%	1.4%	0.5%
Bimodal, Moderately Sorted Slightly Gravelly Sand	Bimodal, Moderately Well Sorted Slightly Gravelly Sand	Bimodal, Moderately Sorted Gravelly Sand	Bimodal, Poorly Sorted Gravelly Sand	Trimodal, Moderately Well Sorted Slightly Gravelly Sand
Slightly Very Fine Gravelly Medium Sand	Slightly Very Fine Gravelly Medium Sand	Very Fine Gravelly Medium Sand	Very Fine Gravelly Medium Sand	Slightly Very Fine Gravelly Medium Sand
367.1	290.6	420.5	436.7	318.1
424.5	231.0	507.5	541.8	227.0
3.852	6.441	3.380	2.969	3.901
18.03	55.13	13.26	10.77	27.02
273.5	250.8	306.3	299.5	268.9
1.884	1.579	1.902	2.063	1.673
1.419	1.052	1.668	1.392	0.717
5.970	7.273	6.566	4.956	4.152
1.870	1.995	1.707	1.740	1.895
0.914	0.659	0.928	1.045	0.743
-1.419	-1.052	-1.668	-1.392	-0.717
5.970	7.273	6.566	4.956	4.152
242.5	239.4	254.9	281.8	245.3
1.725	1.518	1.839	2.088	1.582
-0.087	-0.285	-0.039	0.214	-0.210
1.279	0.879	4.049	1.631	0.967
2.044	2.063	1.972	1.827	2.027
0.786	0.603	0.879	1.062	0.662
0.087	0.285	0.039	-0.214	0.210
1.279	0.879	4.049	1.631	0.967
Fine Sand Moderately Sorted Symmetrical Leptokurtic	Fine Sand Moderately Well Sorted Fine Skewed Platykurtic	Medium Sand Moderately Sorted Symmetrical Extremely Leptokurtic	Medium Sand Poorly Sorted Coarse Skewed Very Leptokurtic	Fine Sand Moderately Well Sorted Fine Skewed Mesokurtic
302.5	302.5	302.5	302.5	302.5
152.5	152.5	152.5	152.5	152.5
				605.0
1.747	1.747	1.747	1.747	1.747
2.737	2.737	2.737	2.737	2.737
				0.747
137.8	138.8	146.4	139.4	139.5
278.1	275.7	291.2	284.0	281.4
583.2	346.7	611.3	691.8	568.7
4.232	2.497	4.176	4.963	4.077
445.4	207.9	464.9	552.4	429.2
2.011	1.934	1.319	2.015	1.989
164.9	153.6	80.97	169.5	164.5
0.778	1.528	0.710	0.532	0.814
1.846	1.859	1.780	1.816	1.830
2.859	2.849	2.772	2.843	2.842
3.676	1.864	3.904	5.348	3.490
2.081	1.320	2.062	2.311	2.028
1.627	1.576	1.253	1.643	1.622
1.008	0.952	0.400	1.011	0.992
3.3%	0.8%	5.7%	6.2%	0.3%
96.7%	99.2%	94.3%	93.8%	99.7%
0.0%	0.0%	0.0%	0.0%	0.0%
0.0%	0.0%	0.0%	0.0%	0.0%
0.0%	0.0%	0.0%	0.0%	0.0%
0.0%	0.0%	0.0%	0.0%	0.0%
0.0%	0.0%	0.0%	0.0%	0.0%
0.0%	0.0%	0.0%	0.0%	0.0%
3.3%	0.8%	5.7%	6.2%	0.3%
2.9%	1.1%	1.1%	3.3%	2.7%
6.7%	4.0%	7.4%	7.7%	11.1%
53.2%	61.2%	63.3%	51.7%	54.2%
32.6%	32.3%	22.0%	30.2%	31.1%
1.3%	0.7%	0.5%	1.0%	0.7%
0.0%	0.0%	0.0%	0.0%	0.0%
0.0%	0.0%	0.0%	0.0%	0.0%
0.0%	0.0%	0.0%	0.0%	0.0%
0.0%	0.0%	0.0%	0.0%	0.0%
0.0%	0.0%	0.0%	0.0%	0.0%
0.0%	0.0%	0.0%	0.0%	0.0%
0.0%	0.0%	0.0%	0.0%	0.0%

RC18	RC09	C06	RC15	RC13
1.2%	0.6%	0.5%	7.4%	0.8%
Trimodal, Poorly Sorted	Bimodal, Poorly Sorted	Unimodal, Well Sorted	Bimodal, Moderately Well Sorted	Trimodal, Moderately Well Sorted
Gravelly Sand	Gravelly Sand	Slightly Gravelly Sand	Slightly Gravelly Sand	Slightly Gravelly Sand
Very Fine Gravelly Medium Sand	Very Fine Gravelly Medium Sand	Slightly Very Fine Gravelly Medium Sand	Slightly Very Fine Gravelly Medium Sand	Slightly Very Fine Gravelly Medium Sand
572.3	471.5	333.0	341.2	301.1
719.5	596.3	239.7	387.3	239.5
1.985	2.706	6.359	4.429	5.425
5.260	8.856	51.40	23.10	43.36
346.0	316.5	295.5	263.7	254.8
2.392	2.092	1.489	1.789	1.643
1.158	1.495	1.322	1.549	1.002
3.412	5.073	11.20	7.270	5.353
1.531	1.660	1.759	1.923	1.972
1.258	1.065	0.574	0.840	0.716
-1.158	-1.495	-1.322	-1.549	-1.002
3.412	5.073	11.20	7.270	5.353
354.6	283.7	295.5	240.6	239.8
2.495	2.056	1.338	1.587	1.568
0.385	0.199	-0.003	-0.202	-0.205
1.681	1.842	2.684	1.008	0.922
1.496	1.818	1.759	2.055	2.060
1.319	1.040	0.420	0.666	0.649
-0.385	-0.199	0.003	0.202	0.205
1.681	1.842	2.684	1.008	0.922
Medium Sand	Medium Sand	Medium Sand	Fine Sand	Fine Sand
Poorly Sorted	Poorly Sorted	Well Sorted	Moderately Well Sorted	Moderately Well Sorted
Very Coarse Skewed	Coarse Skewed	Symmetrical	Fine Skewed	Fine Skewed
Very Leptokurtic	Very Leptokurtic	Very Leptokurtic	Mesokurtic	Mesokurtic
302.5	302.5	302.5	302.5	302.5
152.5	152.5		152.5	152.5
2400.0				605.0
1.747	1.747	1.747	1.747	1.747
2.737	2.737		2.737	2.737
-1.243				0.747
140.8	143.4	169.9	138.0	138.0
291.3	289.8	295.5	276.7	274.0
2138.1	1075.1	352.0	353.4	514.6
15.18	7.496	2.072	2.560	3.728
1997.2	931.6	182.1	215.3	376.5
2.038	1.879	1.244	1.971	2.009
177.7	157.5	64.73	158.8	162.3
-1.096	-0.104	1.506	1.501	0.959
1.779	1.787	1.759	1.854	1.868
2.828	2.802	2.557	2.857	2.857
-2.580	-26.835	1.698	1.904	2.980
3.924	2.906	1.051	1.356	1.898
1.676	1.579	1.197	1.599	1.618
1.027	0.910	0.315	0.979	1.007
12.5%	8.0%	0.9%	2.8%	0.7%
87.5%	92.0%	99.1%	97.2%	99.3%
0.0%	0.0%	0.0%	0.0%	0.0%
0.0%	0.0%	0.0%	0.0%	0.0%
0.0%	0.0%	0.0%	0.0%	0.0%
0.0%	0.0%	0.0%	0.0%	0.0%
0.0%	0.0%	0.0%	0.0%	0.0%
12.5%	8.0%	0.9%	2.8%	0.7%
3.6%	2.5%	1.4%	1.8%	1.4%
6.6%	5.5%	5.8%	4.6%	8.6%
48.6%	58.6%	80.2%	57.3%	53.2%
28.0%	24.6%	11.0%	32.2%	35.8%
0.9%	0.7%	0.8%	1.2%	0.3%
0.0%	0.0%	0.0%	0.0%	0.0%
0.0%	0.0%	0.0%	0.0%	0.0%
0.0%	0.0%	0.0%	0.0%	0.0%
0.0%	0.0%	0.0%	0.0%	0.0%
0.0%	0.0%	0.0%	0.0%	0.0%
0.0%	0.0%	0.0%	0.0%	0.0%
0.0%	0.0%	0.0%	0.0%	0.0%

C13	C05	RC25	C21	C16
-0.1%	0.5%	0.9%	0.4%	0.4%
Bimodal, Moderately Sorted	Bimodal, Moderately Sorted	Bimodal, Moderately Sorted	Bimodal, Moderately Well Sorted	Trimodal, Moderately Sorted
Slightly Gravelly Sand	Gravelly Sand	Slightly Gravelly Sand	Slightly Gravelly Sand	Gravelly Sand
Slightly Very Fine Gravelly Medium Sand	Very Fine Gravelly Medium Sand	Slightly Very Fine Gravelly Medium Sand	Slightly Very Fine Gravelly Medium Sand	Very Fine Gravelly Medium Sand
416.1	473.2	388.0	336.0	616.7
453.2	552.3	437.5	310.9	684.0
3.572	2.910	3.757	5.560	2.069
15.38	10.20	16.99	35.90	5.611
317.9	340.2	292.6	284.9	424.3
1.821	1.944	1.855	1.575	2.088
1.599	1.635	1.456	1.839	1.387
6.569	5.736	6.285	11.01	3.989
1.653	1.555	1.773	1.812	1.237
0.864	0.959	0.891	0.655	1.062
-1.599	-1.635	-1.456	-1.839	-1.387
6.569	5.736	6.285	11.01	3.989
264.0	343.3	250.5	257.5	387.8
1.669	1.831	1.709	1.475	1.793
-0.091	0.491	-0.108	-0.279	0.706
3.512	4.331	1.445	2.562	1.351
1.921	1.542	1.997	1.958	1.367
0.739	0.873	0.773	0.560	0.843
0.091	-0.491	0.108	0.279	-0.706
3.512	4.331	1.445	2.562	1.351
Medium Sand	Medium Sand	Medium Sand	Medium Sand	Medium Sand
Moderately Sorted	Moderately Sorted	Moderately Sorted	Moderately Well Sorted	Moderately Sorted
Symmetrical	Very Coarse Skewed	Fine Skewed	Fine Skewed	Very Coarse Skewed
Extremely Leptokurtic	Extremely Leptokurtic	Leptokurtic	Very Leptokurtic	Leptokurtic
302.5	302.5	302.5	302.5	302.5
152.5	152.5	152.5	152.5	605.0
				2400.0
1.747	1.747	1.747	1.747	1.747
2.737	2.737	2.737	2.737	0.747
				-1.243
154.1	159.5	142.8	152.9	257.0
296.5	300.0	287.7	290.2	317.9
632.9	704.0	598.9	349.4	2116.5
4.108	4.415	4.194	2.285	8.235
478.9	544.6	456.1	196.5	1859.5
1.296	1.296	1.868	1.261	1.994
77.17	78.07	154.5	67.47	276.6
0.660	0.506	0.740	1.517	-1.082
1.754	1.737	1.797	1.785	1.653
2.698	2.649	2.808	2.709	1.960
4.089	5.231	3.797	1.786	-1.812
2.039	2.142	2.068	1.192	3.042
1.239	1.242	1.567	1.207	2.172
0.374	0.374	0.901	0.335	0.995
4.1%	6.8%	3.7%	1.8%	12.0%
95.9%	93.2%	96.3%	98.2%	88.0%
0.0%	0.0%	0.0%	0.0%	0.0%
0.0%	0.0%	0.0%	0.0%	0.0%
0.0%	0.0%	0.0%	0.0%	0.0%
0.0%	0.0%	0.0%	0.0%	0.0%
0.0%	0.0%	0.0%	0.0%	0.0%
4.1%	6.8%	3.7%	1.8%	12.0%
3.3%	3.0%	2.8%	1.4%	2.9%
7.9%	7.7%	7.2%	3.3%	14.3%
67.5%	67.6%	60.6%	75.6%	65.9%
16.8%	14.7%	24.8%	17.6%	4.5%
0.4%	0.2%	1.0%	0.3%	0.3%
0.0%	0.0%	0.0%	0.0%	0.0%
0.0%	0.0%	0.0%	0.0%	0.0%
0.0%	0.0%	0.0%	0.0%	0.0%
0.0%	0.0%	0.0%	0.0%	0.0%
0.0%	0.0%	0.0%	0.0%	0.0%
0.0%	0.0%	0.0%	0.0%	0.0%

RC14	RC06	C25	RC22	C23
1.1%	2.7%	1.6%	1.2%	1.1%
Polymodal, Poorly Sorted Gravelly Sand	Polymodal, Poorly Sorted Gravelly Sand	Polymodal, Poorly Sorted Gravelly Sand	Polymodal, Poorly Sorted Gravelly Sand	Bimodal, Poorly Sorted Gravelly Sand
Very Fine Gravelly Medium Sand	Very Fine Gravelly Medium Sand	Very Fine Gravelly Medium Sand	Very Fine Gravelly Medium Sand	Very Fine Gravelly Medium Sand
878.9	574.3	717.3	742.9	470.2
880.0	689.8	723.5	854.3	578.6
1.014	2.050	1.585	1.304	2.765
2.237	5.642	4.029	2.897	9.308
533.1	362.5	482.8	416.6	321.4
2.635	2.319	2.256	2.732	2.066
0.475	1.063	0.795	0.743	1.436
1.878	3.410	2.620	2.181	5.011
0.908	1.464	1.050	1.263	1.638
1.398	1.214	1.174	1.450	1.047
-0.475	-1.063	-0.795	-0.743	-1.436
1.878	3.410	2.620	2.181	5.011
577.0	323.4	484.9	463.4	292.7
2.663	2.250	2.226	3.027	2.078
0.583	0.294	0.620	0.460	0.223
0.765	1.695	1.191	0.870	3.864
0.793	1.629	1.044	1.110	1.773
1.413	1.170	1.154	1.598	1.055
-0.583	-0.294	-0.620	-0.460	-0.223
0.765	1.695	1.191	0.870	3.864
Coarse Sand	Medium Sand	Medium Sand	Medium Sand	Medium Sand
Poorly Sorted	Poorly Sorted	Poorly Sorted	Poorly Sorted	Poorly Sorted
Very Coarse Skewed	Coarse Skewed	Very Coarse Skewed	Very Coarse Skewed	Coarse Skewed
Platykurtic	Very Leptokurtic	Leptokurtic	Platykurtic	Extremely Leptokurtic
302.5	302.5	302.5	302.5	302.5
2400.0	152.5	2400.0	152.5	152.5
605.0	2400.0	605.0	2400.0	
1.747	1.747	1.747	1.747	1.747
-1.243	2.737	-1.243	2.737	2.737
0.747	-1.243	0.747	-1.243	
167.3	144.5	256.8	141.5	144.7
335.5	300.2	329.6	304.1	292.4
2425.8	2081.2	2178.5	2362.2	1041.5
14.50	14.40	8.482	16.69	7.196
2258.5	1936.7	1921.7	2220.6	896.8
4.737	2.016	2.507	4.047	1.348
1031.3	256.9	424.9	527.7	87.66
-1.278	-1.057	-1.123	-1.240	-0.059
1.576	1.736	1.601	1.718	1.774
2.580	2.791	1.961	2.821	2.789
-2.018	-2.639	-1.746	-2.275	-47.571
3.858	3.848	3.084	4.061	2.847
-4.804	2.040	3.650	4.933	1.276
2.244	1.011	1.326	2.017	0.431
23.5%	11.3%	13.4%	19.8%	7.4%
76.5%	88.7%	86.6%	80.2%	92.6%
0.0%	0.0%	0.0%	0.0%	0.0%
0.0%	0.0%	0.0%	0.0%	0.0%
0.0%	0.0%	0.0%	0.0%	0.0%
0.0%	0.0%	0.0%	0.0%	0.0%
0.0%	0.0%	0.0%	0.0%	0.0%
23.5%	11.3%	13.4%	19.8%	7.4%
7.6%	4.5%	11.4%	4.9%	2.9%
11.7%	9.7%	13.3%	7.8%	7.2%
44.9%	51.2%	56.2%	39.6%	58.7%
11.5%	22.1%	4.9%	27.1%	23.0%
0.8%	1.2%	0.8%	0.8%	0.8%
0.0%	0.0%	0.0%	0.0%	0.0%
0.0%	0.0%	0.0%	0.0%	0.0%
0.0%	0.0%	0.0%	0.0%	0.0%
0.0%	0.0%	0.0%	0.0%	0.0%
0.0%	0.0%	0.0%	0.0%	0.0%
0.0%	0.0%	0.0%	0.0%	0.0%

C17	C04	C22	RC23	RC21	C01
0.3%	-0.2%	-0.1%	2.8%	1.0%	1.8%
Bimodal, Moderately Sorted	Unimodal, Well Sorted	Unimodal, Well Sorted	Polymodal, Poorly Sorted	Trimodal, Poorly Sorted	Trimodal, Poorly Sorted
Gravelly Sand	Slightly Gravelly Sand	Slightly Gravelly Sand	Gravelly Sand	Gravelly Sand	Gravelly Sand
Very Fine Gravelly Medium Sand	Very Fine Gravelly Medium Sand	Very Fine Gravelly Medium Sa	Very Fine Gravelly Medium Sand	Very Fine Gravelly Medium Sand	Very Fine Gravelly Medium Sand
477.8	326.0	319.2	762.5	527.9	657.9
567.5	198.0	176.7	826.3	651.3	723.0
2.870	6.623	7.327	1.337	2.341	1.854
9.794	62.40	78.27	3.024	6.884	4.729
341.2	294.9	292.6	460.4	345.6	440.1
1.947	1.448	1.411	2.575	2.175	2.192
1.710	1.110	0.997	0.599	1.350	1.131
5.984	9.834	10.39	2.420	4.352	3.390
1.551	1.762	1.773	1.119	1.533	1.184
0.961	0.534	0.497	1.364	1.121	1.133
-1.710	-1.110	-0.997	-0.599	-1.350	-1.131
5.984	9.834	10.39	2.420	4.352	3.390
338.2	295.6	295.3	557.2	310.1	451.6
1.808	1.338	1.326	2.654	2.130	2.155
0.485	-0.002	-0.014	0.592	0.274	0.606
4.508	2.637	2.593	1.273	4.046	1.469
1.564	1.758	1.760	0.844	1.689	1.147
0.854	0.420	0.407	1.408	1.091	1.108
-0.485	0.002	0.014	-0.592	-0.274	-0.606
4.508	2.637	2.593	1.273	4.046	1.469
Medium Sand	Medium Sand	Medium Sand	Coarse Sand	Medium Sand	Medium Sand
Moderately Sorted	Well Sorted	Well Sorted	Poorly Sorted	Poorly Sorted	Poorly Sorted
Very Coarse Skewed	Symmetrical	Symmetrical	Very Coarse Skewed	Coarse Skewed	Very Coarse Skewed
Extremely Leptokurtic	Very Leptokurtic	Very Leptokurtic	Leptokurtic	Extremely Leptokurtic	Leptokurtic
302.5	302.5	302.5	302.5	302.5	302.5
152.5			2400.0	152.5	605.0
			605.0	2400.0	2400.0
1.747	1.747	1.747	1.747	1.747	1.747
2.737			-1.243	2.737	0.747
			0.747	-1.243	-1.243
163.1	168.8	170.6	160.8	148.5	254.5
300.0	295.6	295.3	321.7	297.2	321.9
699.9	352.9	351.3	2344.9	1398.0	2196.0
4.292	2.091	2.059	14.58	9.417	8.627
536.9	184.1	180.6	2184.1	1249.6	1941.5
1.284	1.248	1.243	2.591	1.336	2.143
75.28	65.53	64.25	431.8	86.48	317.8
0.515	1.503	1.509	-1.230	-0.483	-1.135
1.737	1.758	1.760	1.636	1.751	1.635
2.616	2.567	2.551	2.637	2.752	1.974
5.083	1.708	1.690	-2.144	-5.693	-1.739
2.102	1.064	1.042	3.866	3.235	3.109
1.232	1.200	1.195	3.703	1.271	2.472
0.361	0.319	0.313	1.374	0.418	1.100
7.4%	0.5%	0.4%	19.0%	10.0%	13.8%
92.6%	99.5%	99.6%	81.0%	90.0%	86.2%
0.0%	0.0%	0.0%	0.0%	0.0%	0.0%
0.0%	0.0%	0.0%	0.0%	0.0%	0.0%
0.0%	0.0%	0.0%	0.0%	0.0%	0.0%
0.0%	0.0%	0.0%	0.0%	0.0%	0.0%
0.0%	0.0%	0.0%	0.0%	0.0%	0.0%
7.4%	0.5%	0.4%	19.0%	10.0%	13.8%
2.4%	1.2%	0.8%	5.7%	3.1%	2.8%
6.6%	7.0%	6.4%	10.8%	6.2%	16.6%
70.1%	79.3%	80.7%	51.5%	60.5%	59.8%
13.3%	11.8%	11.5%	9.7%	19.3%	6.4%
0.3%	0.2%	0.1%	3.3%	0.9%	0.5%
0.0%	0.0%	0.0%	0.0%	0.0%	0.0%
0.0%	0.0%	0.0%	0.0%	0.0%	0.0%
0.0%	0.0%	0.0%	0.0%	0.0%	0.0%
0.0%	0.0%	0.0%	0.0%	0.0%	0.0%
0.0%	0.0%	0.0%	0.0%	0.0%	0.0%
0.0%	0.0%	0.0%	0.0%	0.0%	0.0%
0.0%	0.0%	0.0%	0.0%	0.0%	0.0%

Table A10: ANOVA tests: Nutrient Analysis Summary

Nutrient		Study Site	Reference Site	F-statistic	p-value	Analysis of Variance Table					
Nitrogen (0-15%)	Min	0.02	0.02	1.84 on 5 and 35 DF	0.1306	Response:					
	Q1	0.02	0.03			Df	Sum Sq	Mean Sq	F value	Pr(>F)	
	Median	0.09	0.15			site	1	0.00915	0.009149	0.2065	0.65231
	Q3	0.35	0.33			zone	2	0.36822	0.18411	4.1558	0.02402 *
	Max	0.71	0.71			site:zone	2	0.03012	0.015059	0.3399	0.71416
	Mean	0.20	0.21			Residuals	35	1.55058	0.044302		

						Contrast	Estimate	SE	df	t-ratio	p-value
						LM - MH	-0.115	0.0783	35	-1.465	0.3198
						LM - S	0.123	0.0828	35	1.481	0.3124
						MH - S	0.237	0.0816	35	2.908	0.0168
Nitrogen (15-50) (%)	Min	0.02	0.02	0.377 on 5 and 35 DF	0.8611	Response: tnitrogen					
	Q1	0.02	0.02			site	1	58.1	58.15	0.1867	0.6684
	Median	0.02	0.02			zone	2	407.9	203.93	0.6546	0.5259
	Q3	0.03	0.04			site:zone	2	121.1	60.572	0.1944	0.8242
	Max	0.40	0.40			Residuals	35	10903.2	311.521		
	Mean	0.05	0.05								
						Response: tP2O5					
P2O5 (0-15) (kg/ha)	Min	64.00	32.00	0.3184 on 5 and 35 DF	0.8986	site	1	0.0000207	2.07E-05	0.1651	0.687
	Q1	75.50	72.00			zone	2	0.0001545	7.73E-05	0.6149	0.5464
	Median	110.00	91.00			site:zone	2	0.0000247	1.24E-05	0.0985	0.9065
	Q3	166.00	160.00			Residuals	35	0.0043977	1.26E-04		
	Max	220.00	220.00								
	Mean	122.80	118.19								
						Response: tP2O5					
P2O5 (15-50) (kg/ha)	Min	162.00	162.00	0.1815 on 5 and 35	0.9677	site	1	0.000041	4.126E-05	0.0242	0.8772
	Q1	245.00	246.00			zone	2	0.000249	0.0001243	0.073	0.9297
	Median	279.00	284.00			site:zone	2	0.001255	0.0006274	0.3686	0.6944
	Q3	410.00	410.00			Residuals	35	0.059575	0.0017022		
	Max	508.00	778.00								
	Mean	342.60	337.62								
						Response: tK2O					
K2O (0-15) (kg/ha)	Min	196.00	196.00	0.3911 on 5 and 35 DF	0.8515	site	1	0.000046	4.604E-05	0.0826	0.7755
	Q1	285.50	278.00			zone	2	0.0004614	0.0002307	0.414	0.6642
	Median	465.00	465.00			site:zone	2	0.0005824	0.0002912	0.5225	0.5976
	Q3	759.50	646.00			Residuals	35	0.0195057	0.0005573		
	Max	1356.00	1356.00								
	Mean	559.90	530.29								
						Response: tK2O					
K2O (15-50) (kg/ha)	Min	162.00	162.00	0.7586 on 5 and 35	0.5857	site	1	1.36E-07	1.36E-07	0.0201	0.8879
	Q1	245.00	246.00			zone	2	1.25E-05	6.26E-06	0.9252	0.4059
	Median	279.00	284.00			site:zone	2	1.30E-05	6.51E-06	0.9613	0.3923
	Q3	410.00	410.00			Residuals	35	2.37E-04	6.77E-06		
	Max	508.00	778.00								
	Mean	342.60	337.62								
						Response: tMg					

Mg (0-15)	Min	372.00	0.09	0.3007 on 5 and 35 DF	0.9091	site	1	0.00002	1.957E-05	0.0203	0.8874
(kg/ha)	Q1	634.50	0.23			zone	2	0.000823	0.0004114	0.4273	0.6556
	Median	981.00	0.37			site:zone	2	0.000605	0.0003026	0.3143	0.7324
	Q3	1485.50	0.58			Residuals	35	0.033695	0.0009627		
	Max	2954.00	0.87								
	Mean	1203.00	0.39								
						Response: tMg					
Mg (15-50)	Min	282.00	282.00	1.813 on 5 and 35	0.1358	site	1	4.2E-07	4.17E-07	0.0361	0.85043
(kg/ha)	Q1	544.00	546.00			zone	2	8.177E-05	4.09E-05	3.5345	0.03998 *
	Median	594.00	627.00			site:zone	2	2.268E-05	1.13E-05	0.9803	0.38525
	Q3	852.50	932.00			Residuals	35	0.0004049	1.16E-05		
	Max	3920.00	3920.00								
	Mean	901.50	916.57								
						Contrast	Estimate	SE	df	t-ratio	p-value
						LM - MH	-0.00102	0.00127	35	-0.806	0.7016
						LM - S	-0.00347	0.00134	35	-2.596	0.0356
						MH - S	-0.00245	0.00132	35	-1.861	0.1653
						Response: tCa					
Ca (0-15)	Min	230.00	230.00	0.1903 on 5 and 35 DF	0.9643	site	1	58.1	58.15	0.1867	0.6684
(kg/ha)	Q1	475.00	488.00			zone	2	407.9	203.93	0.6546	0.5259
	Median	753.00	869.00			site:zone	2	121.1	60.572	0.1944	0.8242
	Q3	948.00	960.00			Residuals	35	10903.2	311.521		
	Max	1690.00	1690.00								
	Mean	792.70	802.67								
						Response: tCa					
Ca (15-50)	Min	228.00	228.00	0.1939 on 5 and 35 DF	0.9629	site	1	4.80E-07	4.80E-07	0.0755	0.7851
(kg/ha)	Q1	257.50	258.00			zone	2	5.01E-06	2.50E-06	0.3934	0.6777
	Median	348.00	348.00			site:zone	2	6.81E-07	3.41E-07	0.0535	0.948
	Q3	509.50	604.00			Residuals	35	2.23E-04	6.36E-06		
	Max	1002.00	1140.00								
	Mean	428.80	469.24								
						Response: tIron					
Iron (0-15)	Min	65.00	64.00	0.4192 on 5 and 35 DF	0.8321	site	1	0.00007	6.983E-05	0.0488	0.8264
(ppm)	Q1	118.25	110.00			zone	2	0.001991	0.0009954	0.6961	0.5053
	Median	173.50	173.50			site:zone	2	0.000937	0.0004684	0.3276	0.7229
	Q3	228.50	227.00			Residuals	35	0.050051	0.00143		
	Max	294.00	897.00								
	Mean	192.40	200.00								
						Response: tIron					

Iron (15-50)	Min	3.00	3.00	0.382 on 5 and 35 DF	0.8577	site	1	0.019	0.01925	0.0126	0.9111
(ppm)	Q1	71.75	77.00			zone	2	2.42	1.21004	0.7948	0.4597
	Median	104.50	112.50			site:zone	2	0.469	0.23443	0.154	0.8579
	Q3	165.00	167.00			Residuals	35	53.286	1.52245		
	Max	590.00	590.00								
	Mean	152.50	155.86								
						Response: tSalt					
Salt (0-15)	Min	2.31	2.31	0.4498 on 5 and 35 DF	0.8105	site	1	0.056	0.0558	0.0079	0.9295
(mmhos/cm)	Q1	4.62	4.11			zone	2	12.598	6.2991	0.8964	0.4172
	Median	5.99	5.99			site:zone	2	3.151	1.5754	0.2242	0.8003
	Q3	8.46	8.35			Residuals	35	245.95	7.0271		
	Max	10.96	10.96								
	Mean	6.38	6.30								
						Response: tSalt					
Salt (15-50)	Min	1.77	1.77	0.5864 on 5 and 35 DF	0.7102	site	1	0.00053	0.000531	0.0078	0.93
(mmhos/cm)	Q1	5.03	5.15			zone	2	0.1028	0.051398	0.7565	0.4768
	Median	5.69	5.79			site:zone	2	0.09587	0.047934	0.7056	0.5007
	Q3	6.32	6.42			Residuals	35	2.37781	0.067938		
	Max	8.03	9.74								
	Mean	5.92	5.73								
						Response: tSulfur					
Sulfur (0-15)	Min	154.00	154.00	0.5704 on 5 and 35 DF	0.7221	site	1	0.000013	1.254E-05	0.0084	0.9273
(kg/ha)	Q1	334.00	322.00			zone	2	0.001957	0.0009784	0.6592	0.5236
	Median	583.00	583.00			site:zone	2	0.002264	0.001132	0.7627	0.474
	Q3	794.50	780.00			Residuals	35	0.05195	0.0014843		
	Max	1194.00	3296.00								
	Mean	665.50	695.05								
						Response: tSulfur					
Sulfur (15-50)	Min	106.00	106.00	0.456 on 5 and 35 DF	0.8061	site	1	0.000016	1.645E-05	0.0085	0.9273
(kg/ha)	Q1	288.50	294.00			zone	2	0.002508	0.0012541	0.6445	0.531
	Median	325.00	380.00			site:zone	2	0.001912	0.0009558	0.4912	0.616
	Q3	780.50	704.00			Residuals	35	0.068099	0.0019457		
	Max	1390.00	1390.00								
	Mean	568.85	521.00								

Table A11: Nutrient Analysis Summary Q1, Q2, and Q3.

P2O5 (0-15)		P2O5 (15-50)		K2O (0-15)		K2O (15-50)		Nitrogen (0-15)		Nitrogen (15-50)		Iron (0-15)		Iron (15-50)	
Study Site		Study Site		Study Site		Study Site		Study Site		Study Site		Study Site		Study Site	
Min	64.00	Min	36.00	Min	196.00	Min	162.00	Min	0.02	Min	0.02	Min	65.00	Min	3.00
Q1	75.50	Q1	51.00	Q1	285.50	Q1	245.00	Q1	0.02	Q1	0.02	Q1	118.25	Q1	71.75
Median	110.00	Median	68.00	Median	465.00	Median	279.00	Median	0.09	Median	0.02	Median	173.50	Median	104.50
Q3	166.00	Q3	104.00	Q3	759.50	Q3	410.00	Q3	0.35	Q3	0.03	Q3	228.50	Q3	165.00
Max	220.00	Max	138.00	Max	1356.00	Max	508.00	Max	0.71	Max	0.40	Max	294.00	Max	590.00
Mean	122.80	Mean	77.30	Mean	559.90	Mean	342.60	Mean	0.20	Mean	0.05	Mean	192.40	Mean	152.50
Reference Site		Reference Site		Reference Site		Reference Site		Reference Site		Reference Site		Reference Site		Reference Site	
Min	32.00	Min	36.00	Min	196.00	Min	162.00	Min	0.02	Min	0.02	Min	64.00	Min	3.00
Q1	72.00	Q1	52.00	Q1	278.00	Q1	246.00	Q1	0.03	Q1	0.02	Q1	110.00	Q1	77.00
Median	91.00	Median	73.00	Median	465.00	Median	284.00	Median	0.15	Median	0.02	Median	173.50	Median	112.50
Q3	160.00	Q3	104.00	Q3	646.00	Q3	410.00	Q3	0.33	Q3	0.04	Q3	227.00	Q3	167.00
Max	220.00	Max	188.00	Max	1356.00	Max	778.00	Max	0.71	Max	0.40	Max	897.00	Max	590.00
Mean	118.19	Mean	78.95	Mean	530.29	Mean	337.62	Mean	0.21	Mean	0.05	Mean	200.00	Mean	155.86
Salt (0-15)		Salt (15-50)		Calcium (0-15)		Calcium (15-50)		Mg (0-15)		Mg (15-50)		Sulfur (0-15)		Sulfur (15-50)	
Study Site		Study Site		Study Site		Study Site		Study Site		Study Site		Study Site		Study Site	
Min	2.31	Min	1.77	Min	230.00	Min	228.00	Min	372.00	Min	282.00	Min	154.00	Min	106.00
Q1	4.62	Q1	5.03	Q1	475.00	Q1	257.50	Q1	634.50	Q1	544.00	Q1	334.00	Q1	288.50
Median	5.99	Median	5.69	Median	753.00	Median	348.00	Median	981.00	Median	594.00	Median	583.00	Median	325.00
Q3	8.46	Q3	6.32	Q3	948.00	Q3	509.50	Q3	1485.50	Q3	852.50	Q3	794.50	Q3	780.50
Max	10.96	Max	8.03	Max	1690.00	Max	1002.00	Max	2954.00	Max	3920.00	Max	1194.00	Max	1390.00
Mean	6.38	Mean	5.92	Mean	792.70	Mean	428.80	Mean	1203.00	Mean	901.50	Mean	665.50	Mean	568.85
Reference Site		Reference Site		Reference Site		Reference Site		Reference Site		Reference Site		Reference Site		Reference Site	
Min	2.31	Min	1.77	Min	230.00	Min	228.00	Min	372.00	Min	282.00	Min	154.00	Min	106.00
Q1	4.11	Q1	5.15	Q1	488.00	Q1	258.00	Q1	618.00	Q1	546.00	Q1	322.00	Q1	294.00
Median	5.99	Median	5.79	Median	869.00	Median	348.00	Median	981.00	Median	627.00	Median	583.00	Median	380.00
Q3	8.35	Q3	6.42	Q3	960.00	Q3	604.00	Q3	1480.00	Q3	932.00	Q3	780.00	Q3	704.00
Max	10.96	Max	9.74	Max	1690.00	Max	1140.00	Max	2954.00	Max	3920.00	Max	3296.00	Max	1390.00
Mean	6.30	Mean	5.73	Mean	802.67	Mean	469.24	Mean	1182.67	Mean	916.57	Mean	695.05	Mean	521.00

Table A12: Nutrient Analysis Summary (standard deviations).

Variable	Study Site (0-15)	Study Site (15-50)	Reference Site (0-15)	Reference Site (15-50)
P2O5 kg/ha	54.66	32.92	57.03	33.36
K2O kg/ha	335.09	210.28	327.29	211.11
Nitrogen %	0.295	0.112	0.217	0.1
Iron ppm	69.74	87.33	66.92	82.71
Salt mmhos/cm	2.03	1	2.03	1.09
Calcium kg/ha	293.51	320.68	328.38	366.92
Magnesium kg/ha	879.18	706.25	910.7	793.67
Sulfur kg/ha	376.14	307.56	367.13	338.1